

Understanding Galaxy Light: Dust

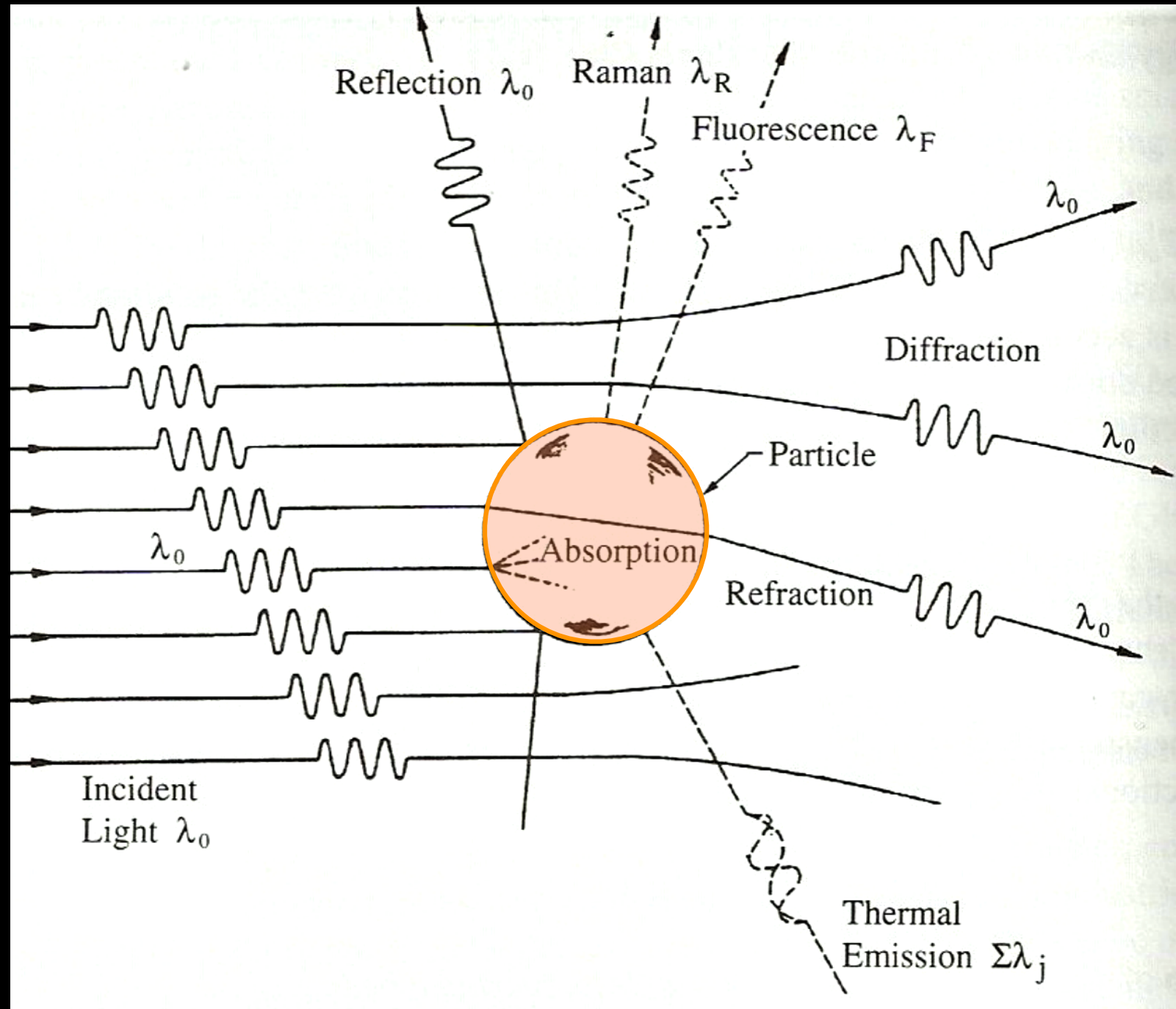
Dust is ubiquitous and must be understood to interpret SEDs



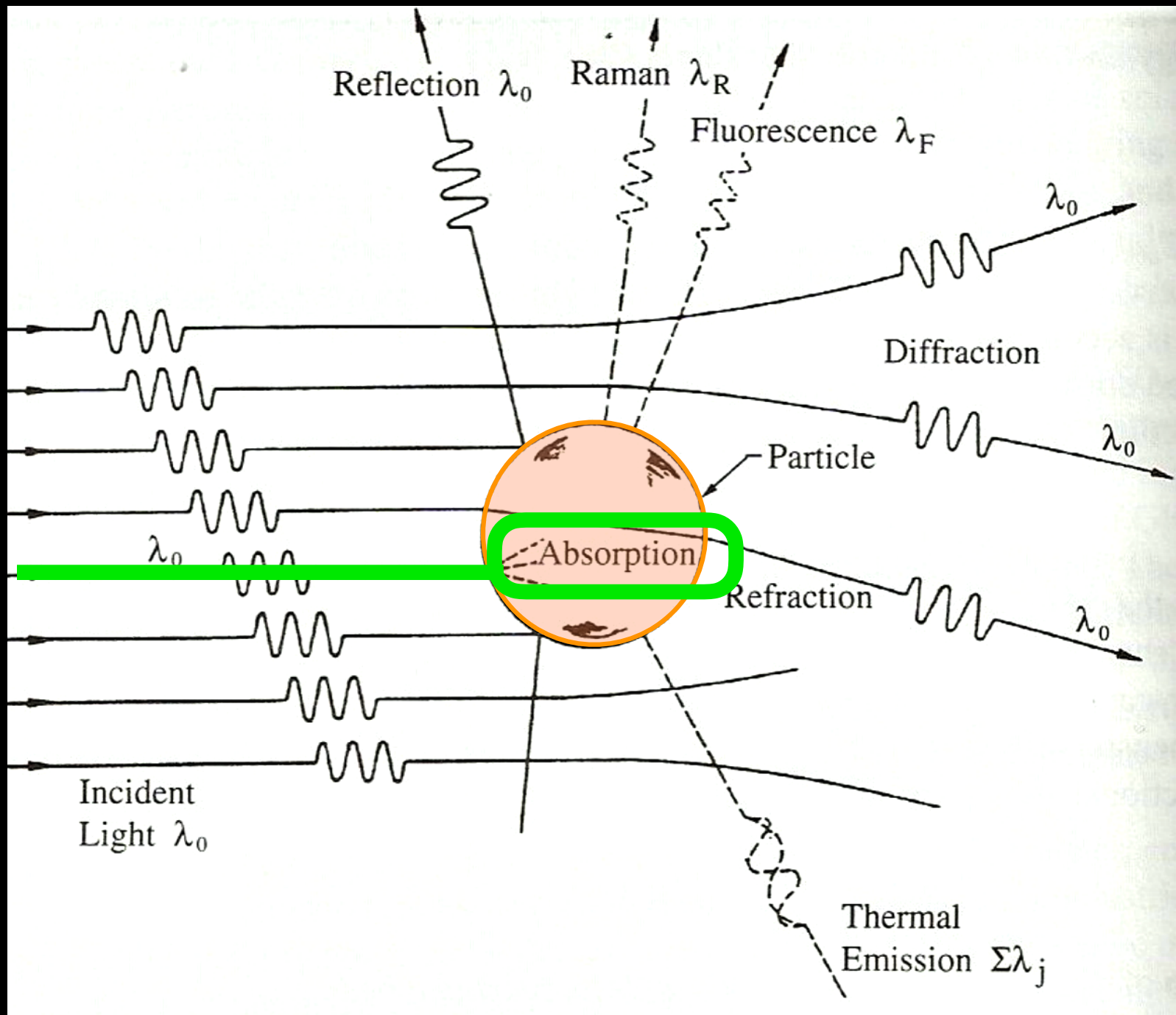
Secondary Roles for Dust

- Locks up metals with low condensation temperatures
- Catalyzes formation of molecules
- Can cause polarization

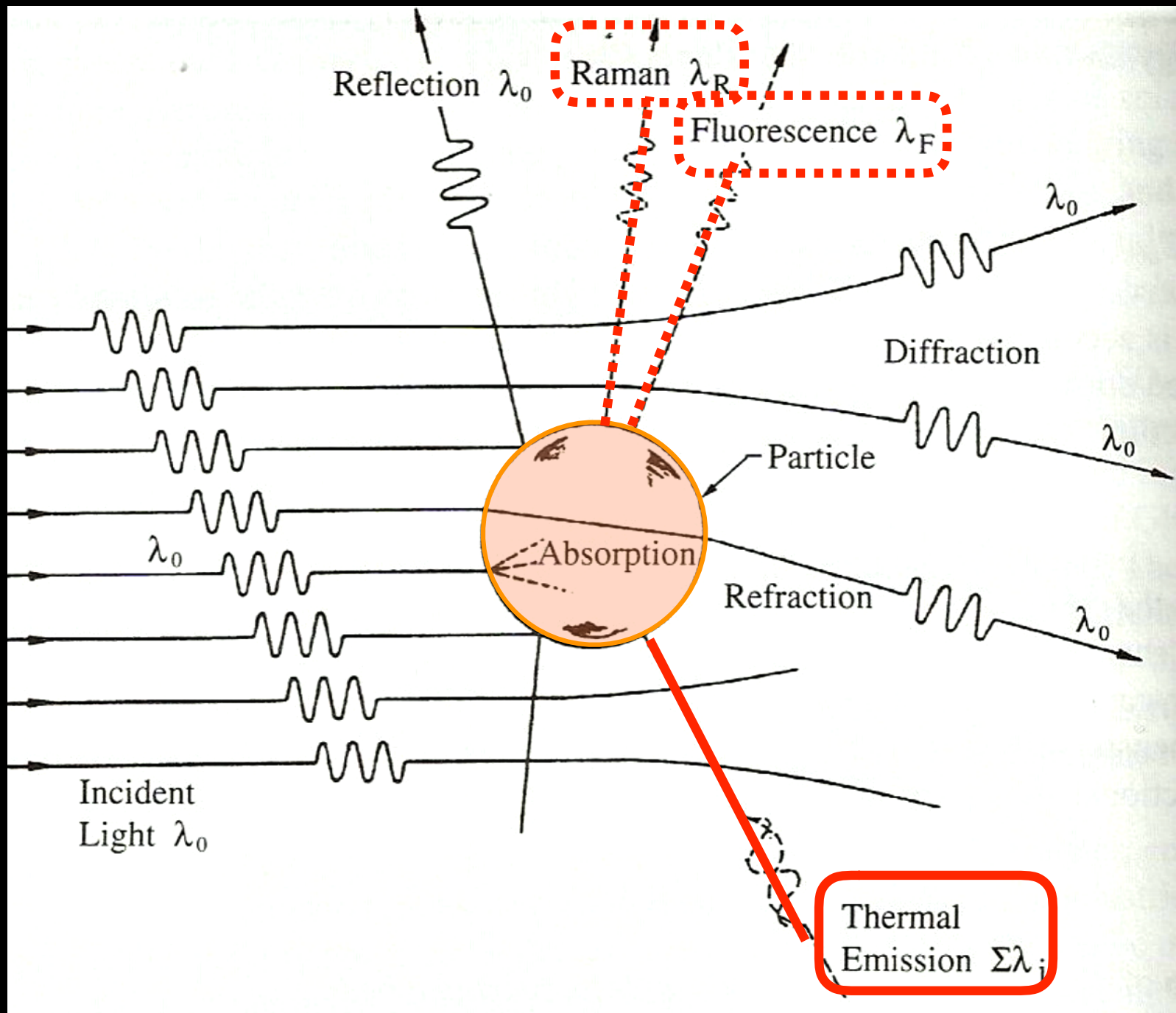
Many interactions between dust & light



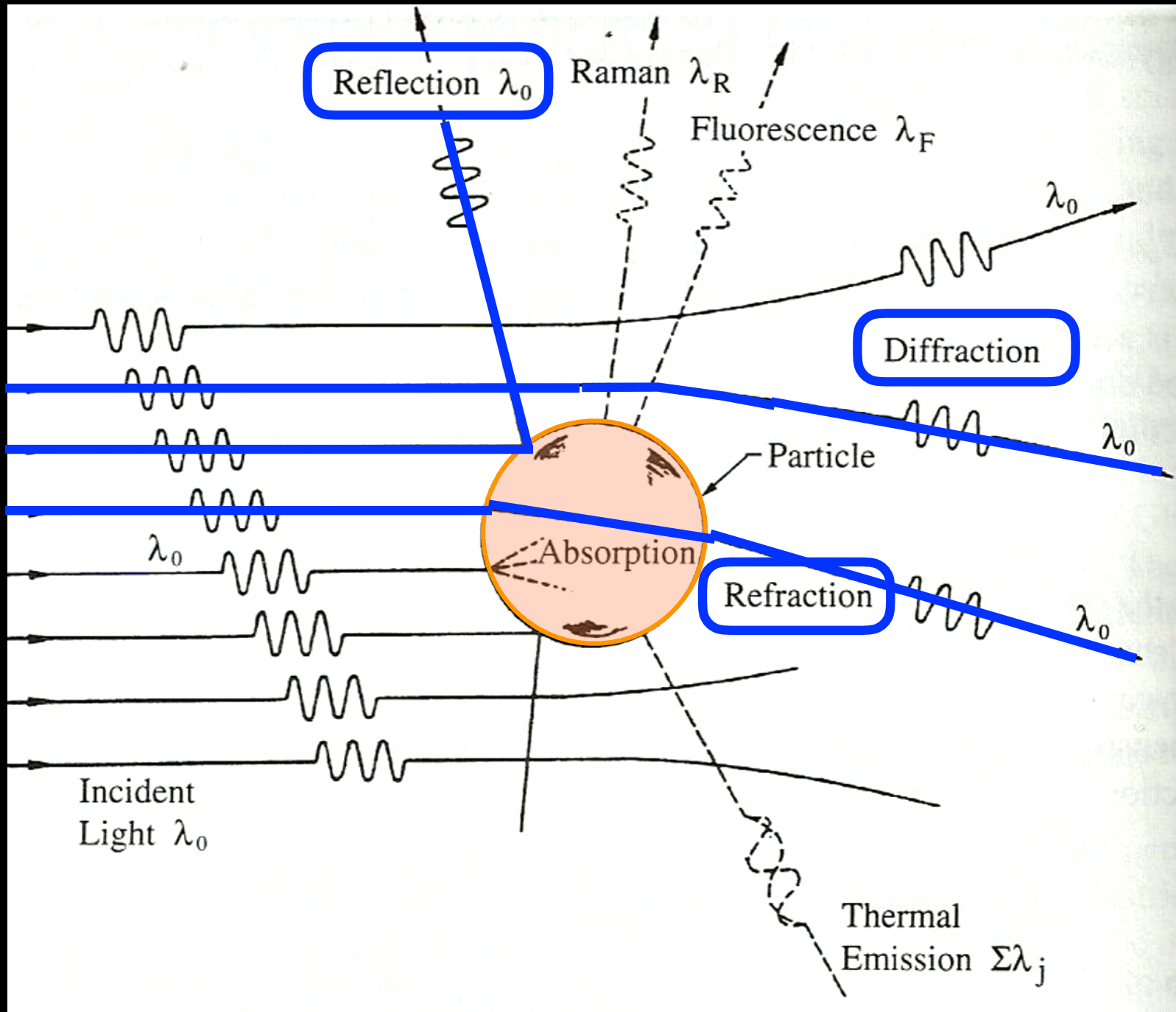
I. Absorption



2. Emission

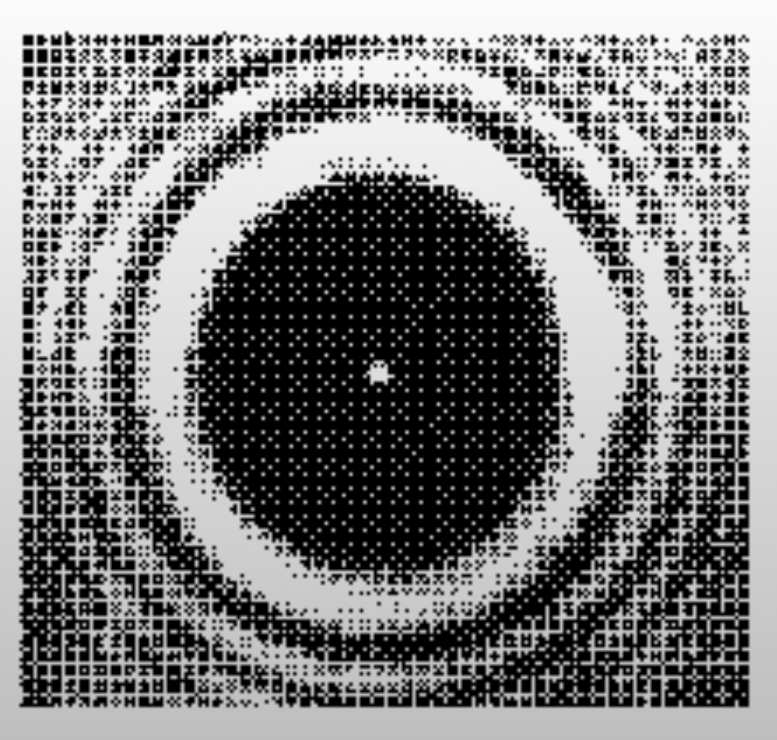


3. Scattering



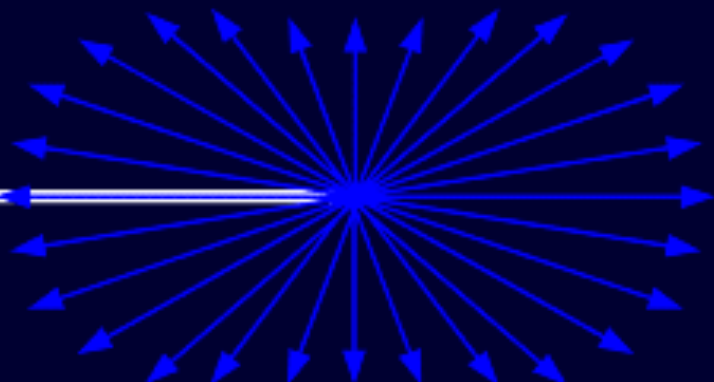
Some scattering is non-isotropic

Diffraction

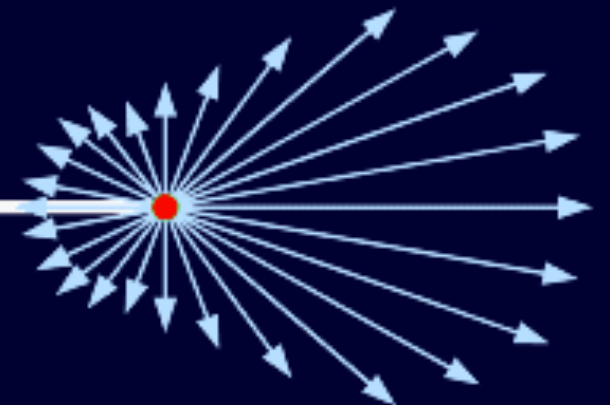


Typically leads to polarization

Rayleigh scattering



Mie Scattering,
small particle



Mie Scattering,
large particle

“forward scattering”



Modeled using Mie (1908) theory for scattering off of uniform spheres of some size. Recommended text is van der Hulst's "Light Scattering by Small Particles".

Behavior depends on dust composition, size a , and wavelength λ of light, characterized by:

- Grain Size:

dimensionless size parameter

$$x = 2\pi a / \lambda$$

- Composition:

complex refractive index

$$m_\lambda = n_\lambda + ik_\lambda$$

real part n_λ : *scattering*

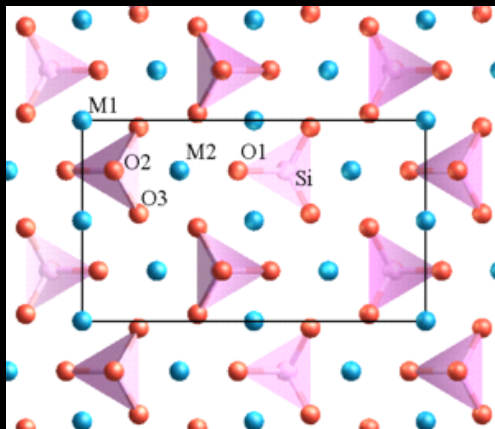
imaginary part k_λ : *absorption*

What is dust?

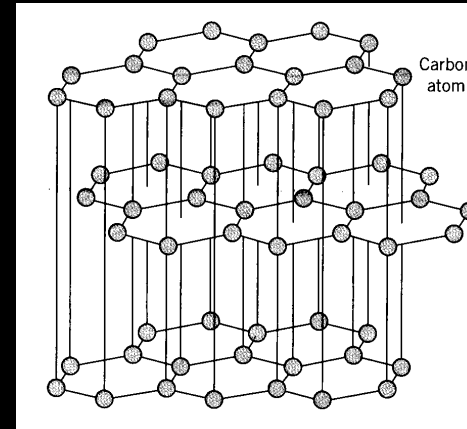
What is dust?

A complex and variable mixture of:

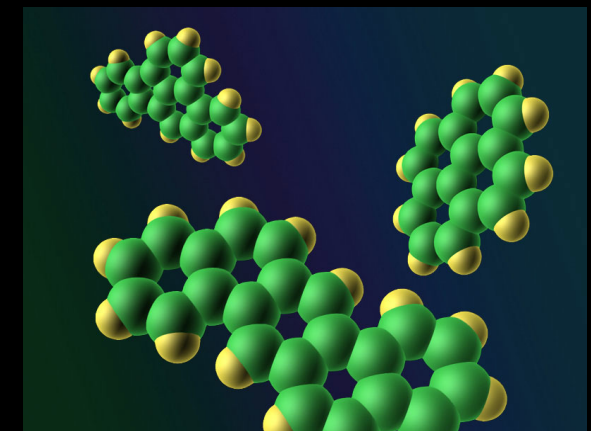
- Large grains ($\sim 0.1 \mu\text{m}$), made of silicates (SiO complexes bonded with Fe or Mg) and graphite.
- “Coal” (200-2000 Å in size)
- “PAH”s: Poly Aromatic Hydrocarbons (like benzene rings)
- “Very small grains” (VSG)



Silicates

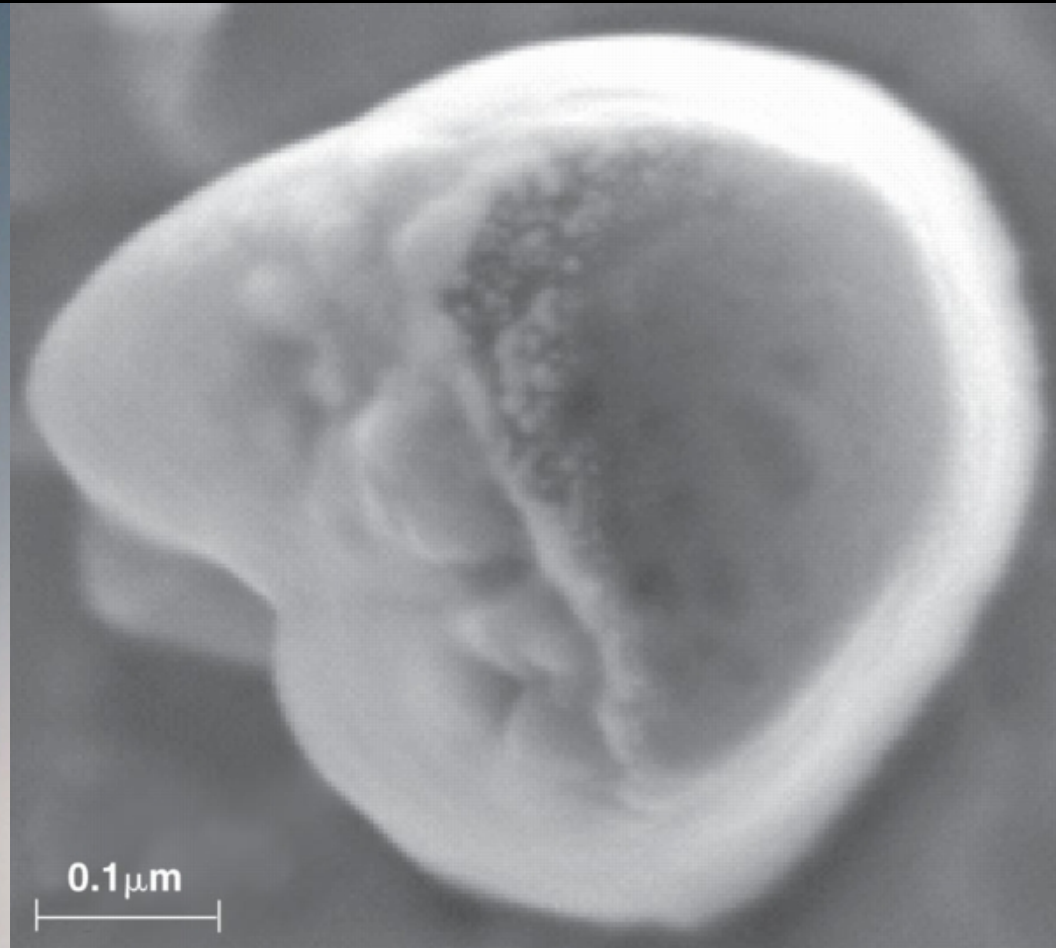
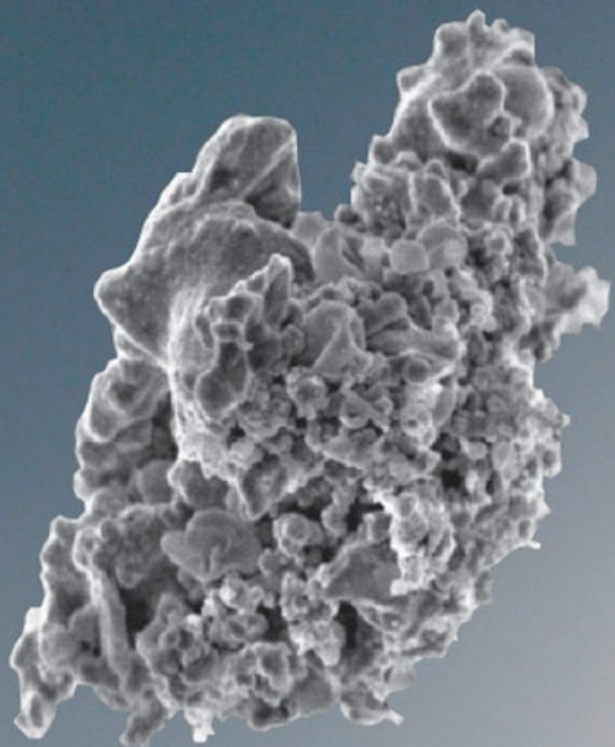


Graphite
Amorphous Carbon



PAHs

Cosmic Dust



J. Freitag and S. Messenger

The dust population evolves

Dust grains are probably created in:

- SN explosions
- Stellar winds (AGB stars in particular)

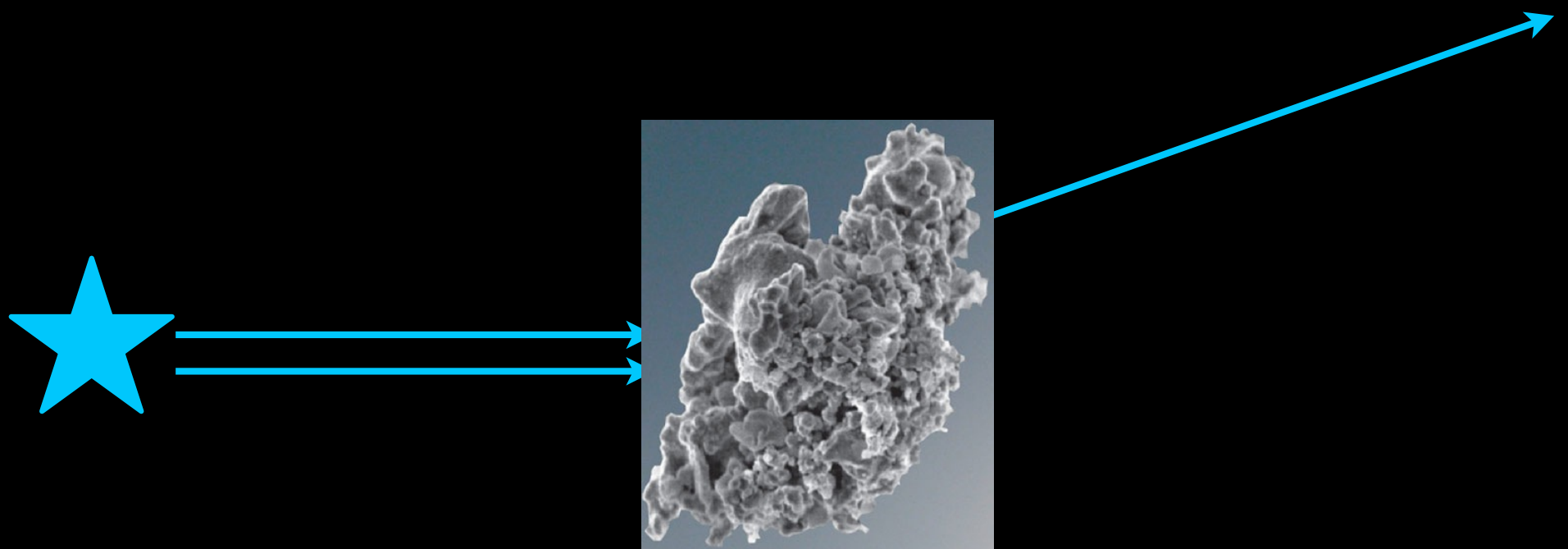
Dust grains are probably destroyed by:

- Shocks (SN explosions & fast stellar winds)
- Intense radiation

“Dust” refers to a complex population of different grains, with different sizes, that will likely change with environment

Dust alters the observed spectrum

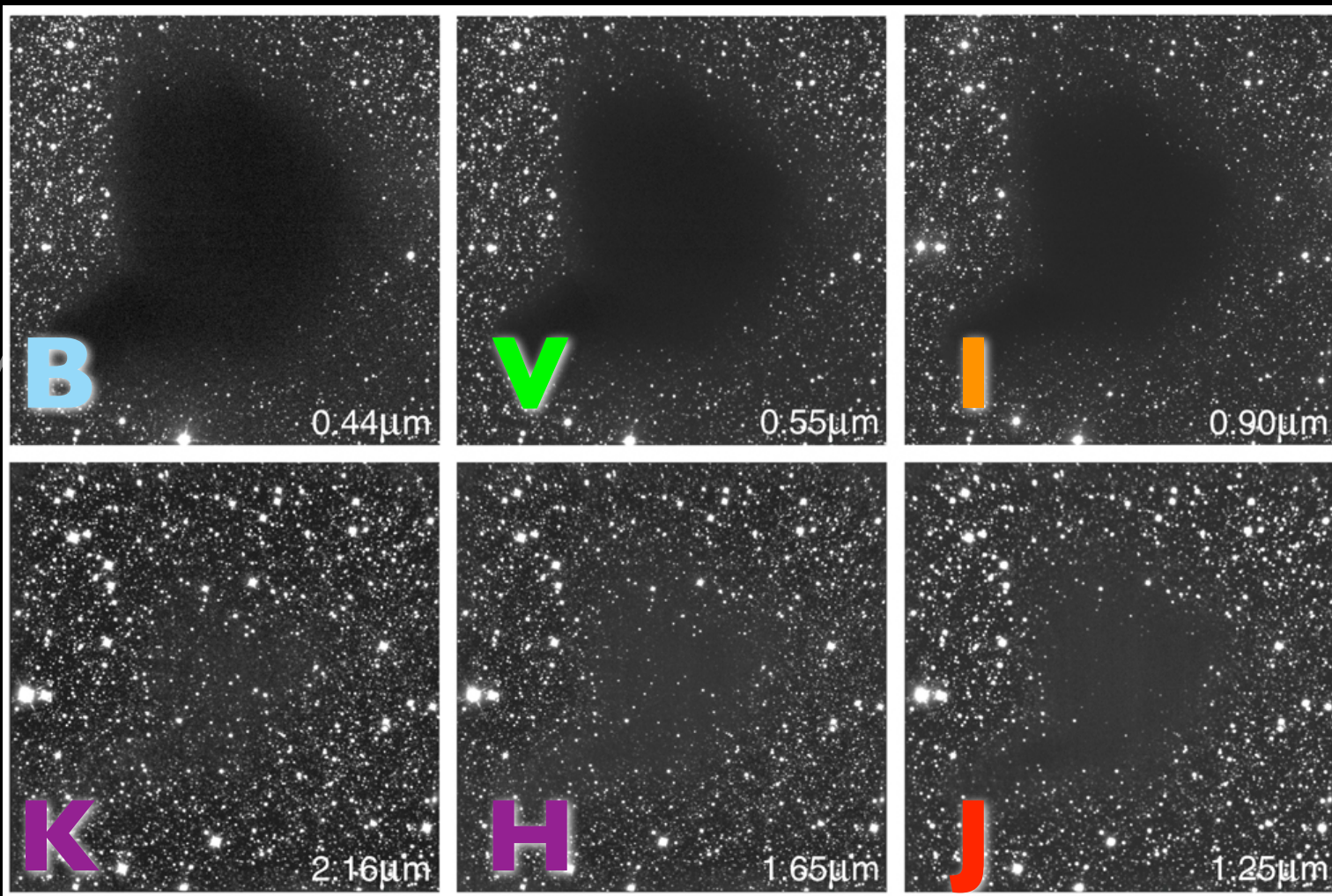
“Extinction”: The combined removal of light by both absorption & scattering



$$\tau_{\text{extinction}} = \tau_{\text{absorption}} + \tau_{\text{scattering}}$$

Dust extinction depends on wavelength

A_V is usually quoted, for historical reasons



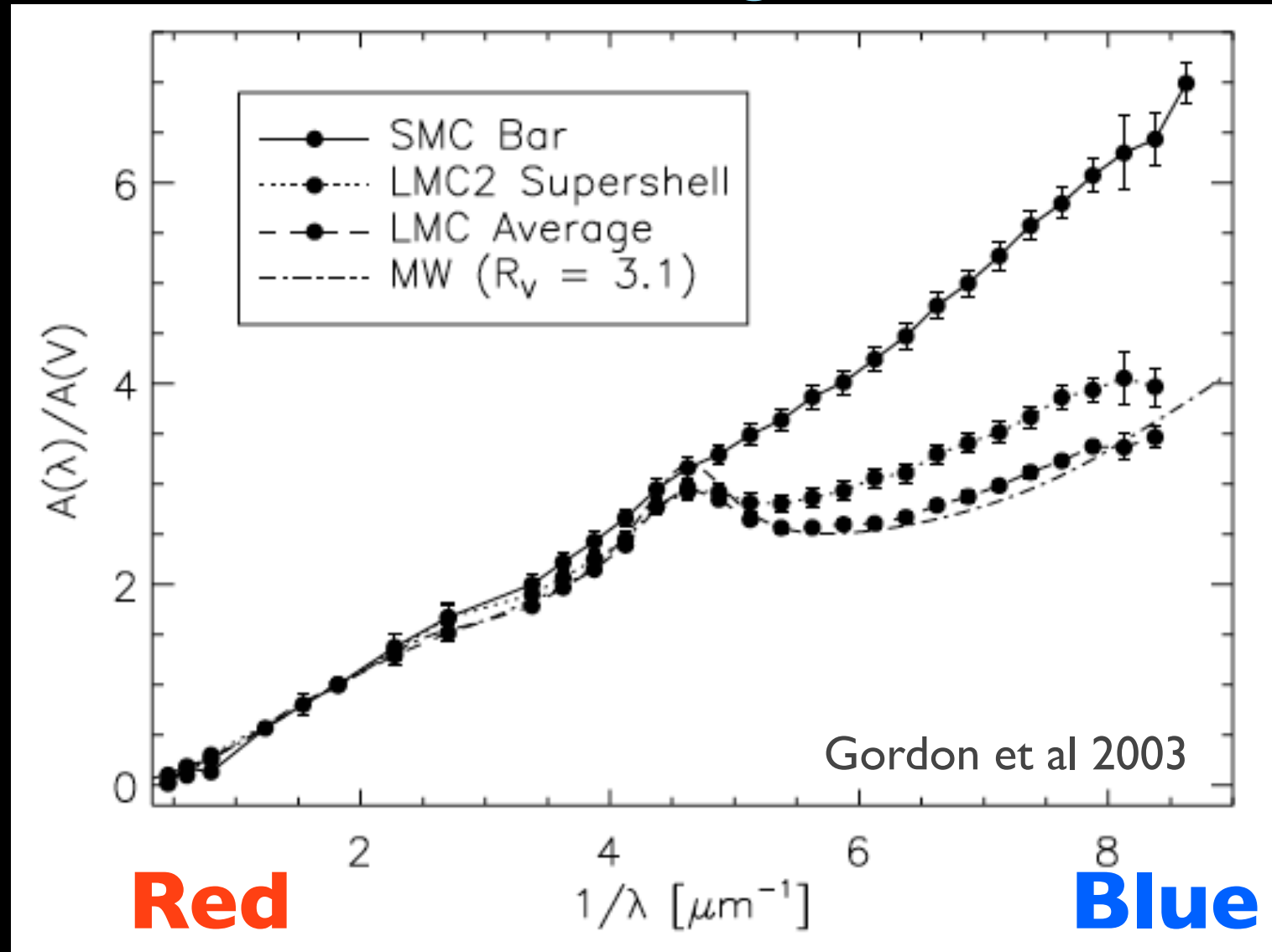
Excellent discussion in
Binney & Merrifield 3.7

Extinction is always tied to a bandpass X (typically V)

$$A_X = (m_{\text{observed}} - m_{\text{true}})_X$$

“Extinction Law”

Describes the *relative extinction* between wavelengths



Extinction: dramatically lower in the IR

INTERSTELLAR EXTINCTION LAW

λ	$E(\lambda - V)/E(B - V)$	A_λ/A_V	van de Hulst No. 15
<i>U</i>	1.64 ^a	1.531	1.555
<i>B</i>	1.00 ^b	1.324	1.329
<i>V</i>	0.0 ^b	1.000	1.000
<i>R</i>	-0.78 ^b	0.748	0.738
<i>I</i>	-1.60 ^b	0.482	0.469
<i>J</i>	-2.22 \pm 0.02	0.282	0.246
<i>H</i>	-2.55 \pm 0.03	0.175	0.155
<i>K</i>	-2.744 \pm 0.024	0.112	0.0885
<i>L</i>	-2.91 \pm 0.03	0.058	0.045
<i>M</i>	-3.02 \pm 0.03	0.023	0.033
<i>N</i>	-2.93	0.052	0.013
8.0 μm	-3.03	0.020 \pm 0.003	
8.5	-2.96	0.043 \pm 0.006	
9.0	-2.87	0.074 \pm 0.011	
9.5	-2.83	0.087 \pm 0.013	
10.0	-2.86	0.083 \pm 0.012	
10.5	-2.87	0.074 \pm 0.011	
11.0	-2.91	0.060 \pm 0.009	
11.5	-2.95	0.047 \pm 0.007	
12.0	-2.98	0.037 \pm 0.006	
12.5	-3.00	0.030 \pm 0.005	
13.0	-3.01	0.027 \pm 0.004	

^a From Nandy *et al.* 1976.

^b From Schultz and Wiemer 1975.

Rieke & Lebofsky 1985

If an object has $A_V = 1$

V band loses 1 mag:

$$f_{\text{observed}}/f_{\text{true}} = 0.4$$

U band loses 1.53

mag:

$$f_{\text{observed}}/f_{\text{true}} = 0.24$$

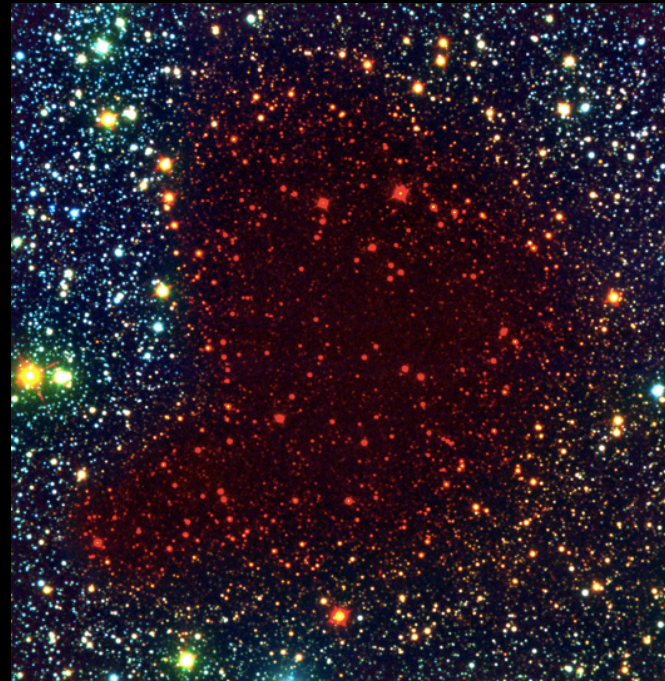
K band loses 0.11

mag:

$$f_{\text{observed}}/f_{\text{true}} = 0.9$$

Reddening (or “color excess”)

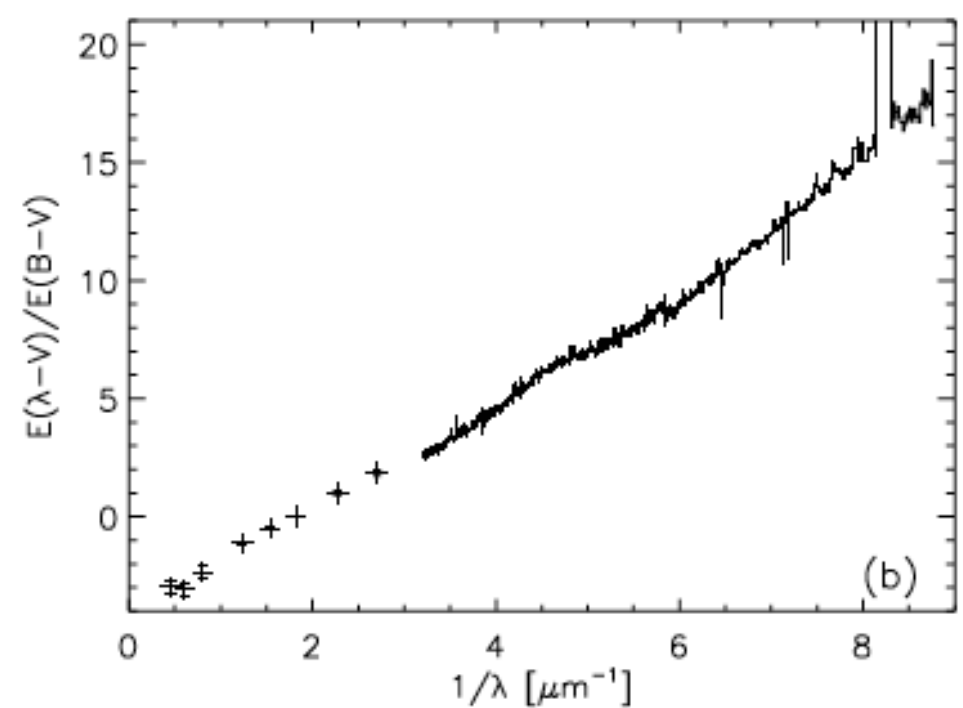
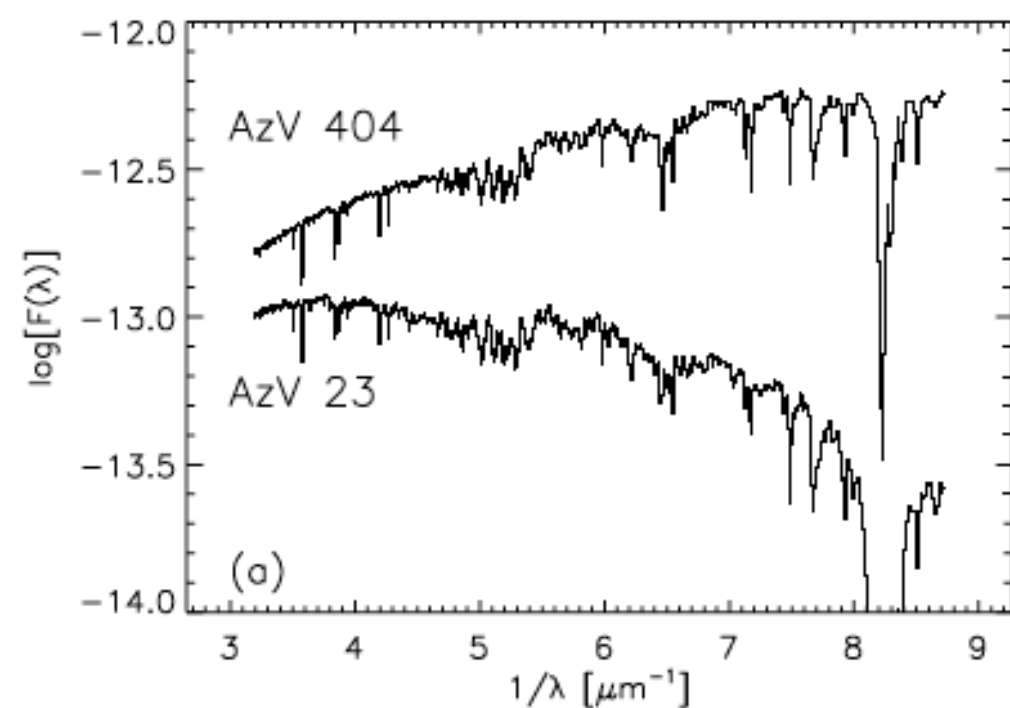
Color-dependent extinction leads to
“reddening”



$$\begin{aligned} E(X-Y) &= (m_X - m_Y)_{\text{observed}} - (m_X - m_Y)_{\text{true}} \\ &= (m_{\text{observed}} - m_{\text{true}})_X - (m_{\text{observed}} - m_{\text{true}})_Y \\ &= A_X - A_Y \end{aligned}$$

$E(B-V)$ is usually quoted, for historical reasons

Measuring the Attenuation Law



Use pairs of stars with identical spectral types
(i.e. identical absorption features)

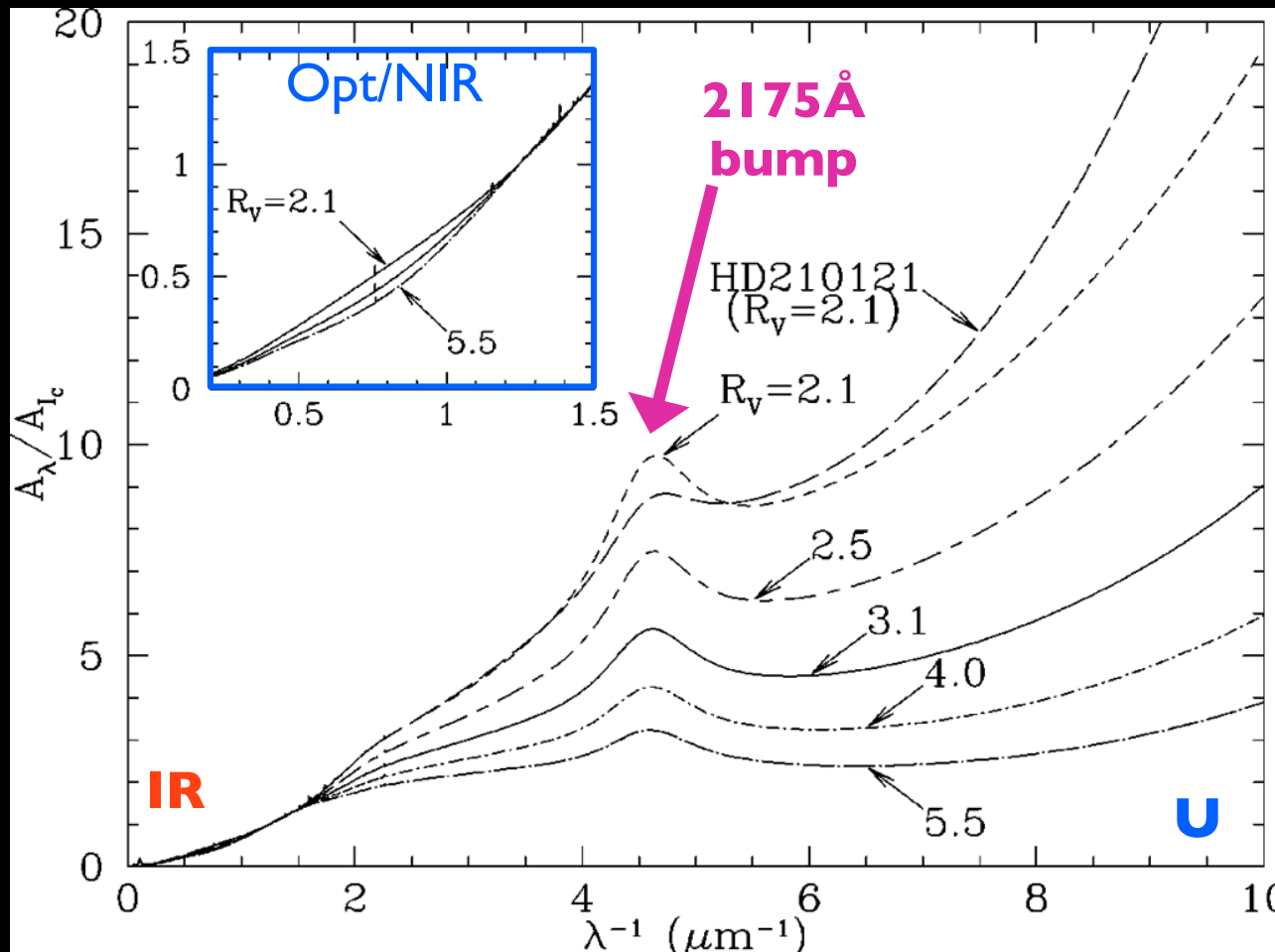
Attenuation laws characterized by R_V

$$R_V = A_V / (A_B - A_V) = A_V / E(B-V)$$

Related to the slope of the extinction curve near the V band

See
Draine 2003
ARA&A

Functional
forms found
in: Cardelli,
Clayton, &
Mathis
(CCM) 1989
Fitzpatrick
1999



Smaller R_V =
More
wavelength
dependence,
more
reddening for
a given
extinction A_V

Wide variation, but $R_V=3.1$ is “typical”

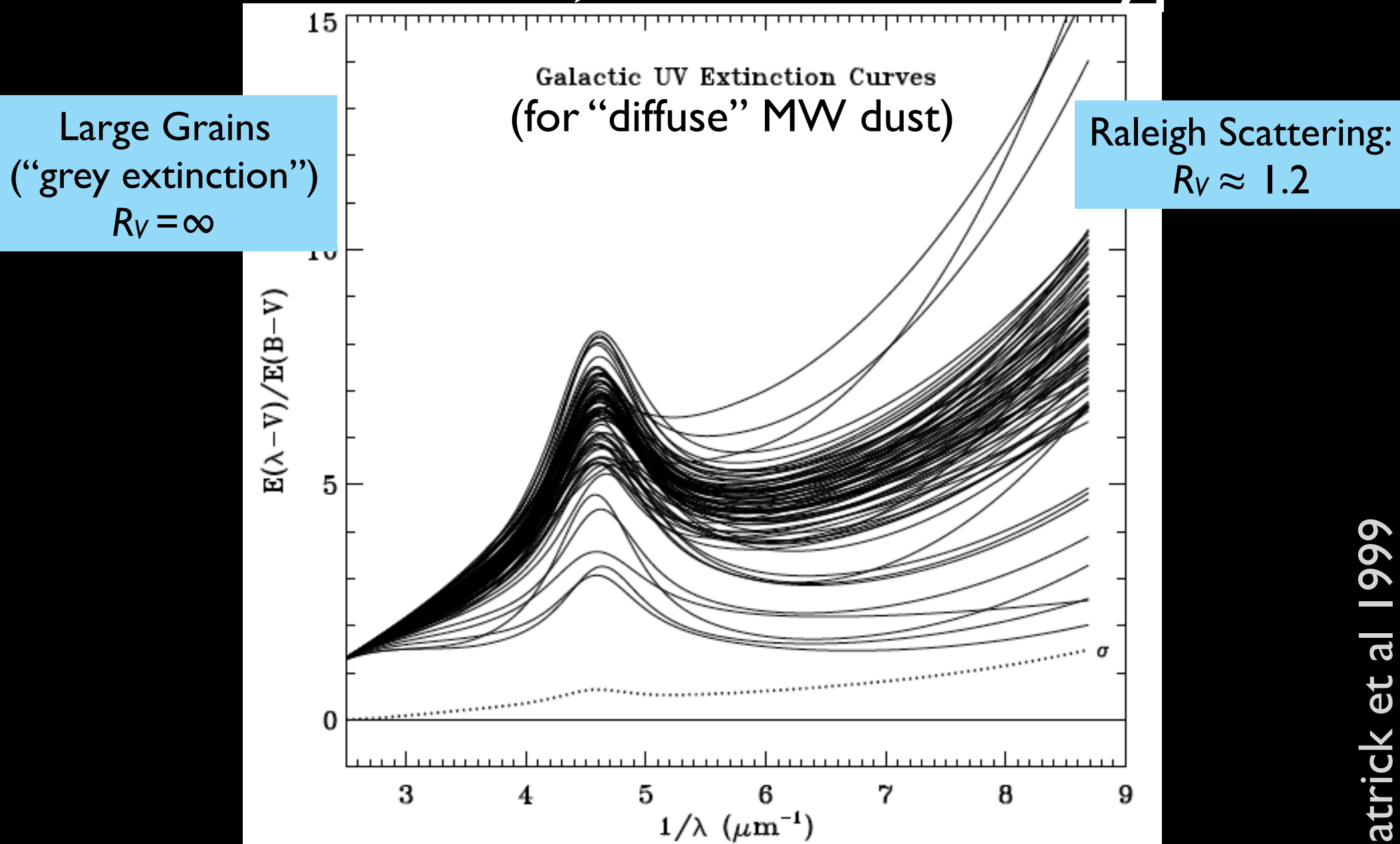
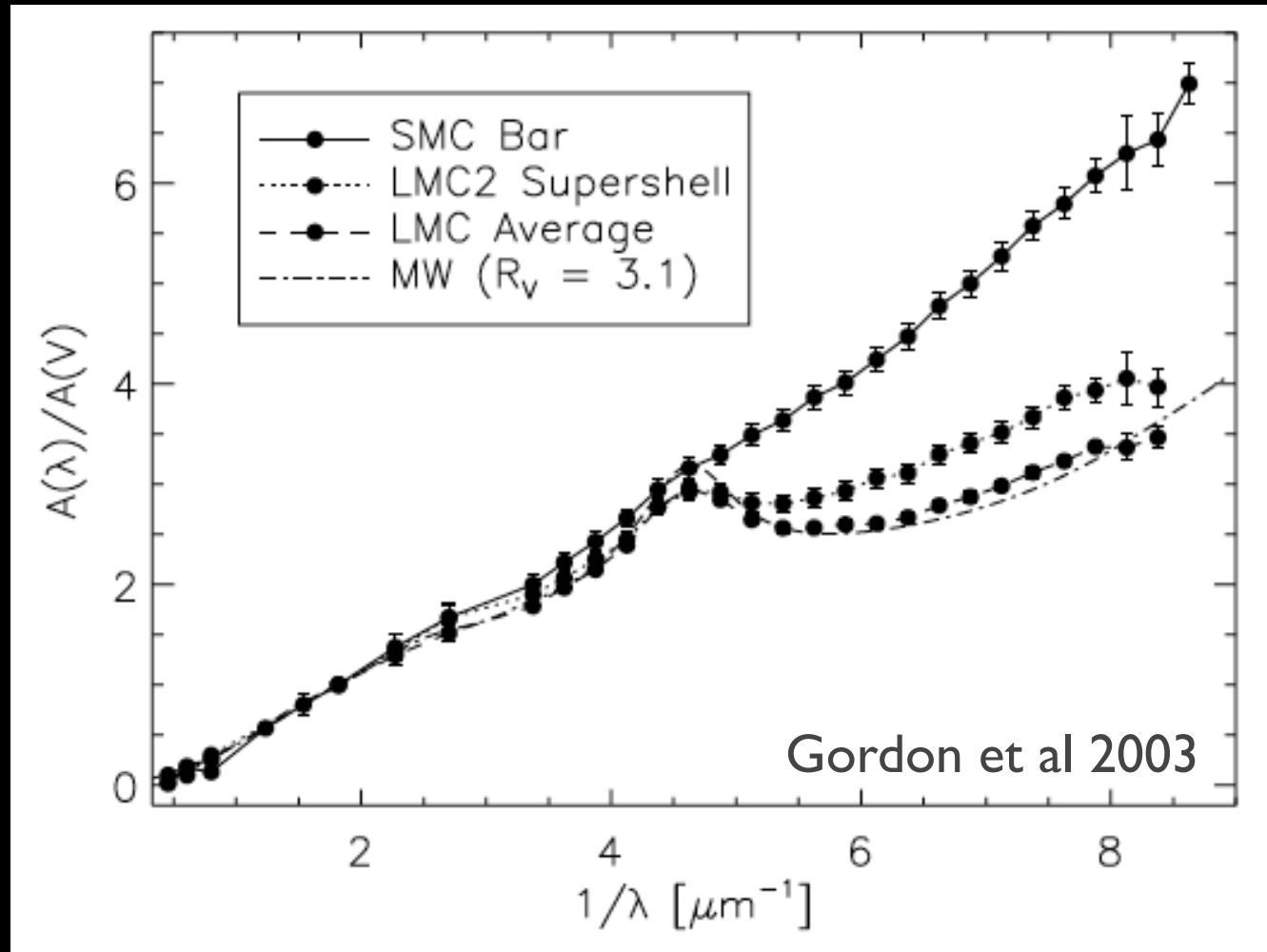


FIG. 2.— Examples of 80 Galactic UV extinction curves derived from *IUE* satellite observations. Analytical fits to the curves are shown, based on the work of Fitzpatrick & Massa 1990. The curves are taken from the Fitzpatrick & Massa catalog, with the addition of the lines-of-sight toward HD 210121 from Welty & Fowler 1992 and HD 62542 from Cardelli & Savage 1988. This figure demonstrates the enormous range of properties exhibited by UV extinction in the Milky Way. The dotted line, labeled “ σ ,” shows the standard deviation of the sample scaled to the value $\sigma(1500) = 0.74$, as derived from *ANS* satellite data (see §3.1).

Different galaxies have different mean extinction curves



Different average dust composition

Different types & sizes of grains produce different features

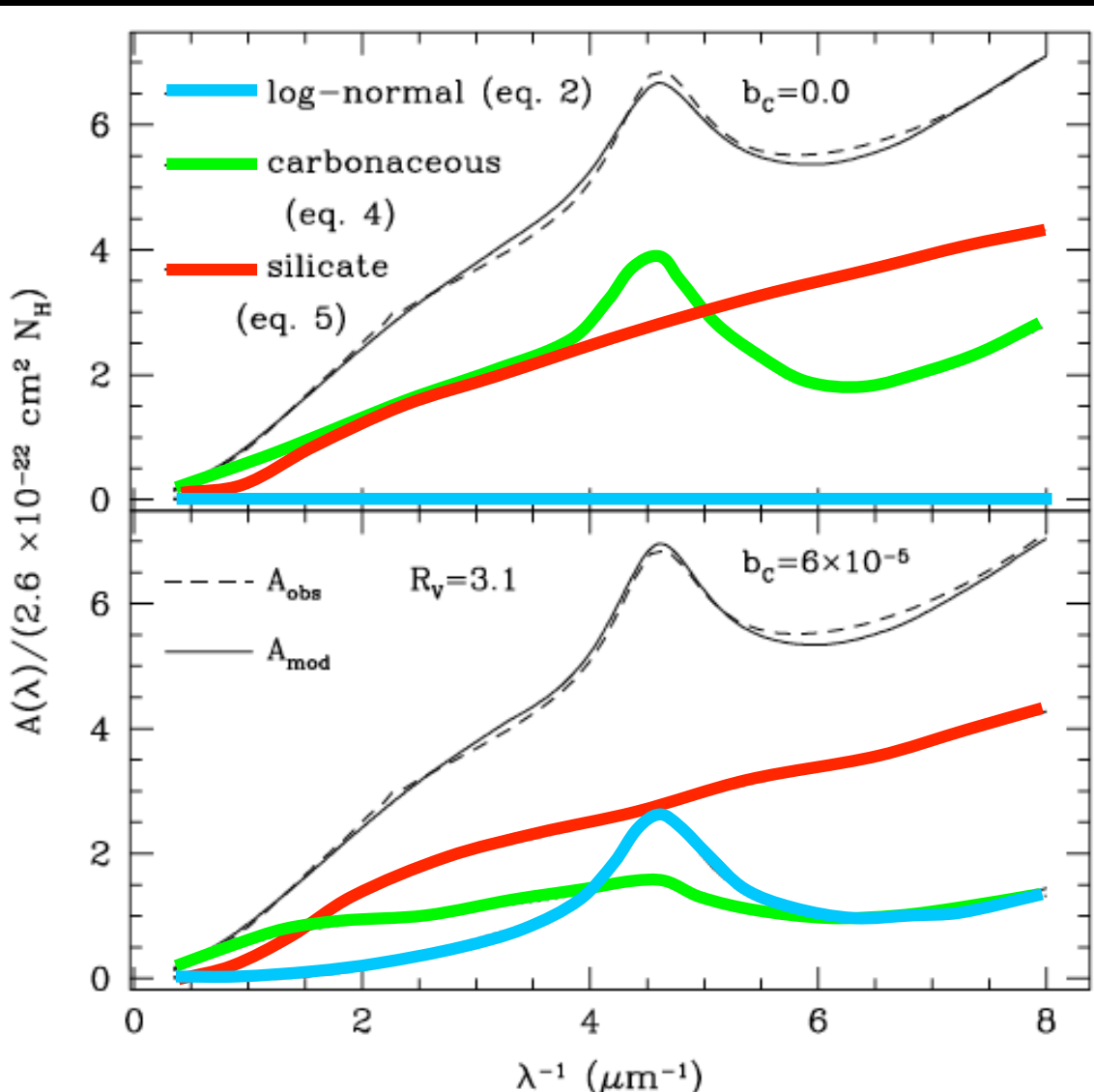
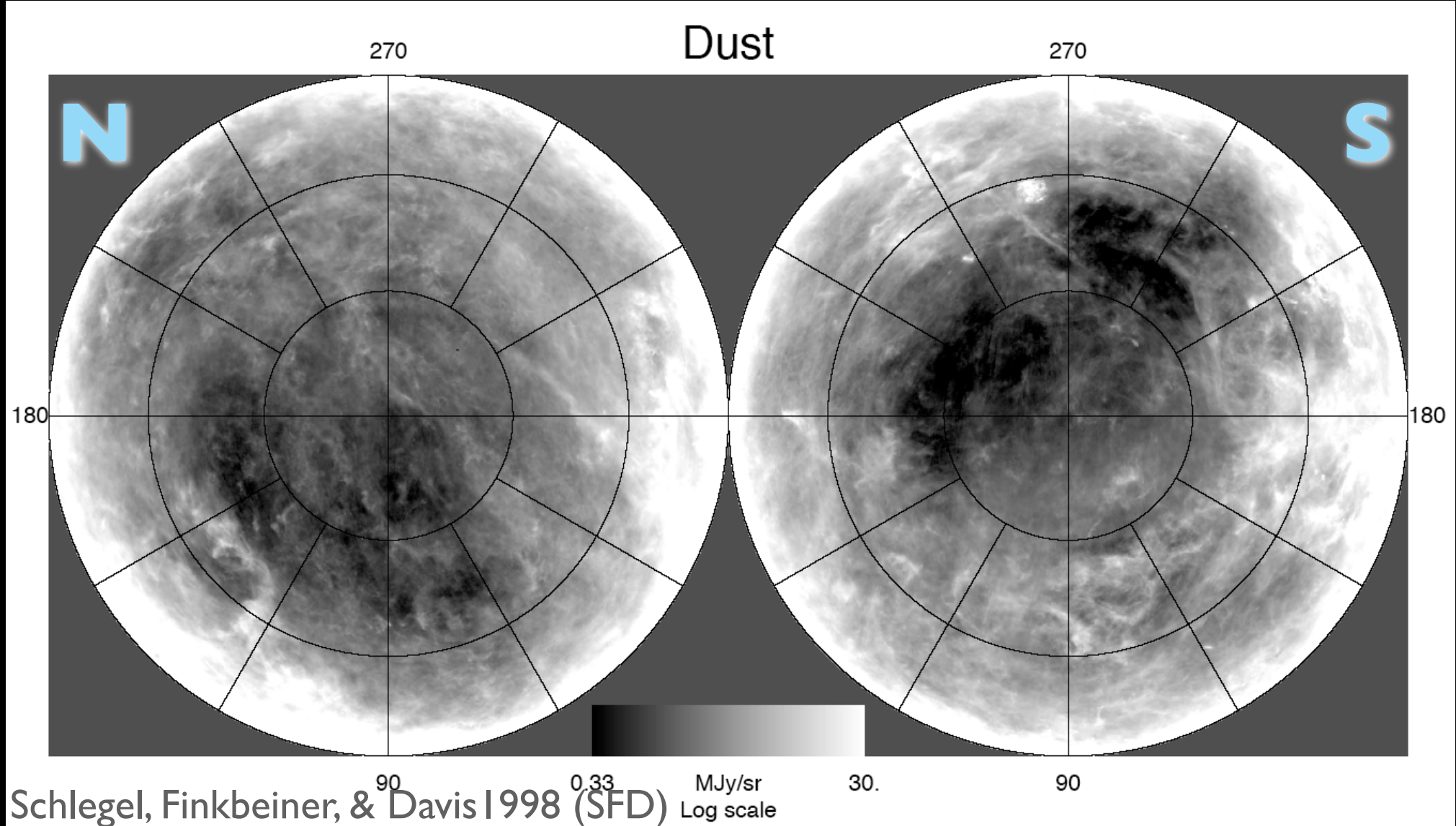


FIG. 8.—Extinction curve A_{mod} resulting from the grain distribution of eqs. (4) and (5), with parameters optimized to fit A_{obs} (see text) for $R_V = 3.1$ (also shown), for $b_c = 0.0$ and 6.0×10^{-5} . The contributions from the three grain distribution components are also shown.

silicates
PAHs + carbonaceous
very small grains
silicates
very small grains
PAHs + carbonaceous

All extragalactic observations need to
be corrected for dust in the Milky Way

Milky Way has no “dust free” sightlines



All extragalactic observations must correct for this

Note: See Schlafly & Finkbeiner 2011 for PS-I recalibrated maps

Dust server: <https://irsa.ipac.caltech.edu/applications/DUST/>

- Thermal Emission-based Maps:

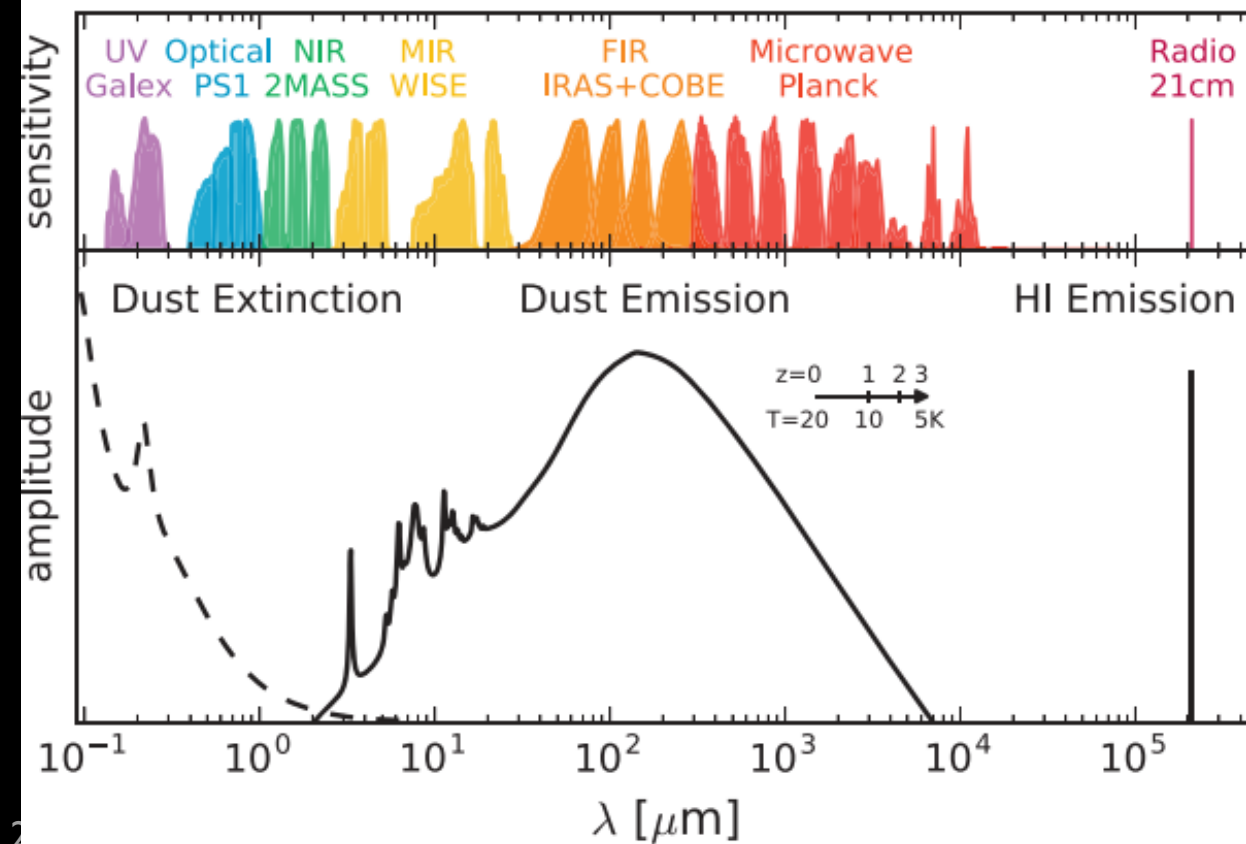


- Stellar Reddening Maps:



- HI-based Map:

Lenz Hensley Doré 17

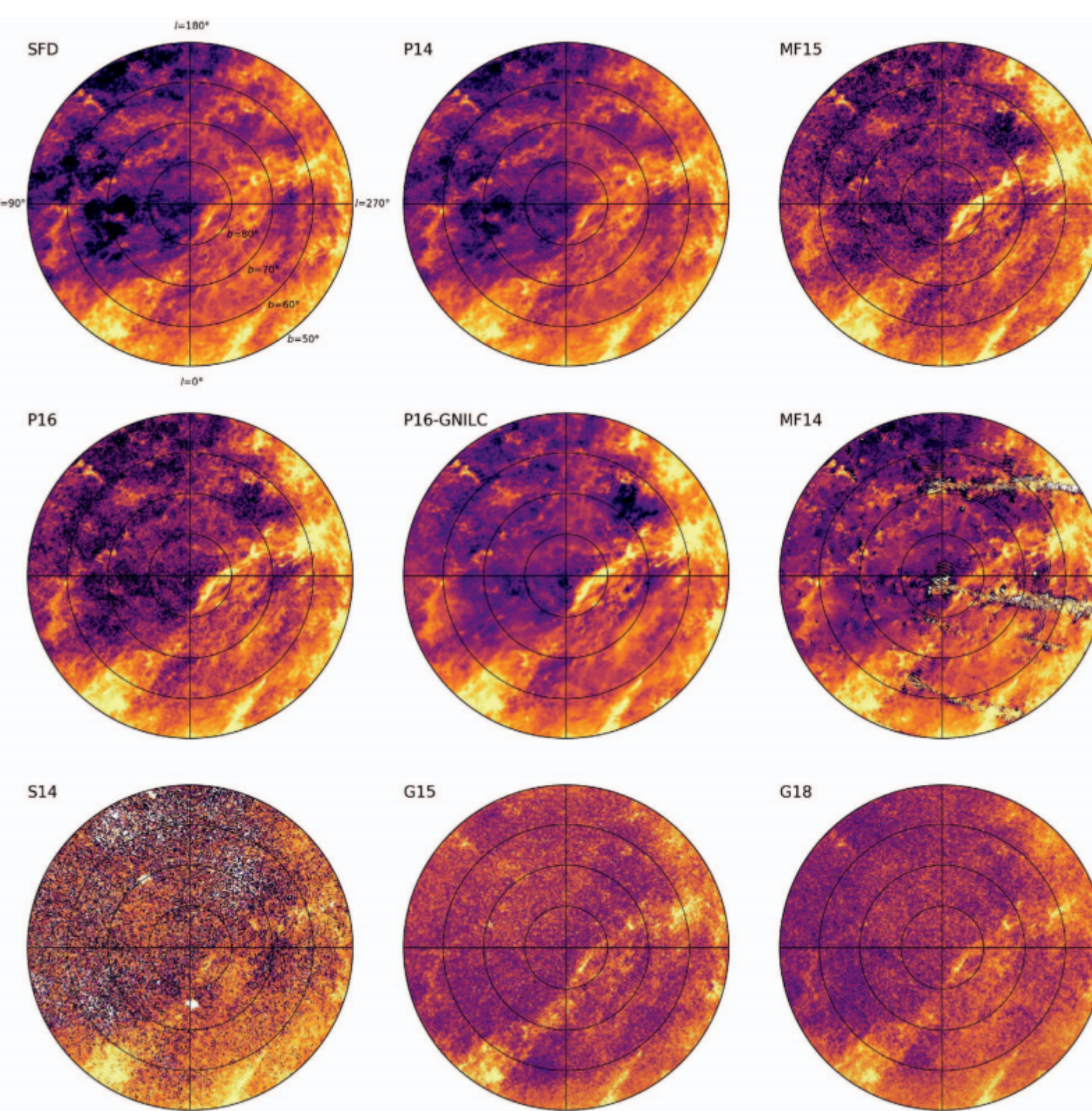


Modern maps of MW dust are derived in a variety of ways

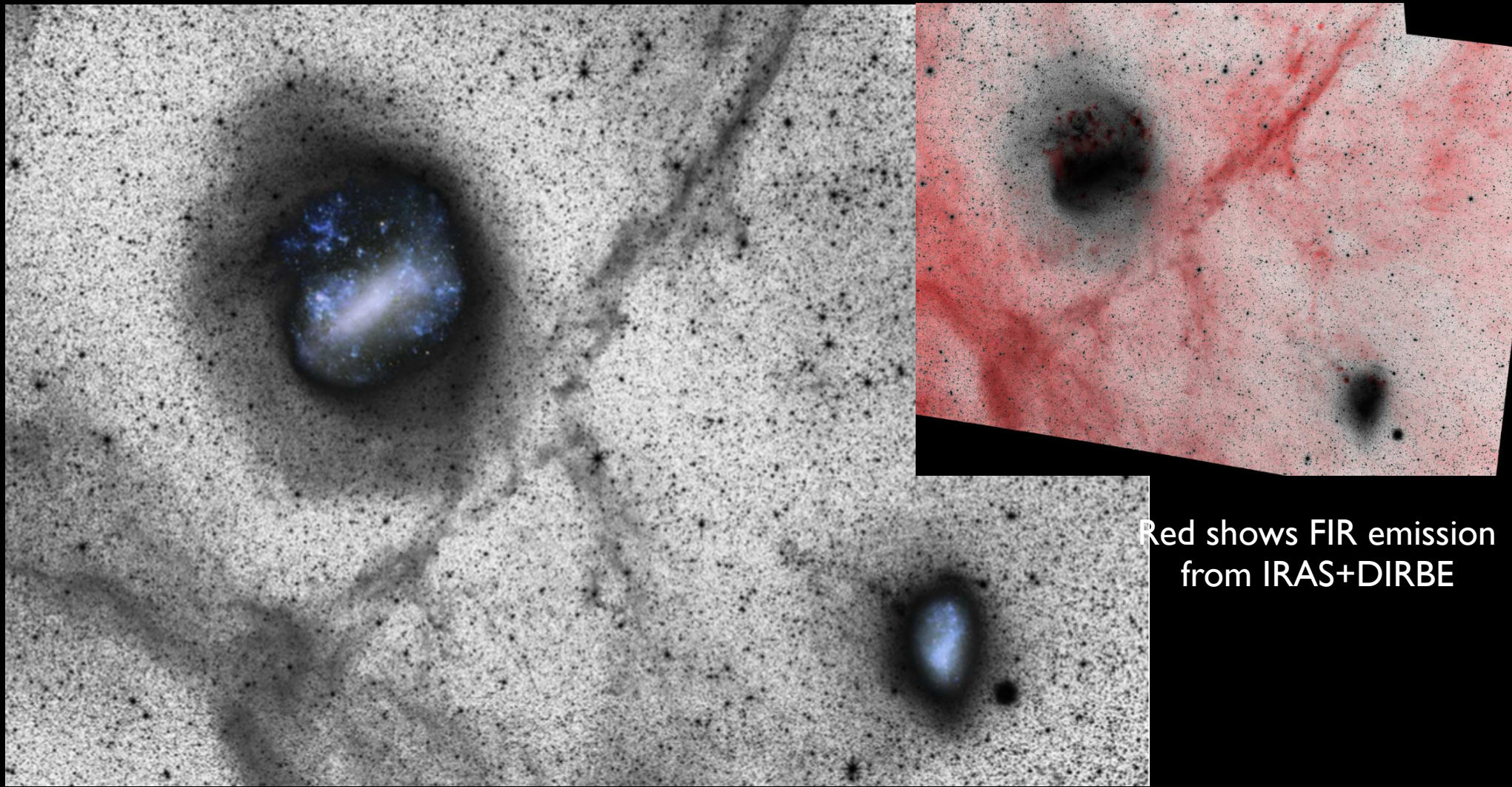
Note: Different methods will have different sources of contamination

E(B-V) maps of the north galactic cap

Chiang & Ménard 2019

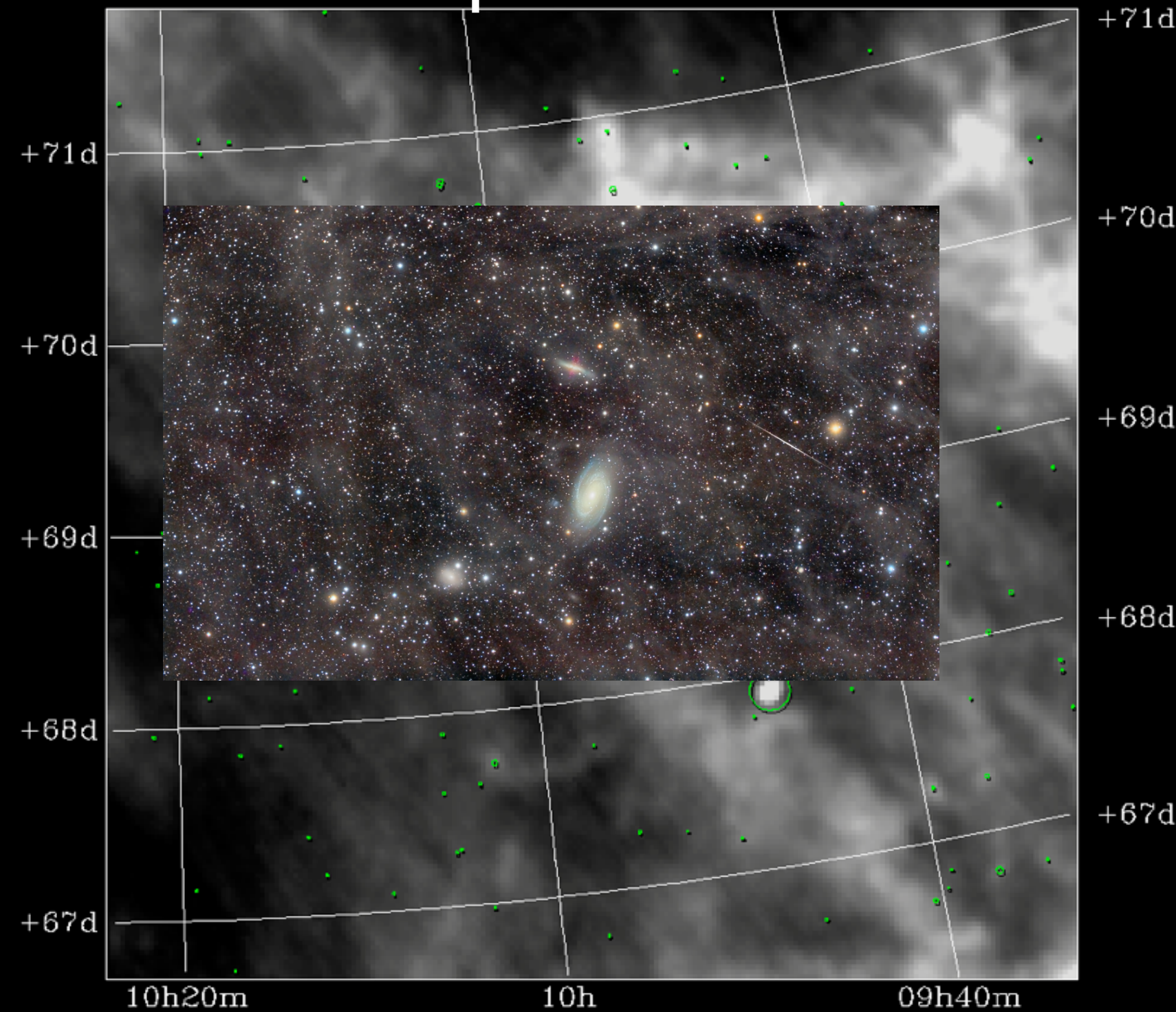


The dusty “high-latitude cirrus” emits at red optical wavelengths



- Probably due to photoluminescence of dust.
- Sometimes referred to as ERE “extended red emission”

Diffuse 100μm emission of M81 group



Dominant limitation on faint surface photometry



Dust Content & Behavior Questions

- What is the composition of individual dust grains & the associated scattering behavior?
- How is dust formed and destroyed?
- What drives the variations in dust properties with environment, as traced by the extinction law?
- How relevant is “Milky Way dust” or “LMC/SMC dust” to studies of distant galaxies?

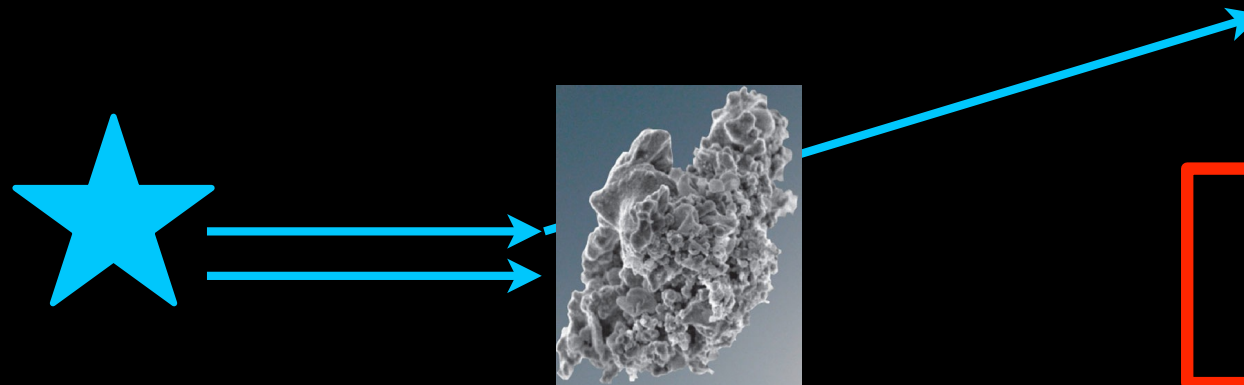
**Extragalactic observations often need
to be corrected for their own dust**

(if you want to know the true luminosity &
color of the underlying stellar populations)

“*Internal Extinction Corrections*”
are fundamentally complicated

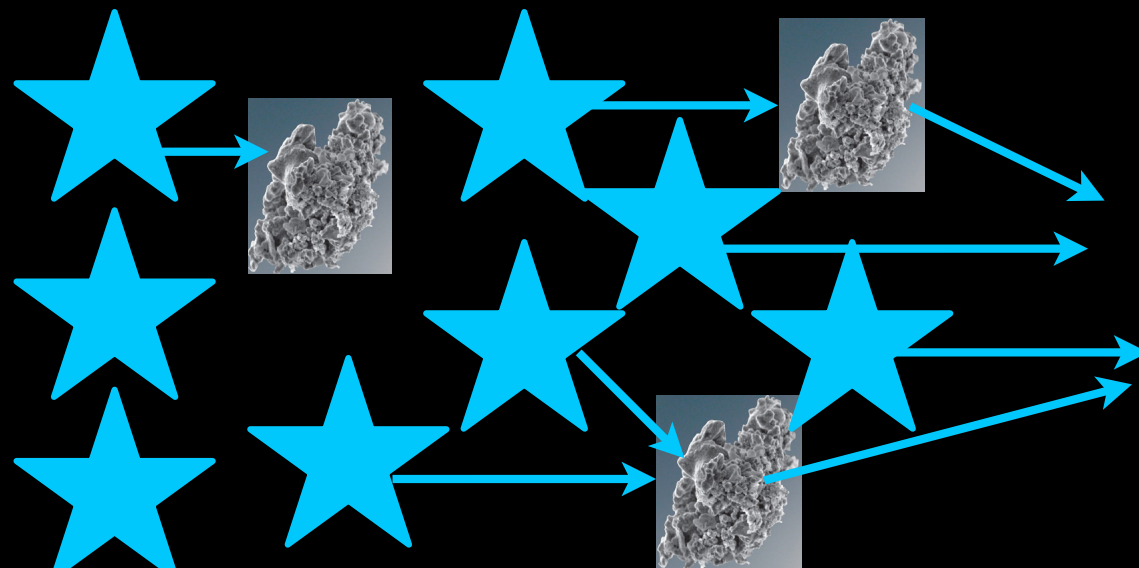
Depends on dust+star geometry

“Attenuation”, not Extinction



“Extinction” is loss
from a single star

Depends only on dust properties



“Attenuation” is net
effect of mix of
dust+stars,
absorption, &
scattering in and out
of the line of sight

*Depends on dust properties and
star+dust geometry*

“Inclination Corrections”

- Brings all galaxy magnitudes to those expected if the galaxy were seen face-on.
- Depends on inclination, wavelength, and galaxy luminosity/type
- Usually a “statistical” correction (i.e., based on average properties of similar galaxies)

Edge-On Galaxy NGC 4013



“Internal Attenuation Corrections”

- Corrects for dust along the line of sight *within* the galaxy
- Not statistical — based on estimates of attenuation for each individual galaxy.

Three common methods

- Modeling the entire spectrum or SED
- “Balmer Decrement”
- UV Slope

Internal attenuation #1: Estimate correction from “Balmer Decrement”

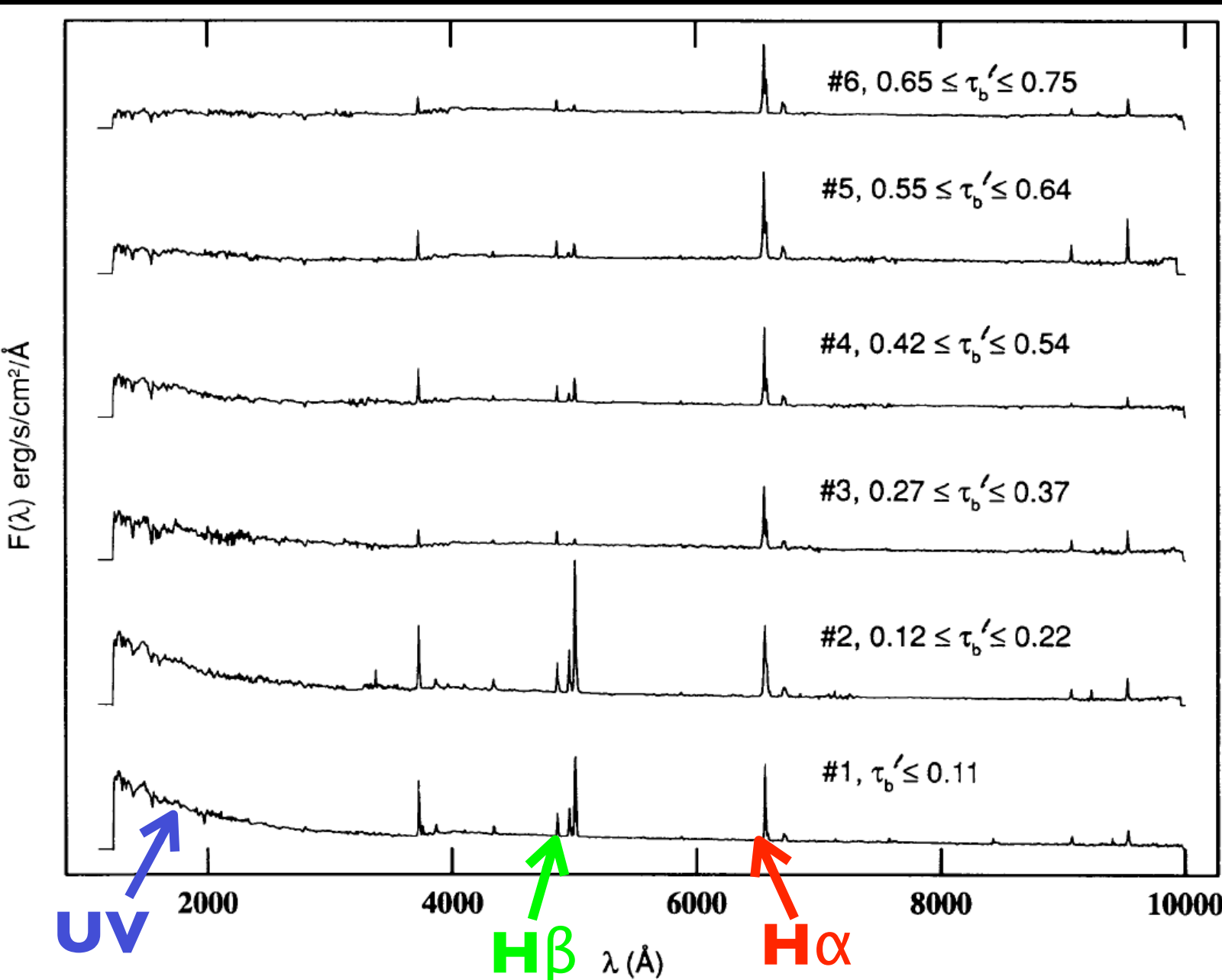
The value of the Balmer extinction is derived from the observed ratio of H α and H β line intensities using the relation

$$C(\text{H}\beta) = \frac{1}{f(\text{H}\beta) - f(\text{H}\alpha)} \log \frac{I(\text{H}\alpha)/I(\text{H}\beta)}{I^0(\text{H}\alpha)/I^0(\text{H}\beta)} \quad (1)$$

where $I^0(\text{H}\alpha)/I^0(\text{H}\beta)$ is the intrinsic intensity ratio of these two lines and $f(\text{H}\beta) - f(\text{H}\alpha)$ is equal to 0.335. The value

- In “case B” recombination, H α and H β are always emitted in the same ratio.
- H β is emitted at a **shorter** wavelength, and will thus suffer more attenuation than H α .
- The observed ratio of H α /H β **increases** with attenuation

Average galaxy templates, binned by attenuation



Decreasing
reddening



Note
simultaneous
change in
UV slope!

FIG. 17.—The spectra of the six templates are shown for increasing values of the extinction parameter τ_b^l , from the bottom to the top of the figure.

Internal attenuation #2: Estimate correction from the slope β of the UV spectrum

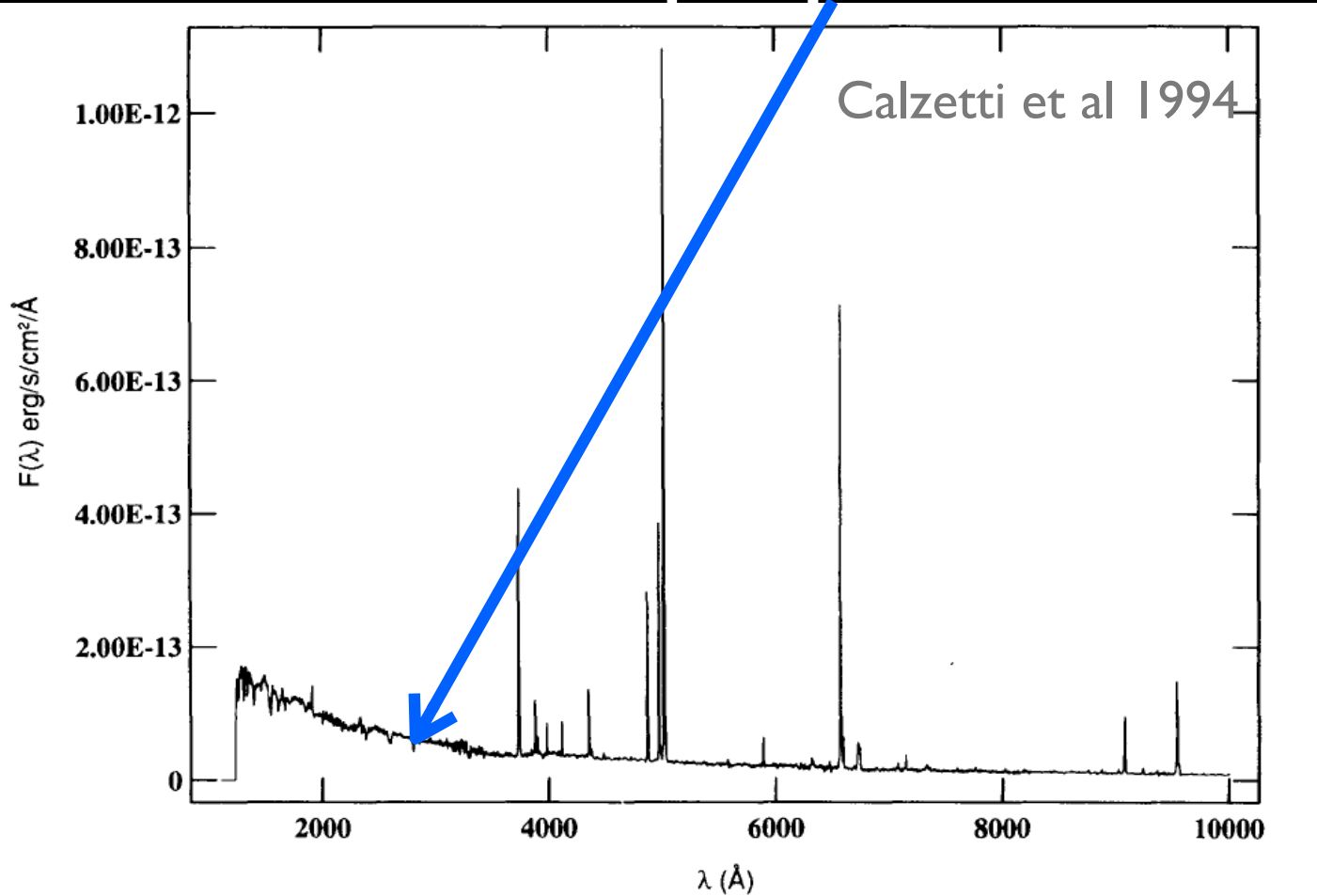


FIG. 2.—An example of UV and optical spectrum with *no normalization between the two wavelength ranges*. The galaxy is NGC 5253. The flux in $\text{ergs cm}^{-2} \text{ s}^{-1} \text{\AA}^{-1}$ is plotted as a function of the wavelength λ in the range 1220–10000 Å. The joining point between the UV and optical is at 3200 Å.

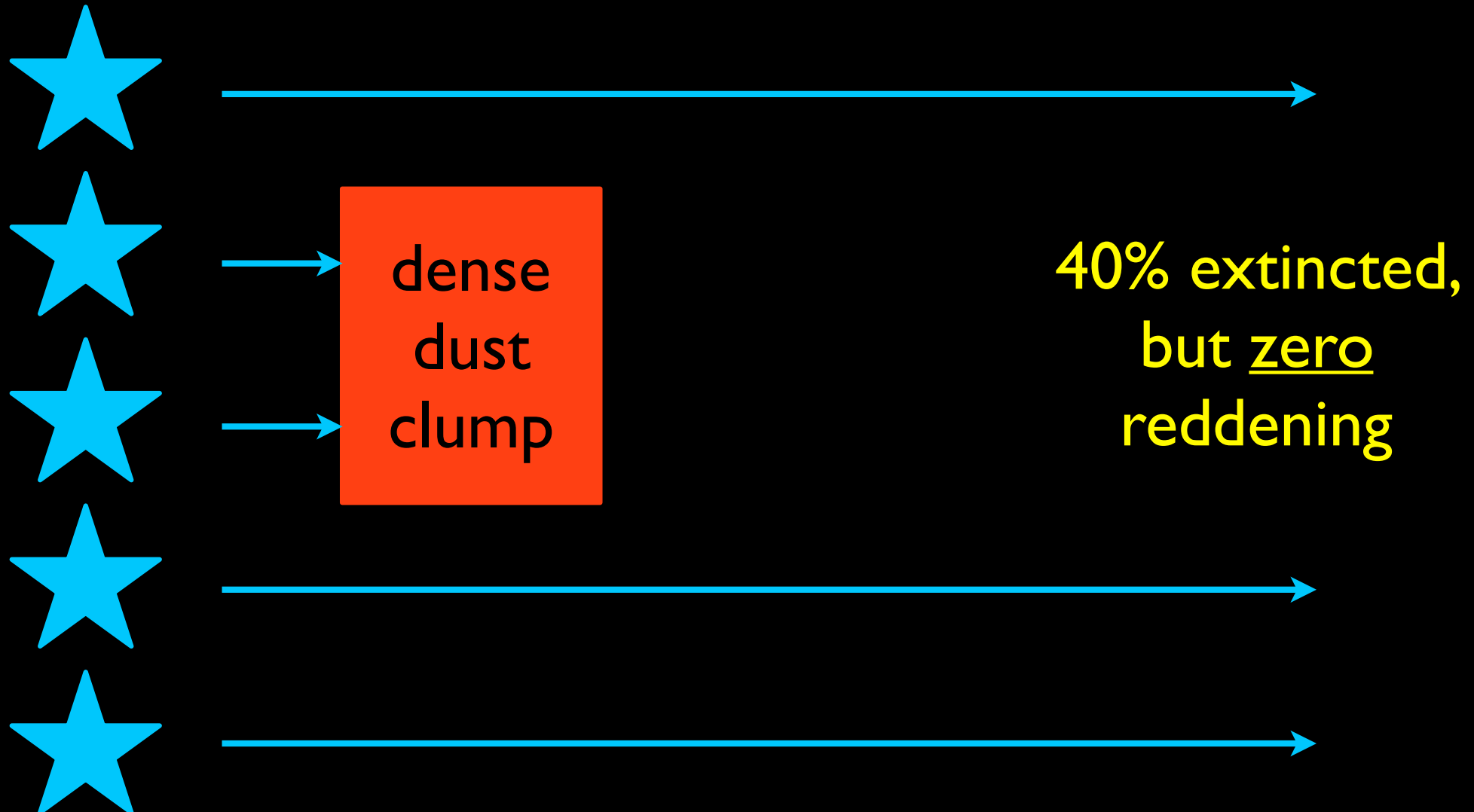
Most star bursts have a reasonably constant power-law slope at UV wavelengths (tail of O/B star blackbody).

If redder, then probably due to dust

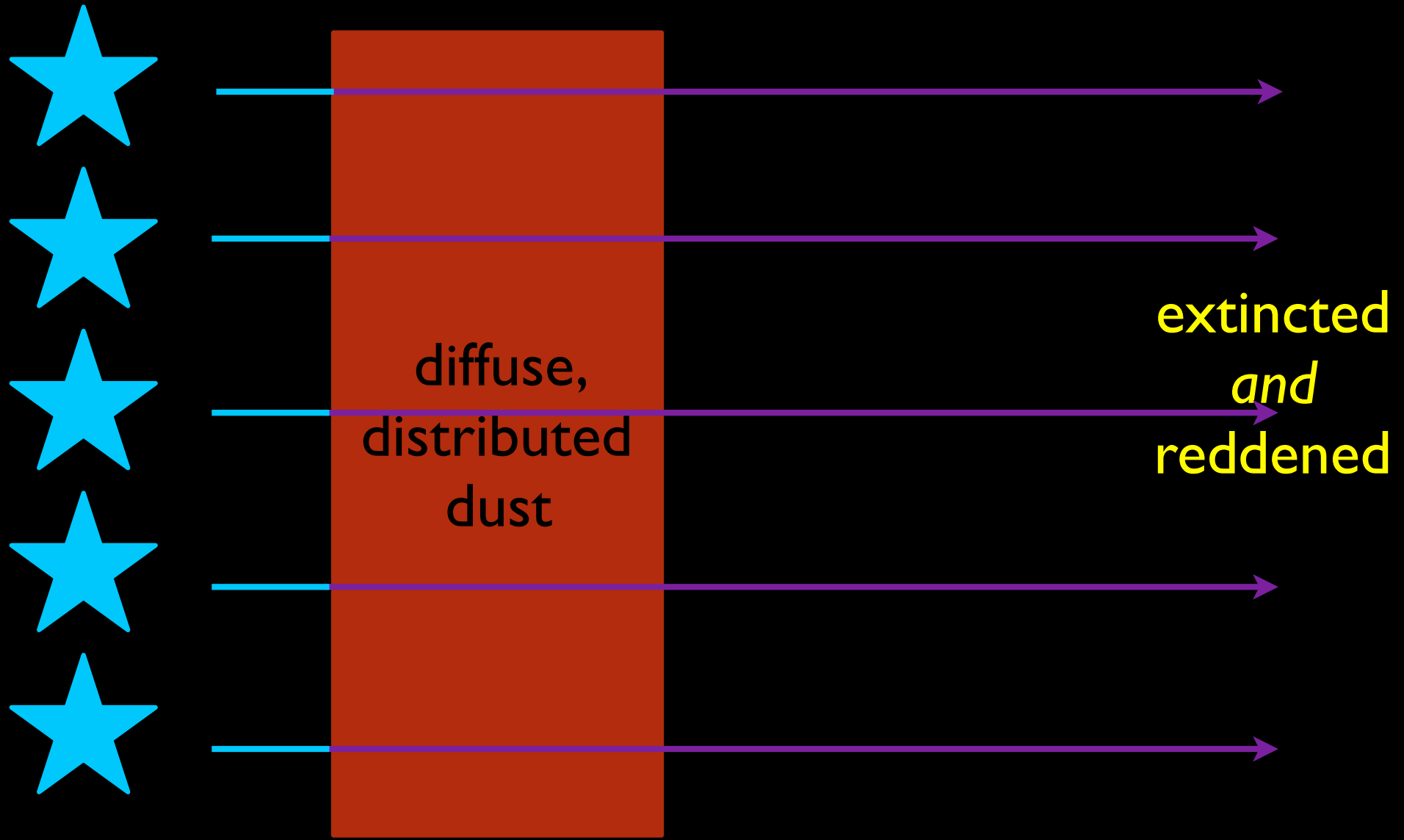
Warning: Reddening (observed Balmer decrement &/or UV slope) \neq **Total extinction**

Problem #1: Varying the relative distributions and clumpiness of the dust and the stars can produce arbitrary relations between reddening & extinction

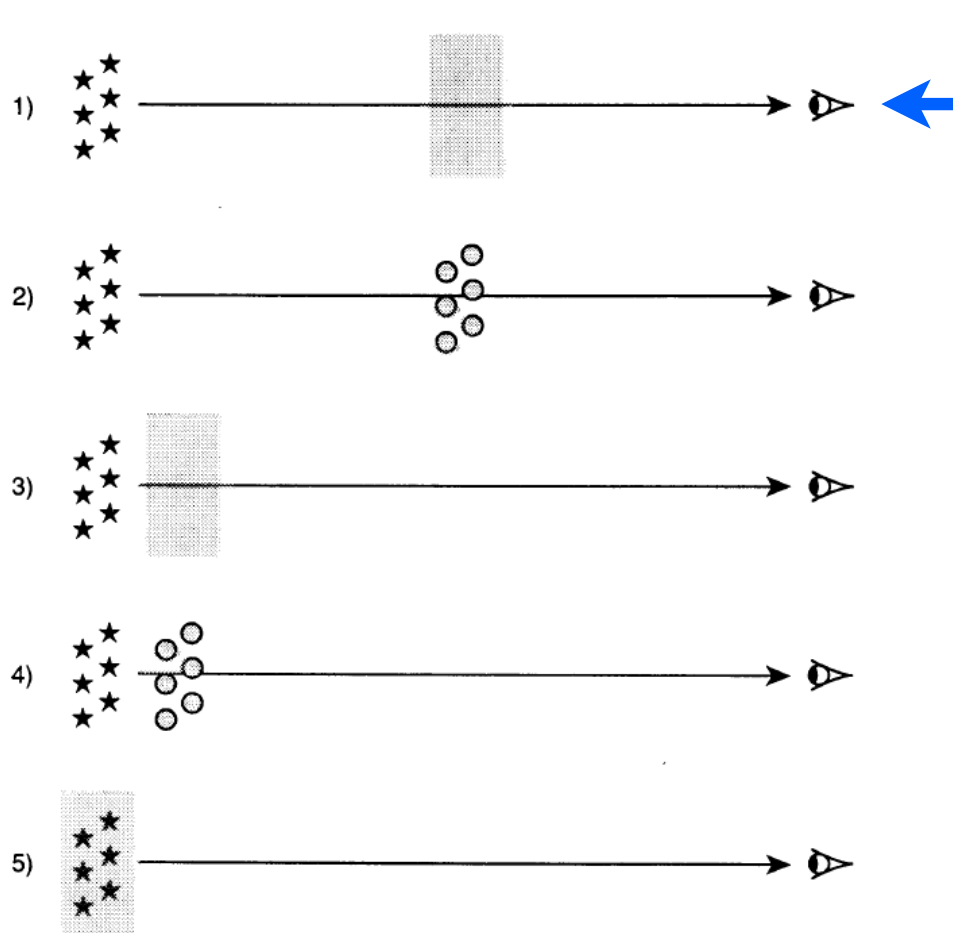
Why dust geometry decouples reddening and extinction:



Why dust geometry decouples reddening and extinction:



Reddening (observed Balmer decrement & UV slope) \neq Total extinction

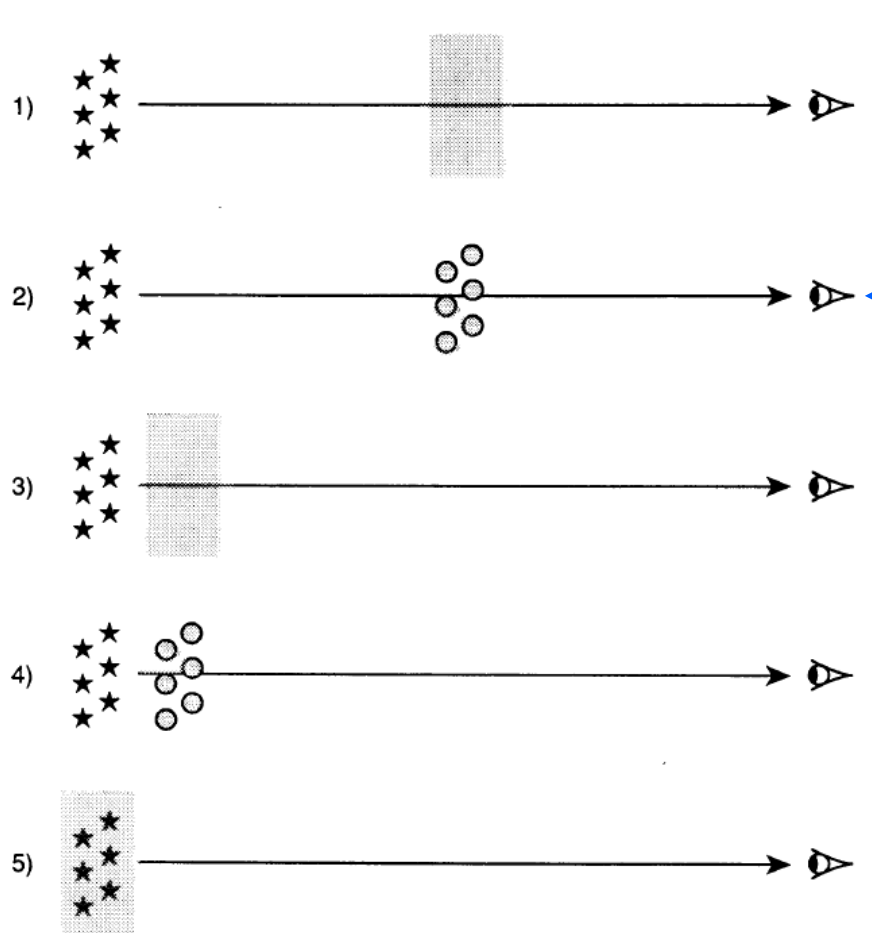


Everything reddened,
everything extinguished, little
scattering

FIG. 8.—A schematic representation of the five configurations of dust/ionized gas discussed in § 4. From top to bottom, they are (1) the uniform dust screen; (2) the clumpy dust screen; (3) the uniform scattering slab; (4) the clumpy scattering slab; (5) the internal dust model.

Calzetti et al 1994

Reddening (observed Balmer decrement & UV slope) \neq Total extinction

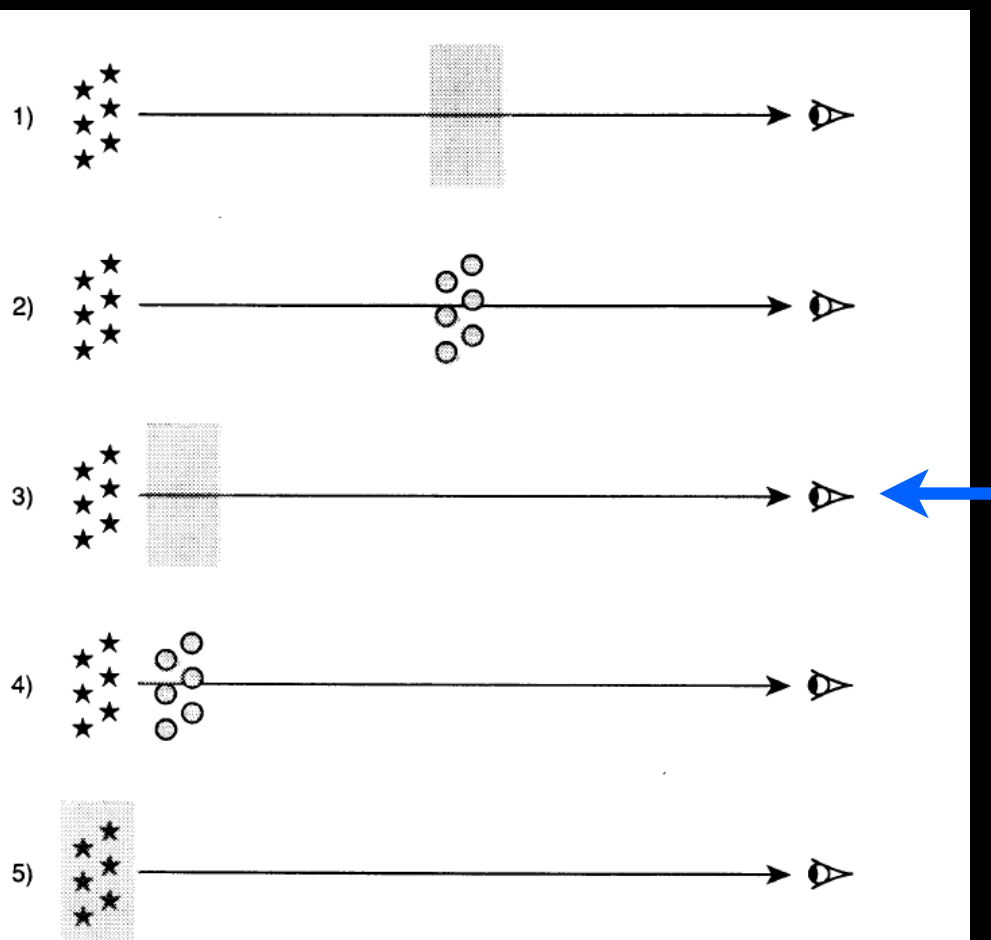


Some stars reddened
and more heavily
extincted, other stars
unobscured, little
scattering

FIG. 8.—A schematic representation of the five configurations of dust/ionized gas discussed in § 4. From top to bottom, they are (1) the uniform dust screen; (2) the clumpy dust screen; (3) the uniform scattering slab; (4) the clumpy scattering slab; (5) the internal dust model.

Calzetti et al 1994

Reddening (observed Balmer decrement & UV slope) \neq Total extinction

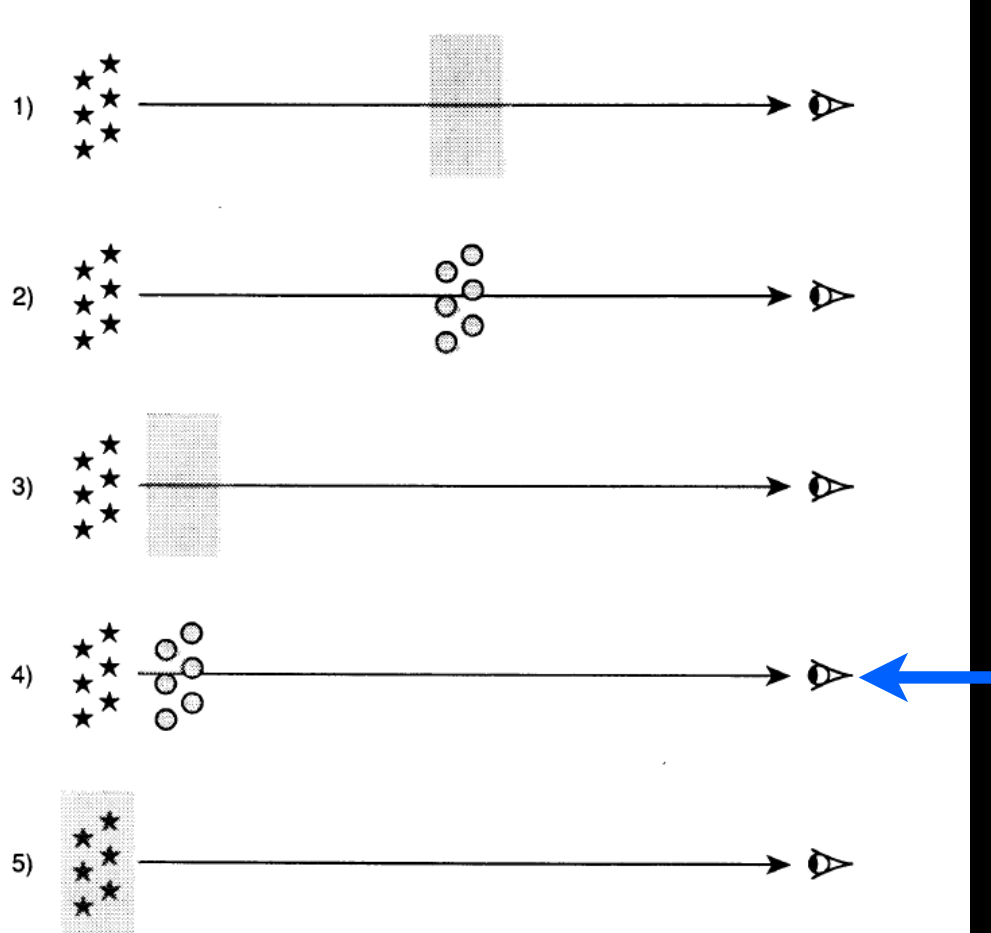


Everything reddened,
everything extinguished,
lots of scattering

FIG. 8.—A schematic representation of the five configurations of dust/ionized gas discussed in § 4. From top to bottom, they are (1) the uniform dust screen; (2) the clumpy dust screen; (3) the uniform scattering slab; (4) the clumpy scattering slab; (5) the internal dust model.

Calzetti et al 1994

Reddening (observed Balmer decrement & UV slope) \neq Total extinction



Some stars reddened
and more heavily
extincted, other stars
unobscured, lots of
scattering

FIG. 8.—A schematic representation of the five configurations of dust/ionized gas discussed in § 4. From top to bottom, they are (1) the uniform dust screen; (2) the clumpy dust screen; (3) the uniform scattering slab; (4) the clumpy scattering slab; (5) the internal dust model.

Reddening (observed Balmer decrement & UV slope) \neq Total extinction

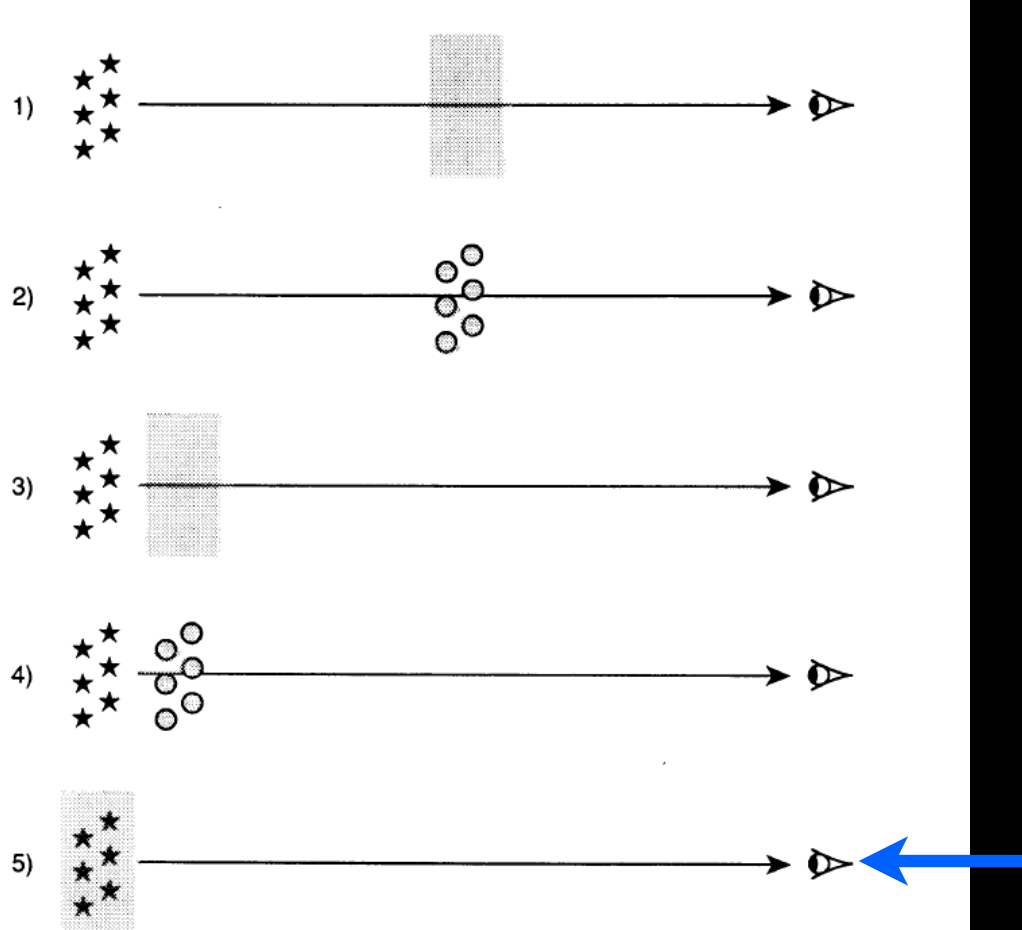


FIG. 8.—A schematic representation of the five configurations of dust/ionized gas discussed in § 4. From top to bottom, they are (1) the uniform dust screen; (2) the clumpy dust screen; (3) the uniform scattering slab; (4) the clumpy scattering slab; (5) the internal dust model.

Range of reddening and extinction for stars, lots of scattering

These effects were first calculated by Disney et al 1989

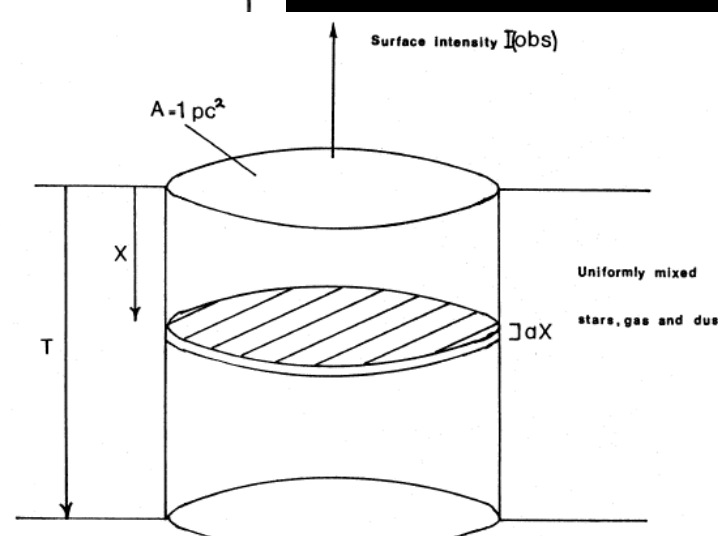
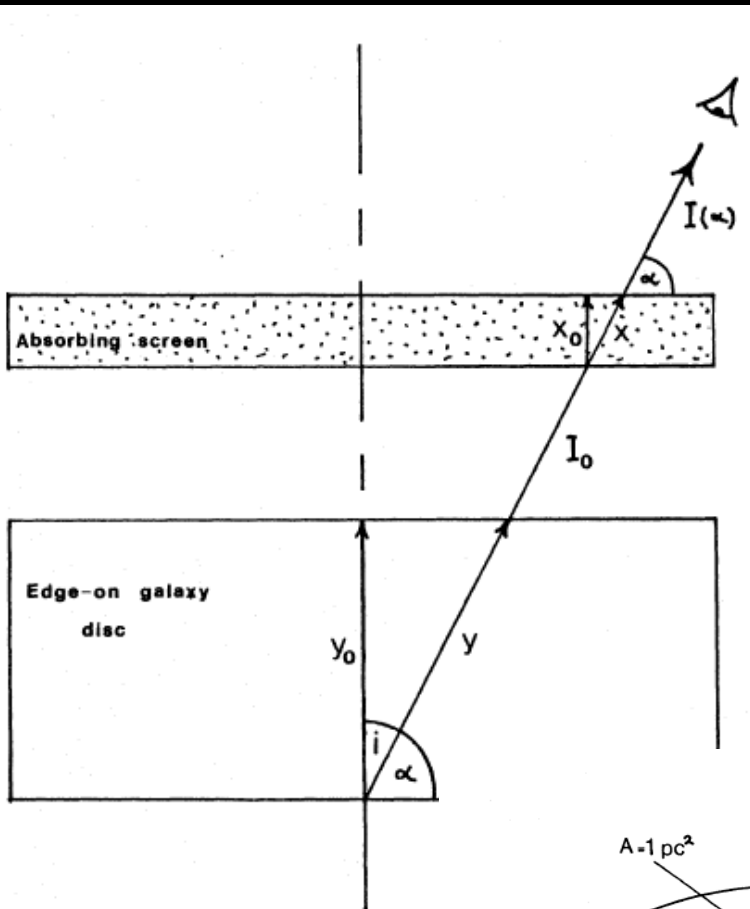


Figure 1. Geometry of the slab model.

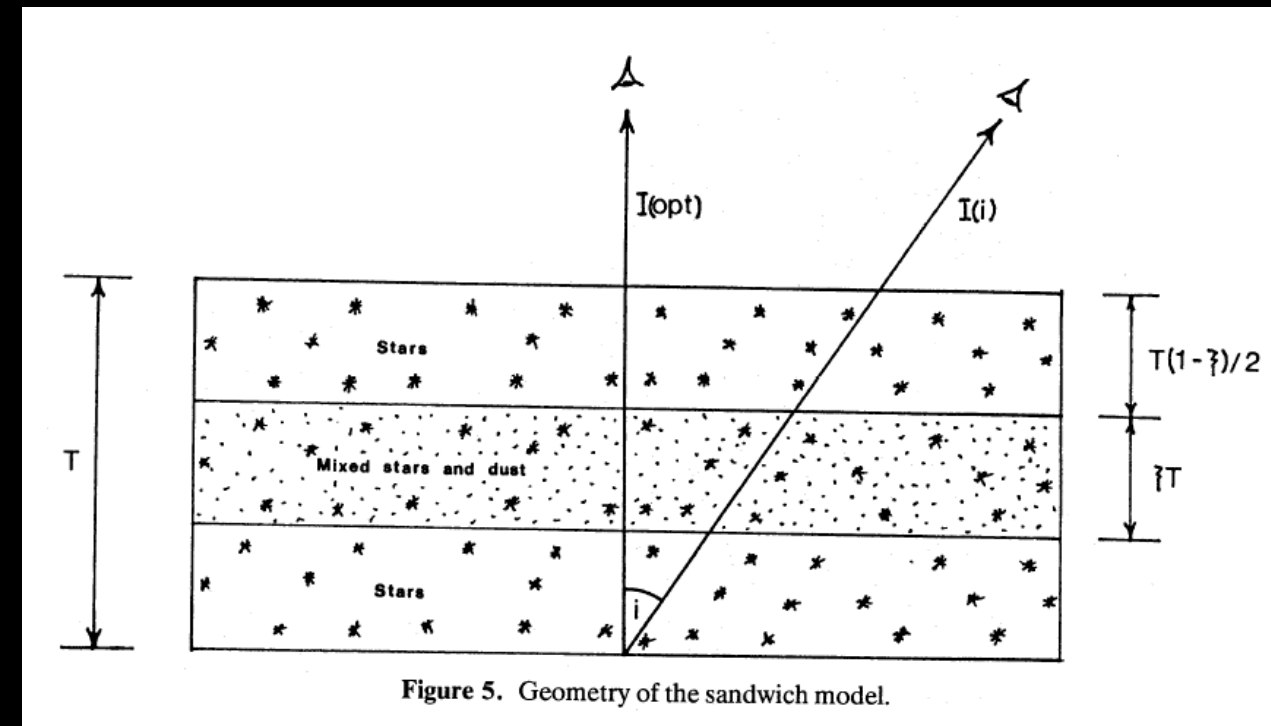


Figure 5. Geometry of the sandwich model.

- uniformly mixed
- “screen”
- “sandwich”
- “triplex” (mixed exponentials)

Clumpier dust lets more unextincted UV light through

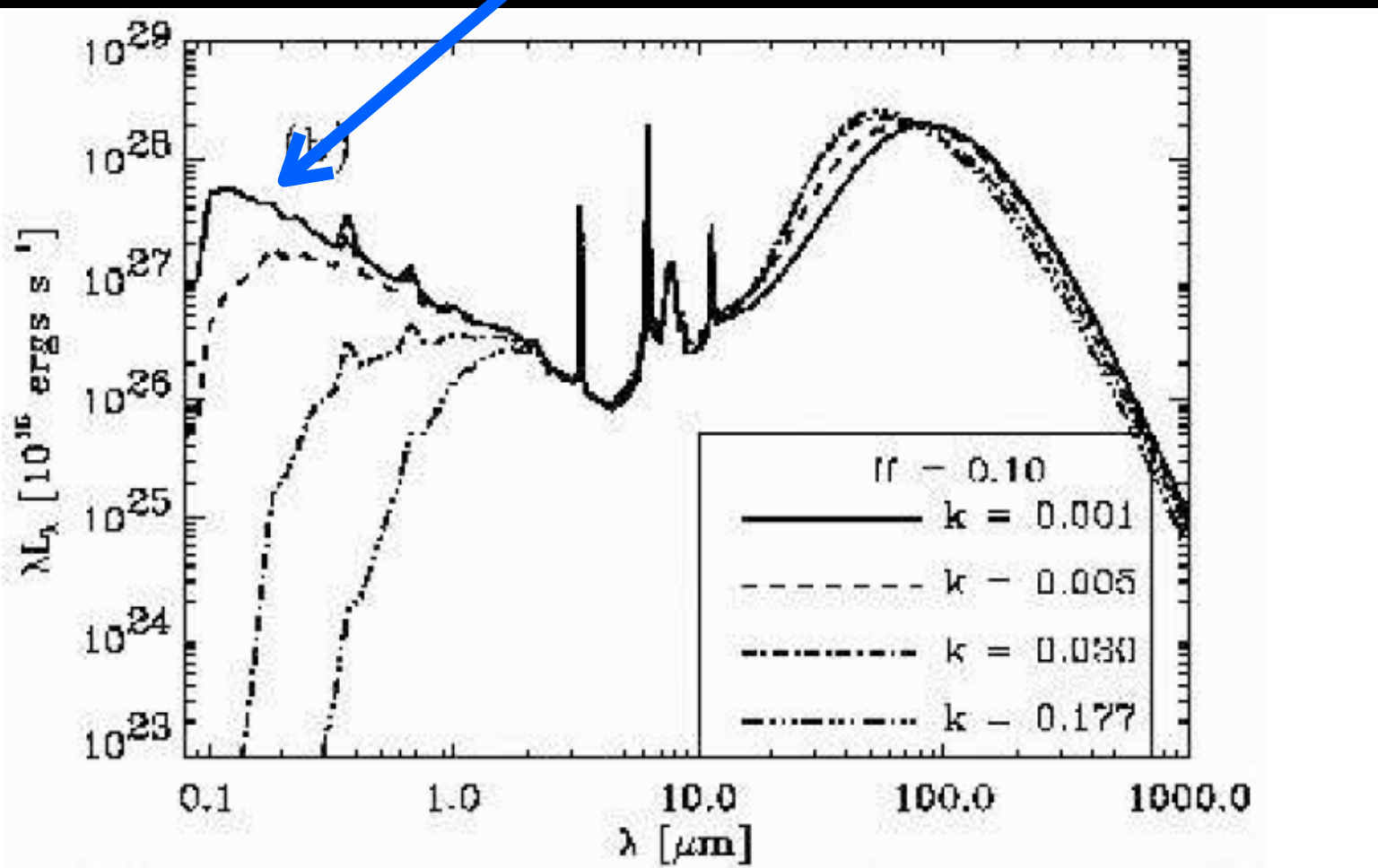


FIGURE 14. The effect of “passive” clumps on the FIR/submm SEDs, taken from Misselt et al. [41]. Model SEDs are for a range of density ratios k between the diffuse and clumpy media and for a filling factor $ff = 0.1$. All models are calculated assuming a spherical shell geometry. It is obvious that the effect of increasing the degree of clumpiness (decreasing k) is to make the SEDs cooler.

Warning: Reddening (observed Balmer decrement &/or UV slope) ≠ **Total extinction**

Problem #2: The attenuation and/or reddening in different parts of the spectrum may be caused by different dust structures

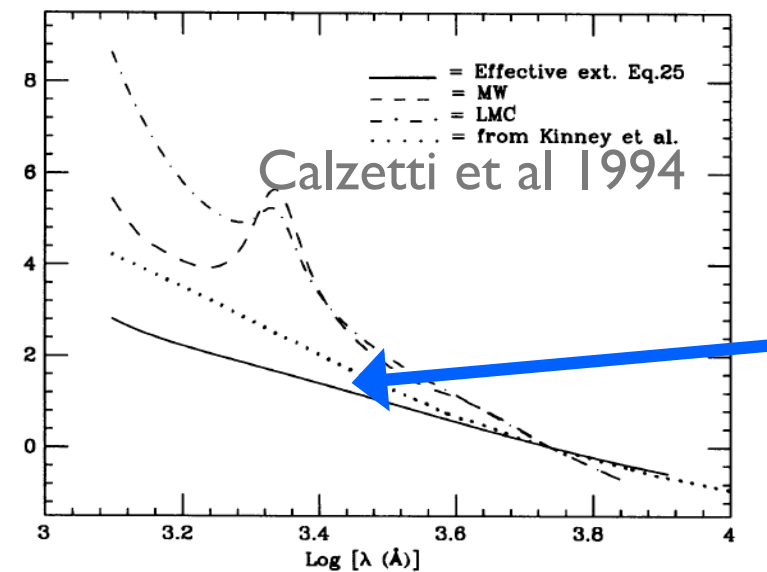
Dust in HII regions

- # Dust near exposed O/B stars
- # Dust in field stars that dominate the red continuum



Warning: **Reddening** (observed Balmer decrement &/or UV slope) \neq Total extinction

Problem #3: The attenuation law may vary from galaxy to galaxy, or within different parts of the same spectrum, due to variations in dust content/geometry

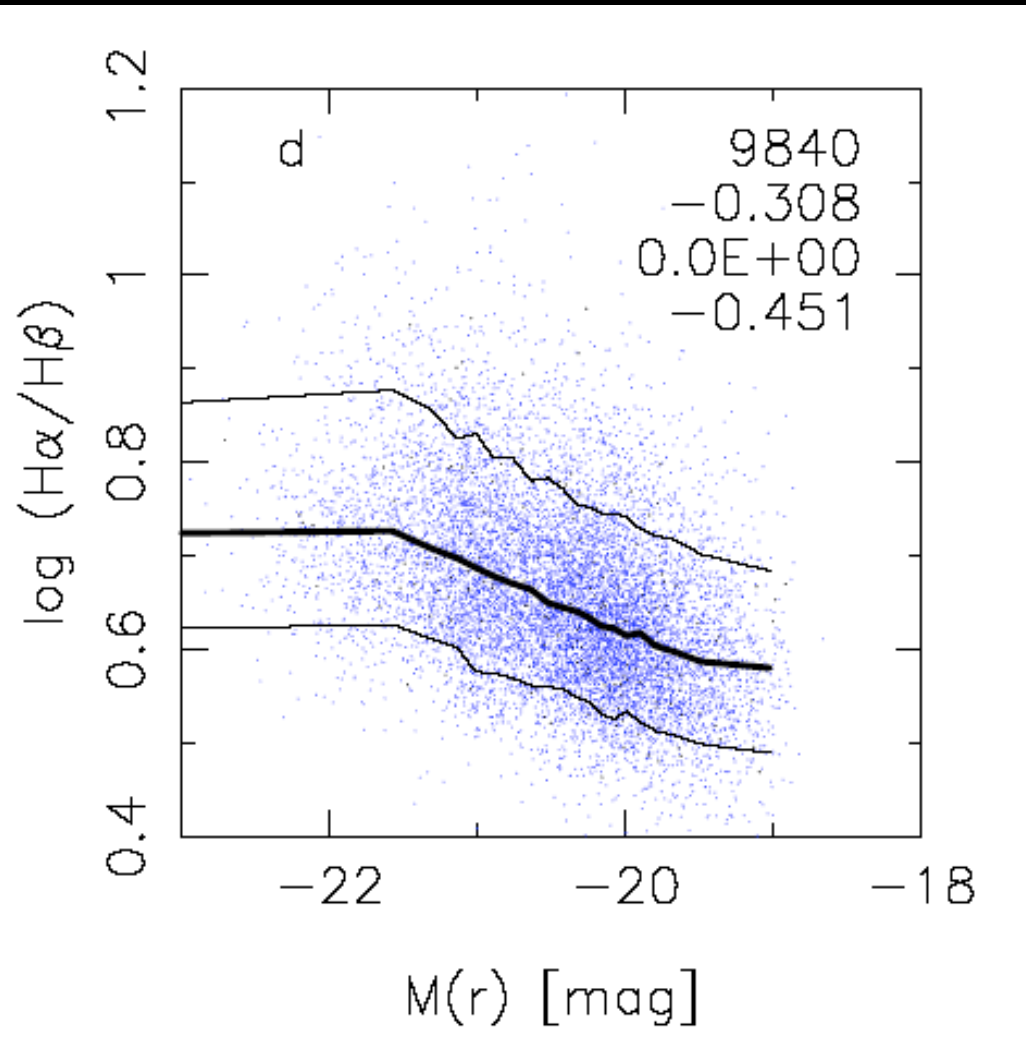


Attenuation law for HII regions & UV in starbursts seems “greyer” than typical MW extinction for single stars

FIG. 21.—The extinction law derived in this work (eq. [25], continuous line) is compared with the Milky Way (dashed line) and the LMC (dot-dashed line) extinction laws. The extinction law derived by Kinney et al. (1994b) is also shown (dotted line). The zero point of the four curves is arbitrary and has been chosen to be the value $Q(5500) = 0.0$.

How does typical internal attenuation
vary among & within galaxies?

Lower mass, late-type disks have less reddening.



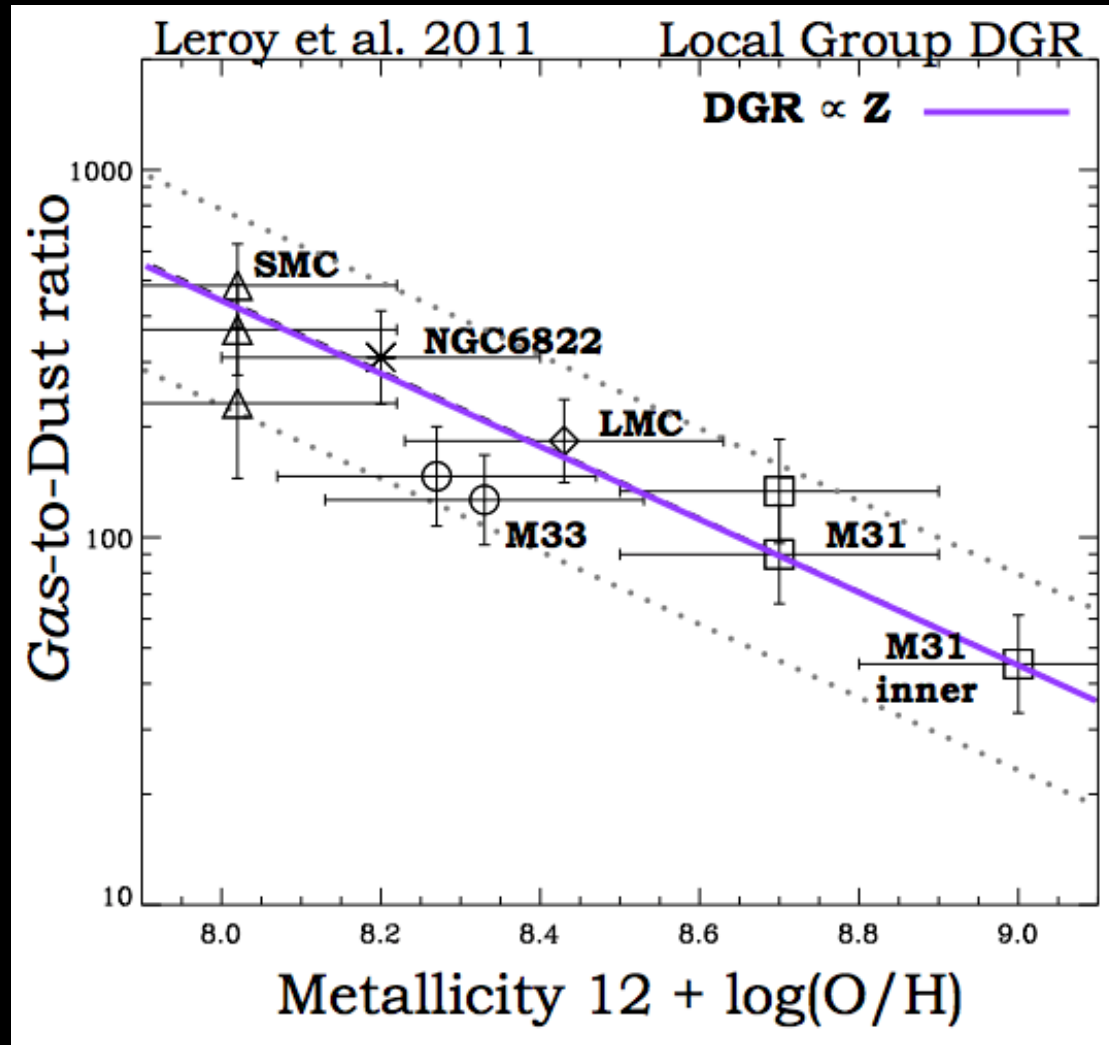
Probably less
reddening due to less
dust, which is due to
lower metal content

Fig. 6. The relation between $\log(\text{H}\alpha/\text{H}\beta)$ and various properties of the galaxies. The meaning of the numbers in the upper right is the same as in Fig. 5. The thick curve represents the median value of $\log(\text{H}\alpha/\text{H}\beta)$. The thin curves delimit the zone containing 80% of the data points (see Sect. 3.1).

SDSS:

Stasinska et al 2004

Normalized dust content tracked by “dust-to-gas ratio” = $\Sigma_{\text{dust}} / \Sigma_{\text{gas}}$

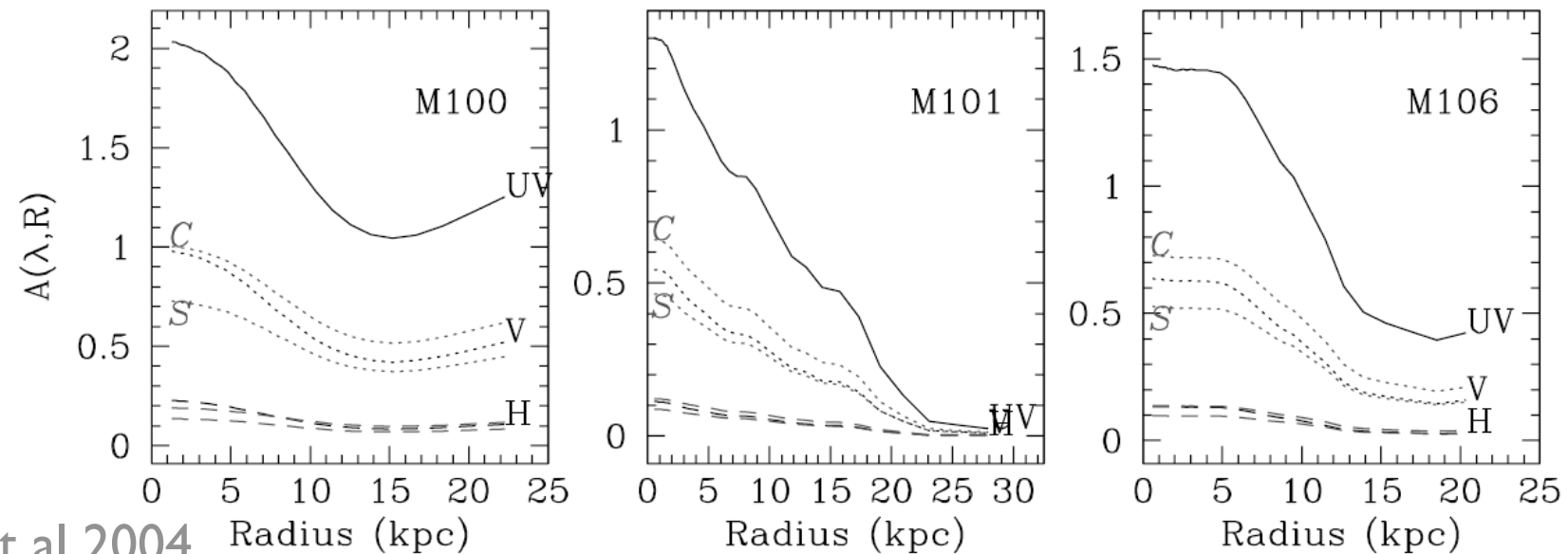


Confirms that amount of dust scales with raw materials, to first order

See also Sandstrom et al 2013 for internal variation within galaxies

$$\Sigma_{\text{gas}} \approx 1.36(\Sigma_{\text{HI}} + \Sigma_{\text{H}_2}), \text{ to correct for He}$$

Within spiral disks, extinction & dust to gas ratio drops with radius



Bossier et al 2004

Fig. 9. Extinction profiles in the UV, V and H. $A(\text{UV})$ is obtained from the FIR/UV ratio. The black line shows the extinction profiles in V and H as derived for a sandwich model with dust to star scale-height ratio ξ depending on the wavelength. For each of these two bands, the others curve show the predicted extinction for a dust screen with Milky-Way-type dust (S) and the Calzetti (1999) law (C).

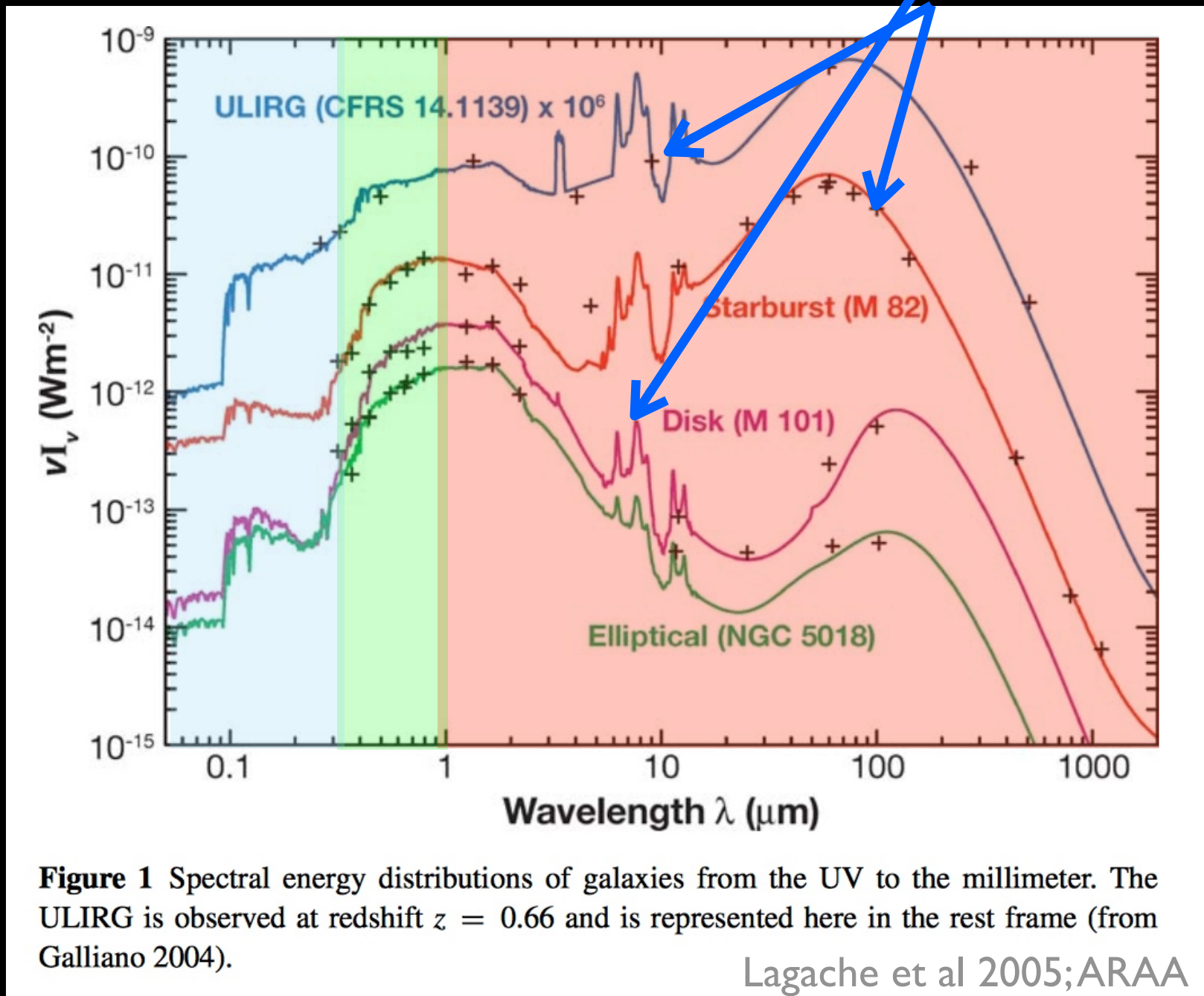
- Outer regions of disks have similar properties to the inner regions of low mass, low surface density disks.

Dust in Galaxies Questions

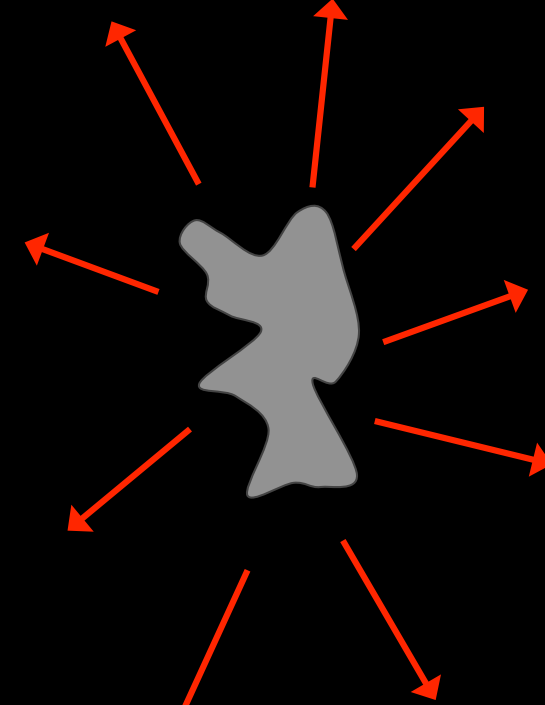
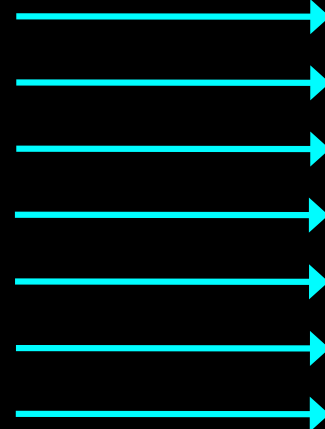
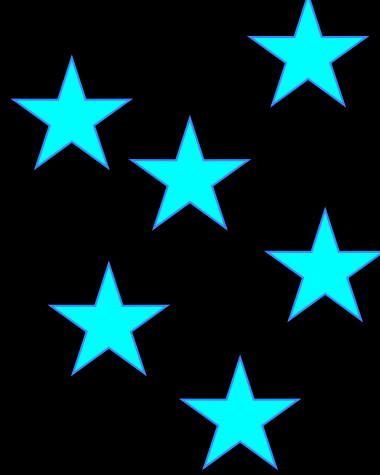
- What is the most effective way to bootstrap measures of reddening into measures of extinction?
- How is dust geometry affecting our measurements of reddening & extinction?
- What physics drives variations in typical extinction within and among galaxies? Is it more than just metallicity?

Dust *emits* strongly in
the mid- and far-IR

Dust is a major part of a galaxy SED



Emission from dust is dominated by light “reprocessed” into the IR

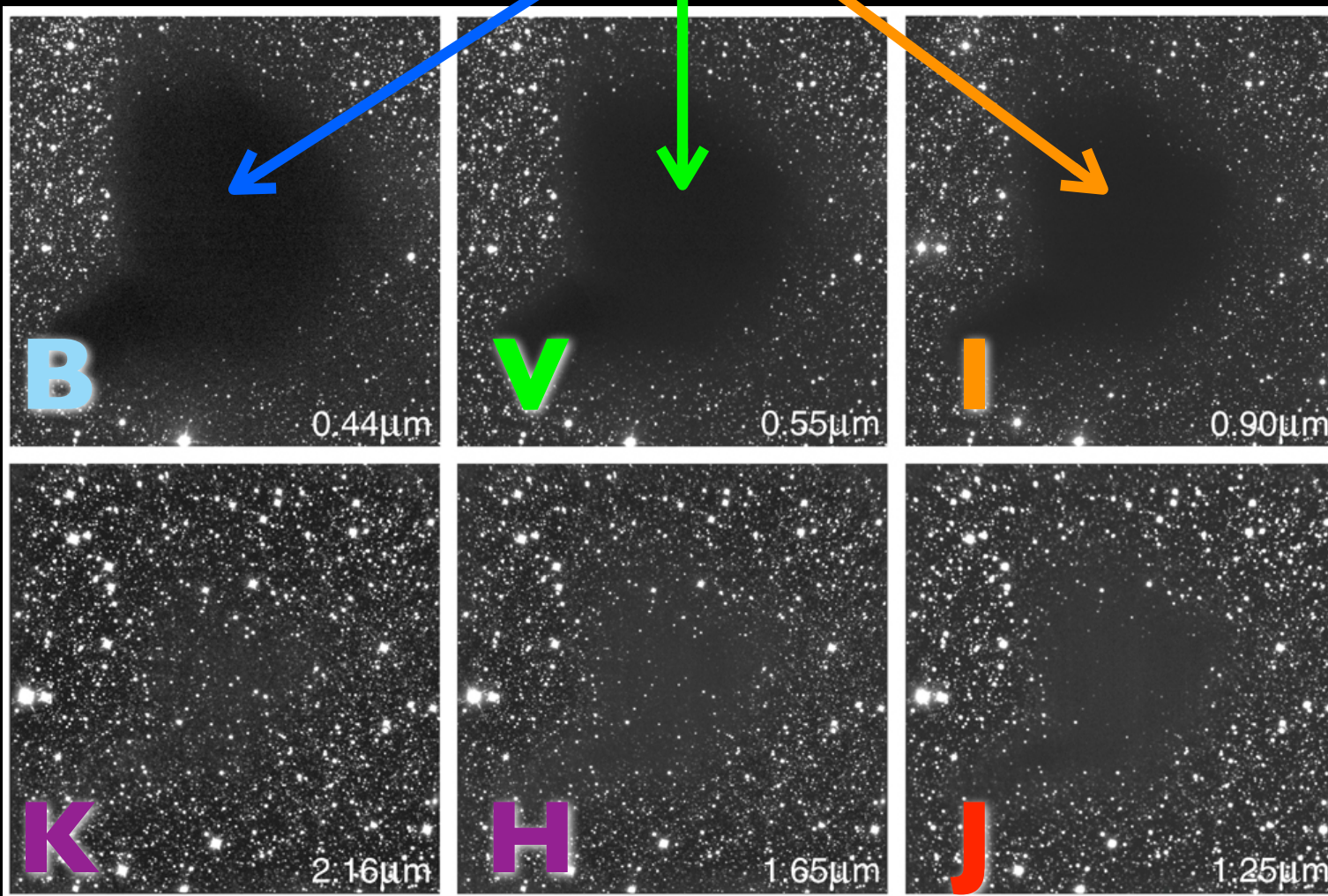


UV & optical light is absorbed by dust...

...which heats up to 10-100K and radiates like a greybody at 10-300 μ m

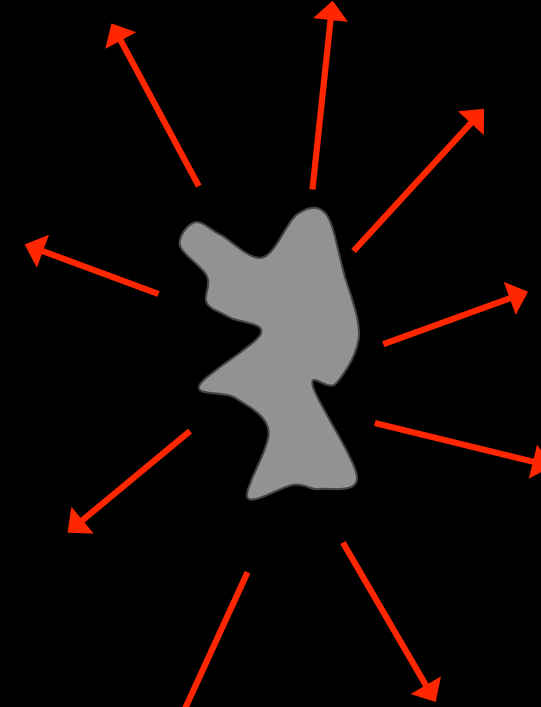
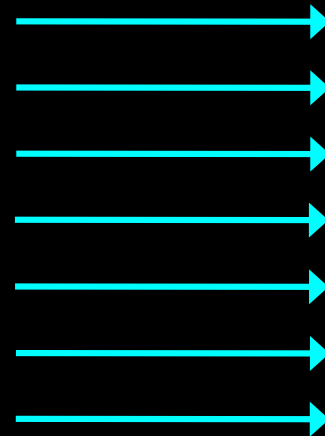
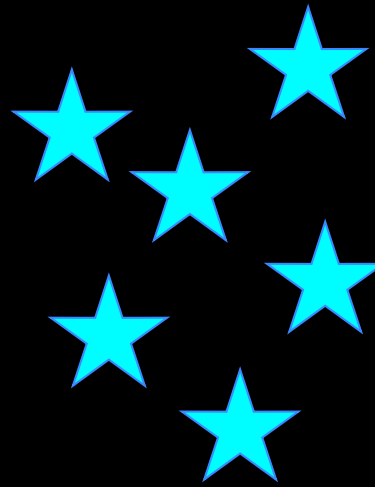
Conservation of energy, basically

Energy absorbed here...



..must be re-emitted somewhere, once the dust reaches a steady-state temperature...

More incident light and/or more dust = more mid- and far-IR emission

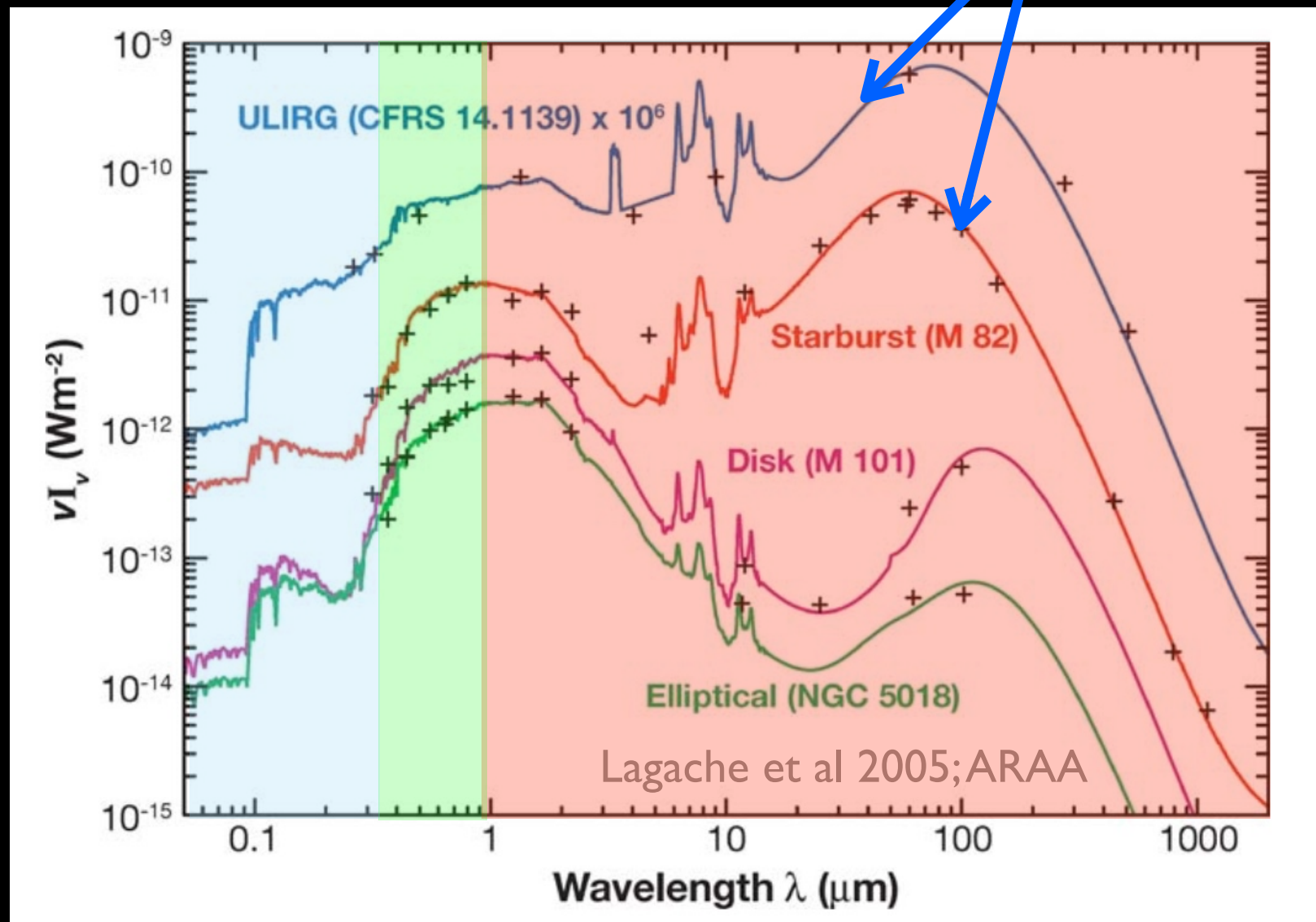


If the “interstellar
radiation field” (ISRF)
goes up...

...dust equilibrates to a
higher temperature, and
this emission increases.

*For large dust grains...

Reprocessing makes dust dominate SED for high SFR



Lots of UV radiation is absorbed & reprocessed

Note: Heating is a bit different for PAH's & small dust grains

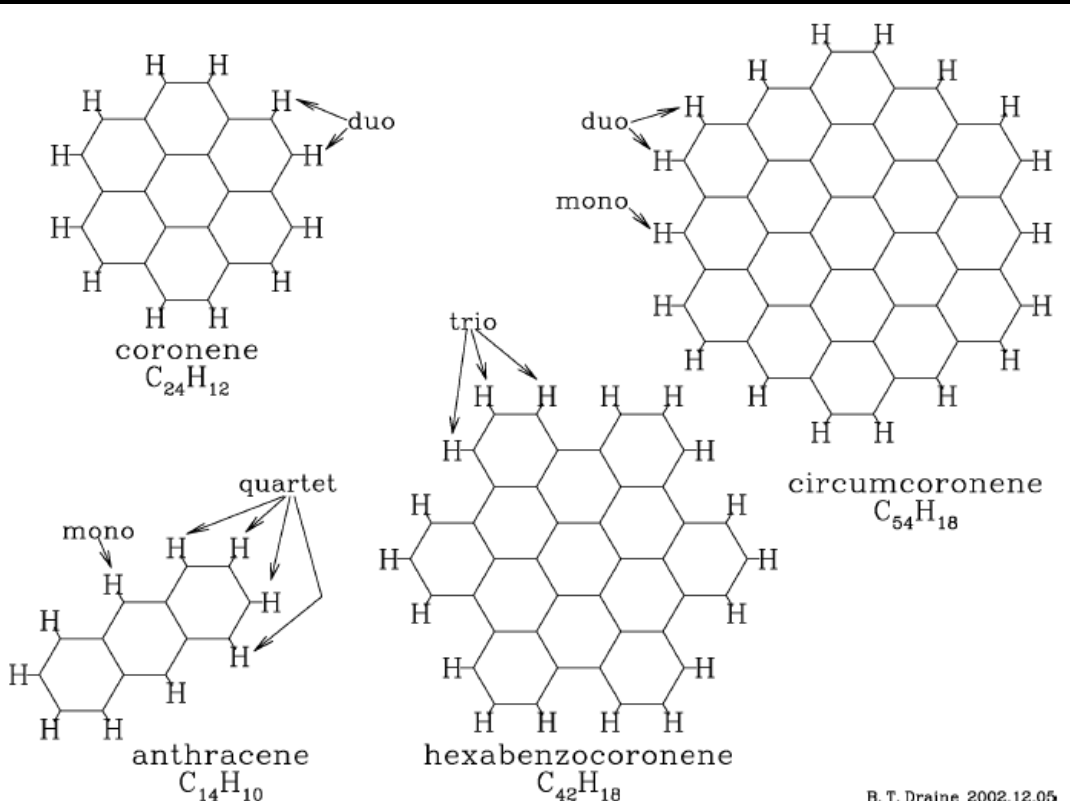


Figure 7 The structure of 4 PAH molecules. Examples of mono, duo, trio, and quartet H sites are indicated.

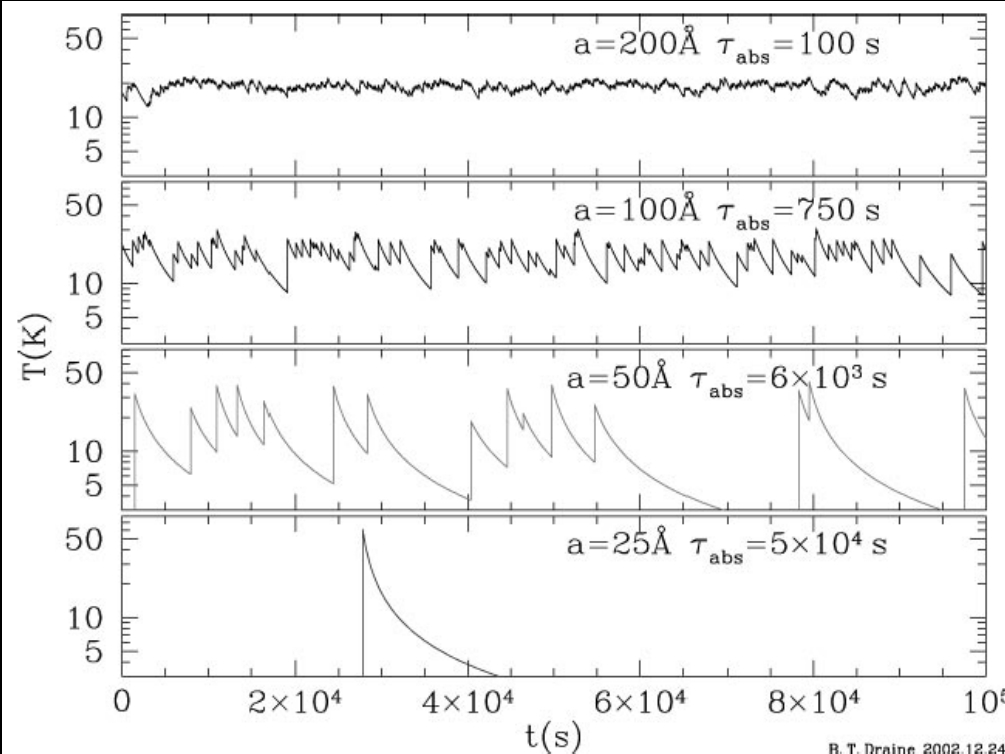
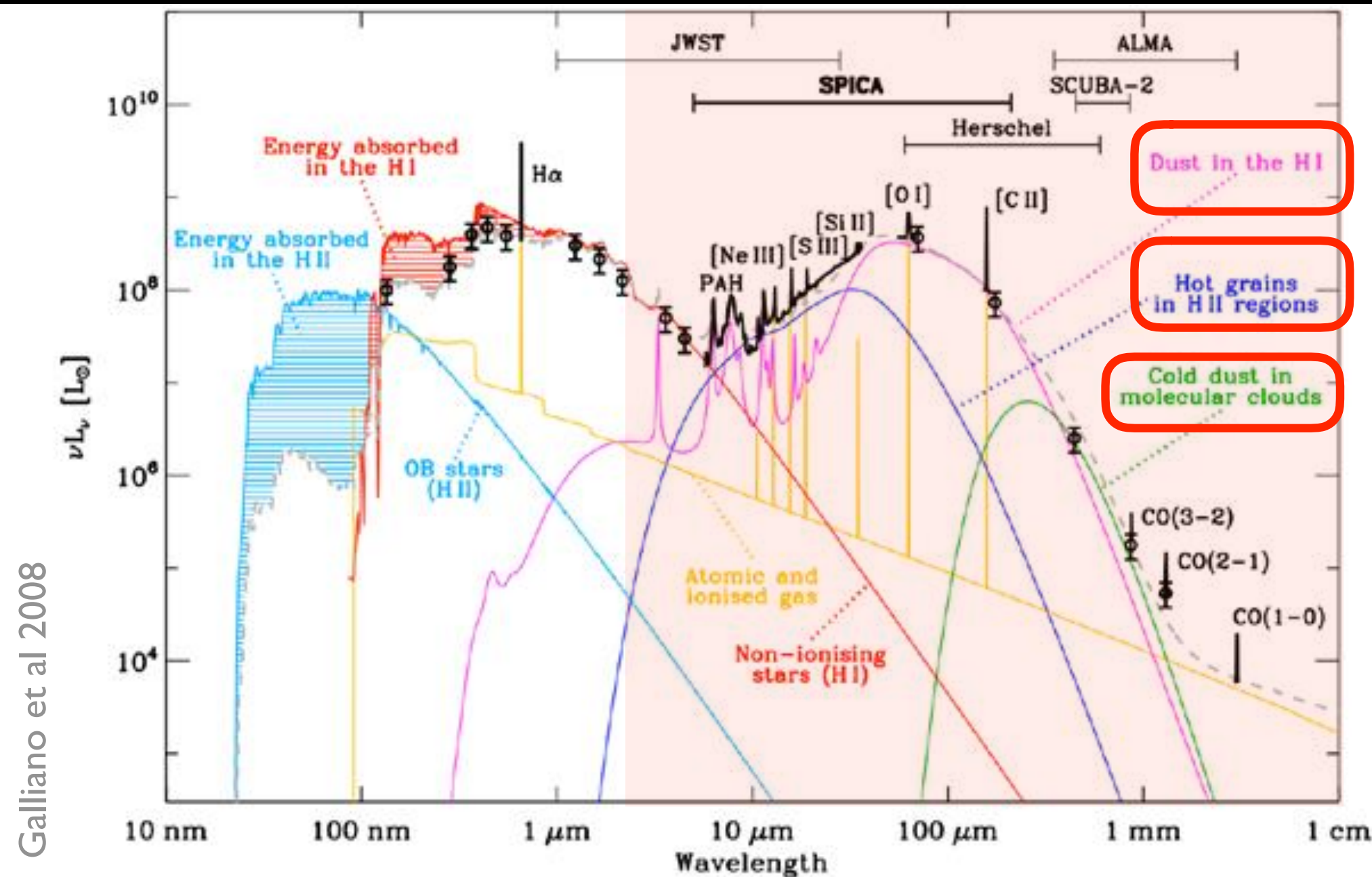


Figure 13 A day in the life of four carbonaceous grains, heated by the local interstellar radiation field. τ_{abs} is the mean time between photon absorptions (Draine & Li 2001).

- Heating can be stochastic when cooling is rapid
- Can heat to high temps, but for very short periods of time

Disentangling dust emission

Dust emission is from a variety of sources w/ different characteristic temperatures (10-100K)



Dust emission components

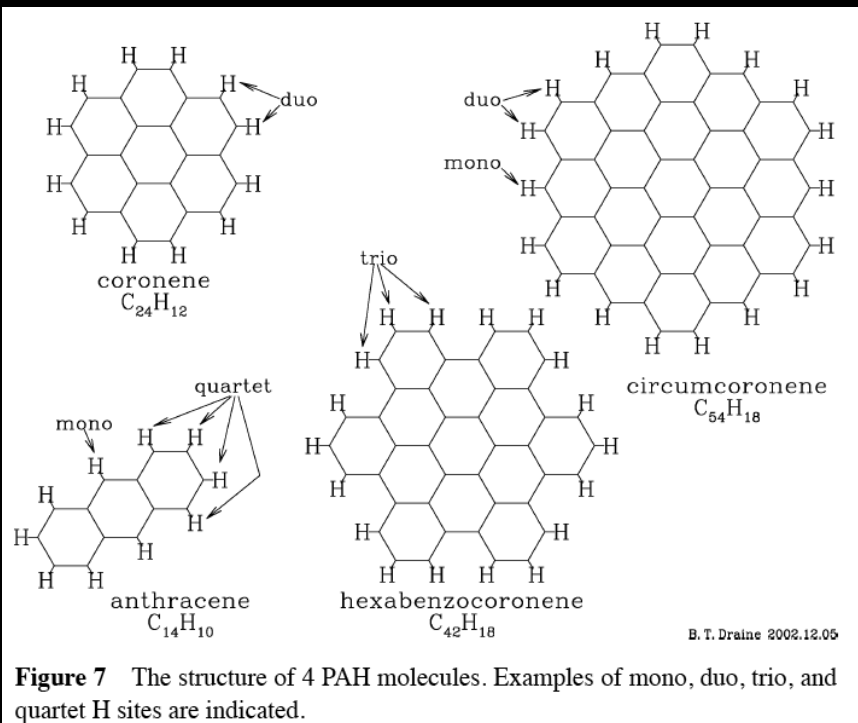


Figure 7 The structure of 4 PAH molecules. Examples of mono, duo, trio, and quartet H sites are indicated.

I. Broad line emission from PAH molecules

- Small enough that quantum mechanical molecular effects are important
- Heating can be stochastic when cooling is rapid

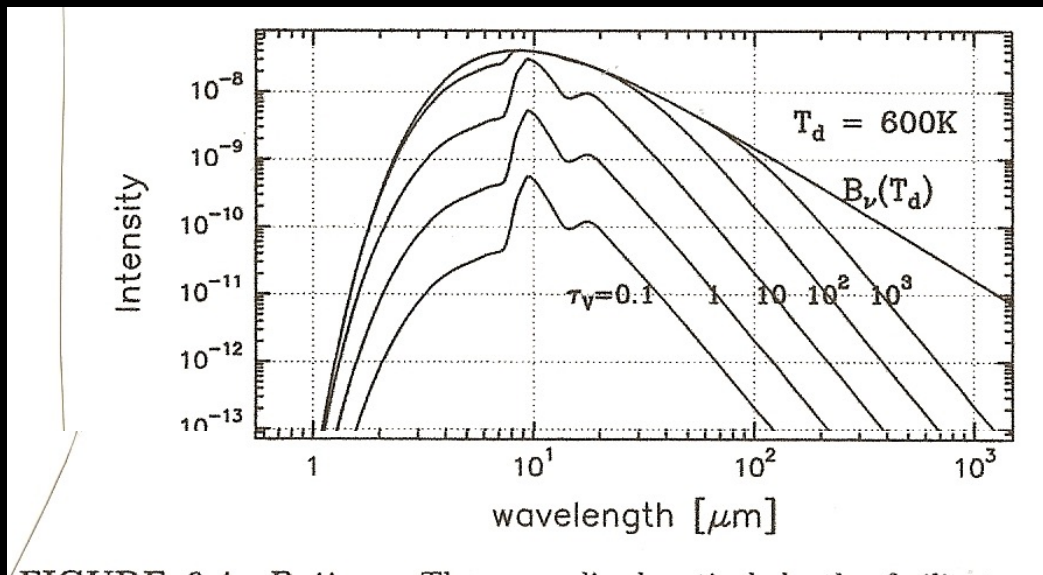


FIGURE 6.4 Bottom: The normalized optical depth of silicate grains with 600Å radius. The wavelength scale starts at 0.55 μ m where $\tau_\lambda/\tau_V = 1$. **Top:** The intensity (in units $\text{erg s}^{-1} \text{cm}^{-2} \text{Hz}^{-1} \text{ster}^{-1}$) towards a cloud of temperature $T = 600 \text{ K}$ filled with such grains for visual optical thickness τ_V from 0.1 and 1000.

2. Near blackbody, depending on optical depth

& grain properties

- Temperature of dust grains depends on balance of heating (ISRF) & cooling (i.e. emission)
- Can have multiple pops with different temps

Deviations from blackbody are typically characterized by a “dust emissivity index” β

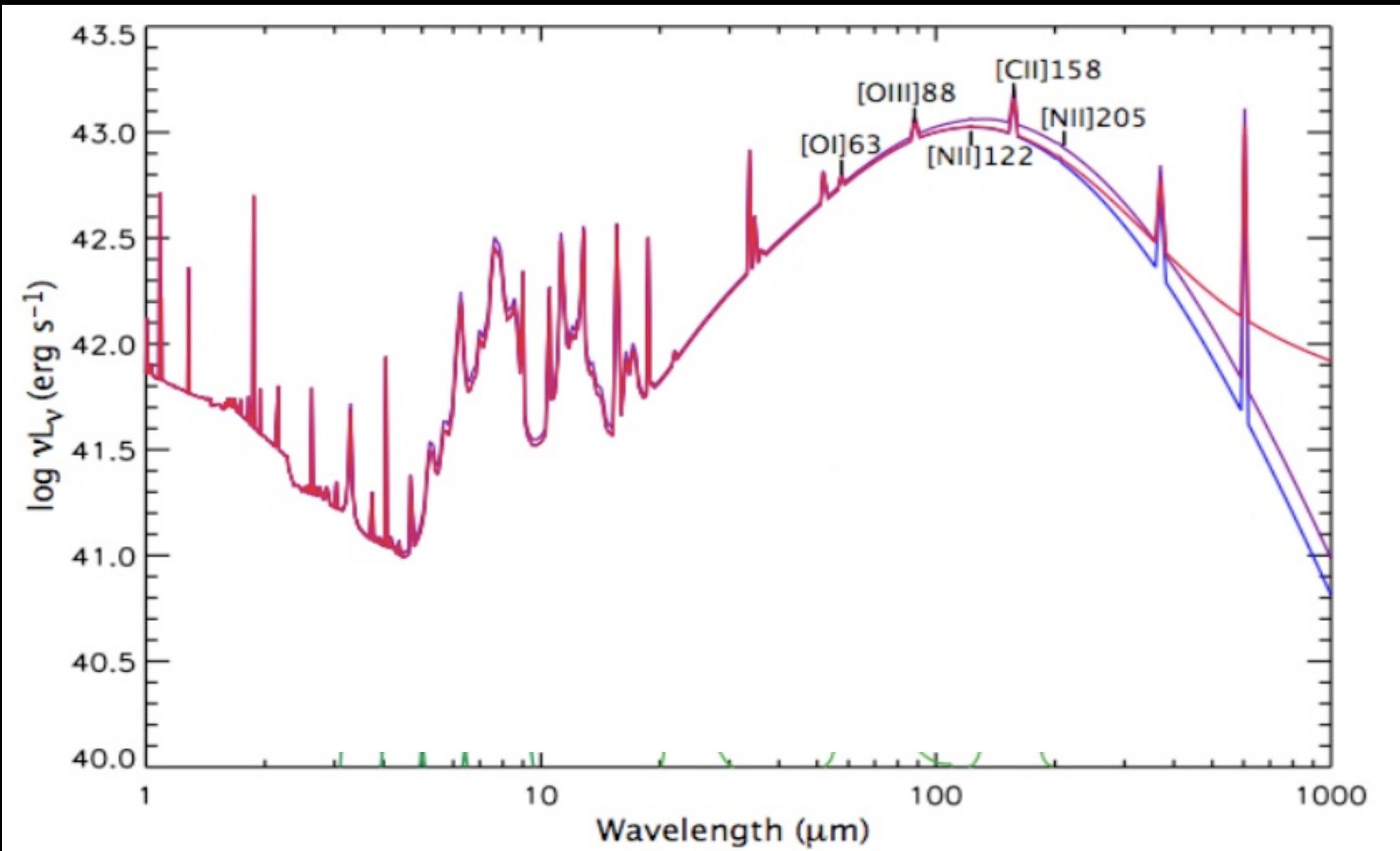
The new MIPS data combined with existing *IRAS* and SCUBA measurements can be used to estimate the dust component temperatures and masses using composite grey-body curves (e.g., Vlahakis et al. 2005). For two components these are:

$$F_\nu = A_w \nu^\beta B_\nu\left(\frac{\nu}{1+z}, T_w\right) + A_c \nu^\beta B_\nu\left(\frac{\nu}{1+z}, T_c\right) \quad (1)$$

where A_w and A_c are the relative contributions due to the warm and cold dust components. The masses can be

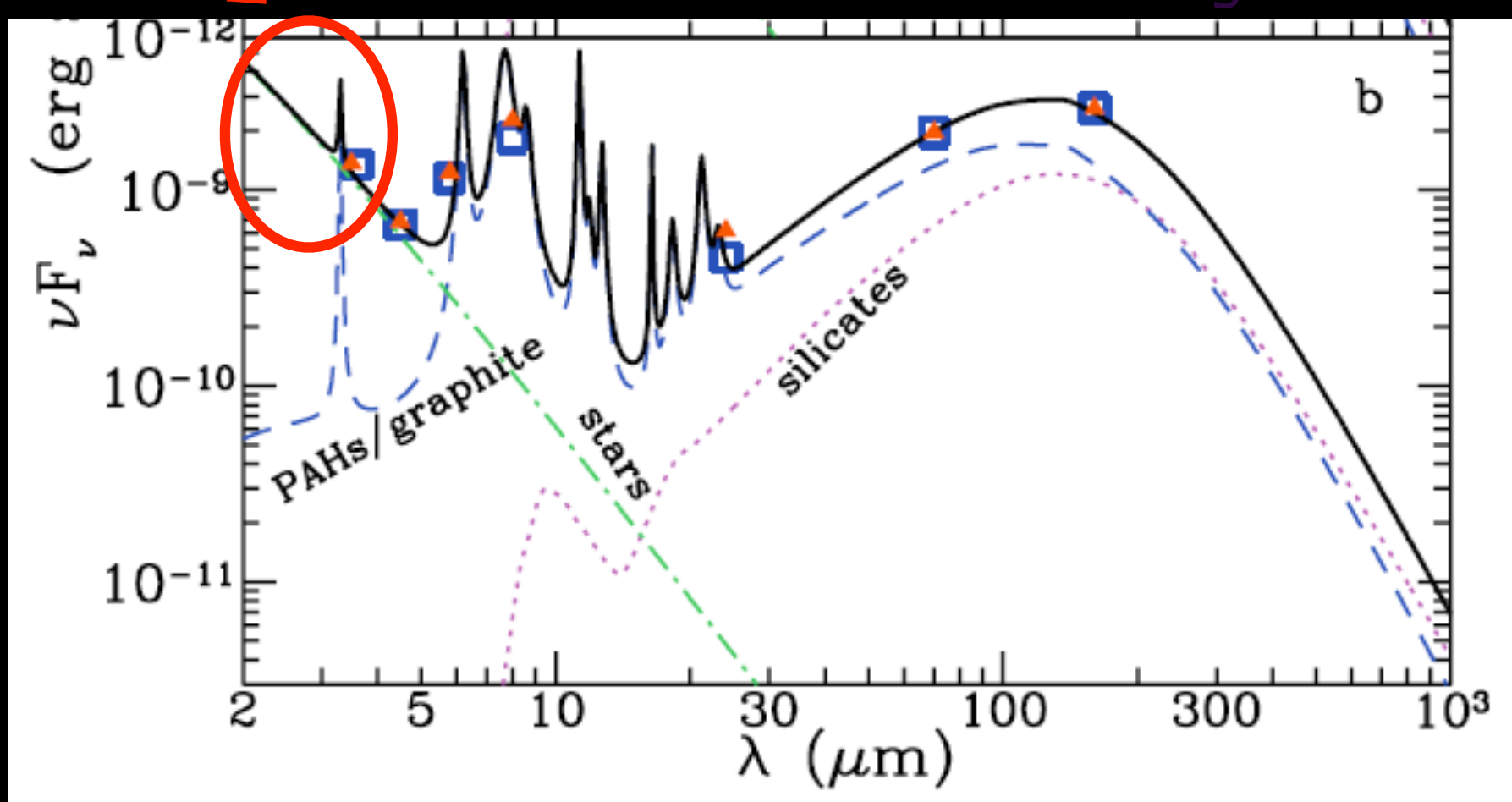
Comparing extinction maps to emission suggests
“dust emissivity index” $\beta \sim 1.5 - 2$

Contributions to NIR/MIR/FIR Spectra



Stars dominate continuum at $\lambda < 3-4\mu$

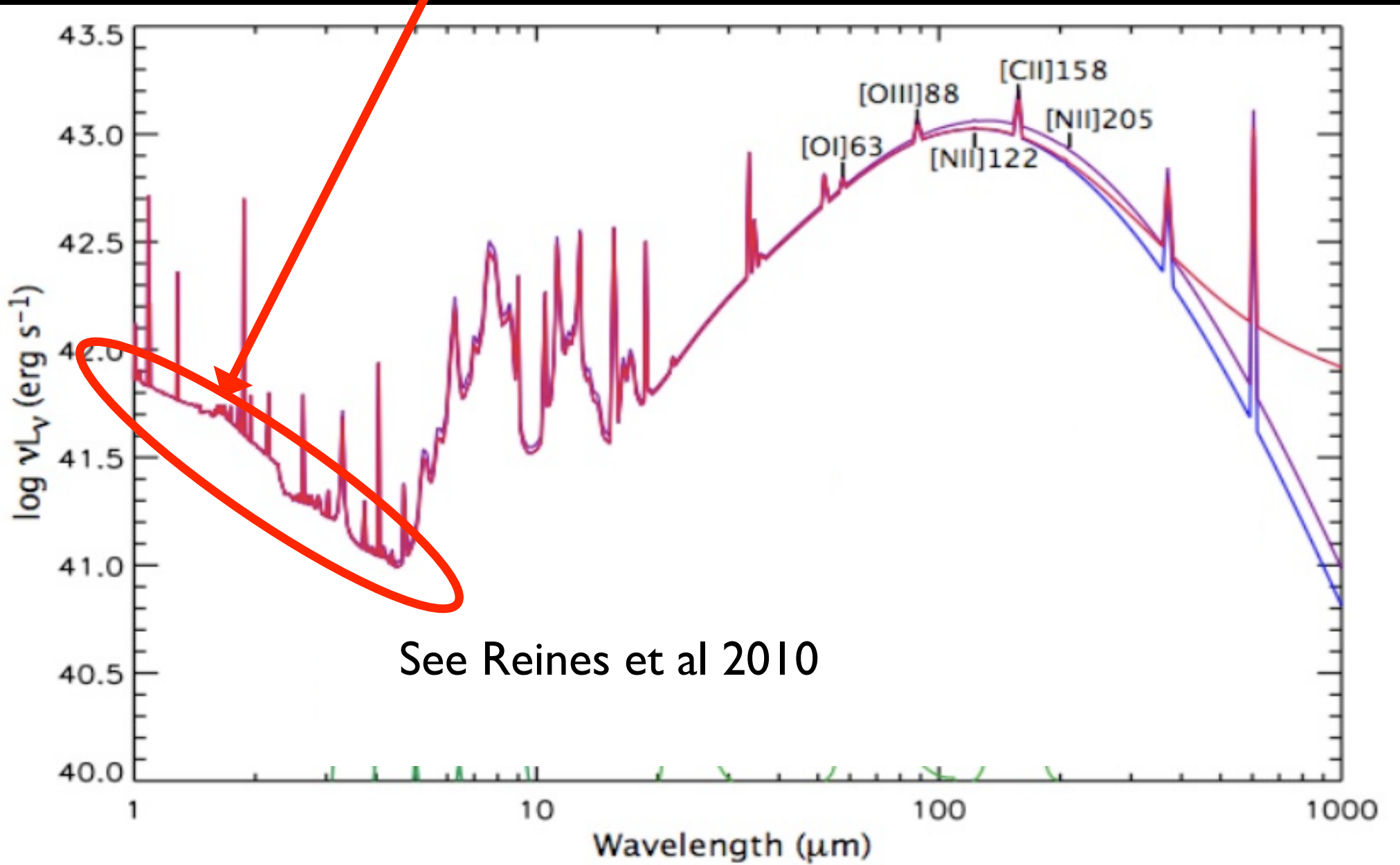
(Power law, with little dependence
on stellar age or metallicity)



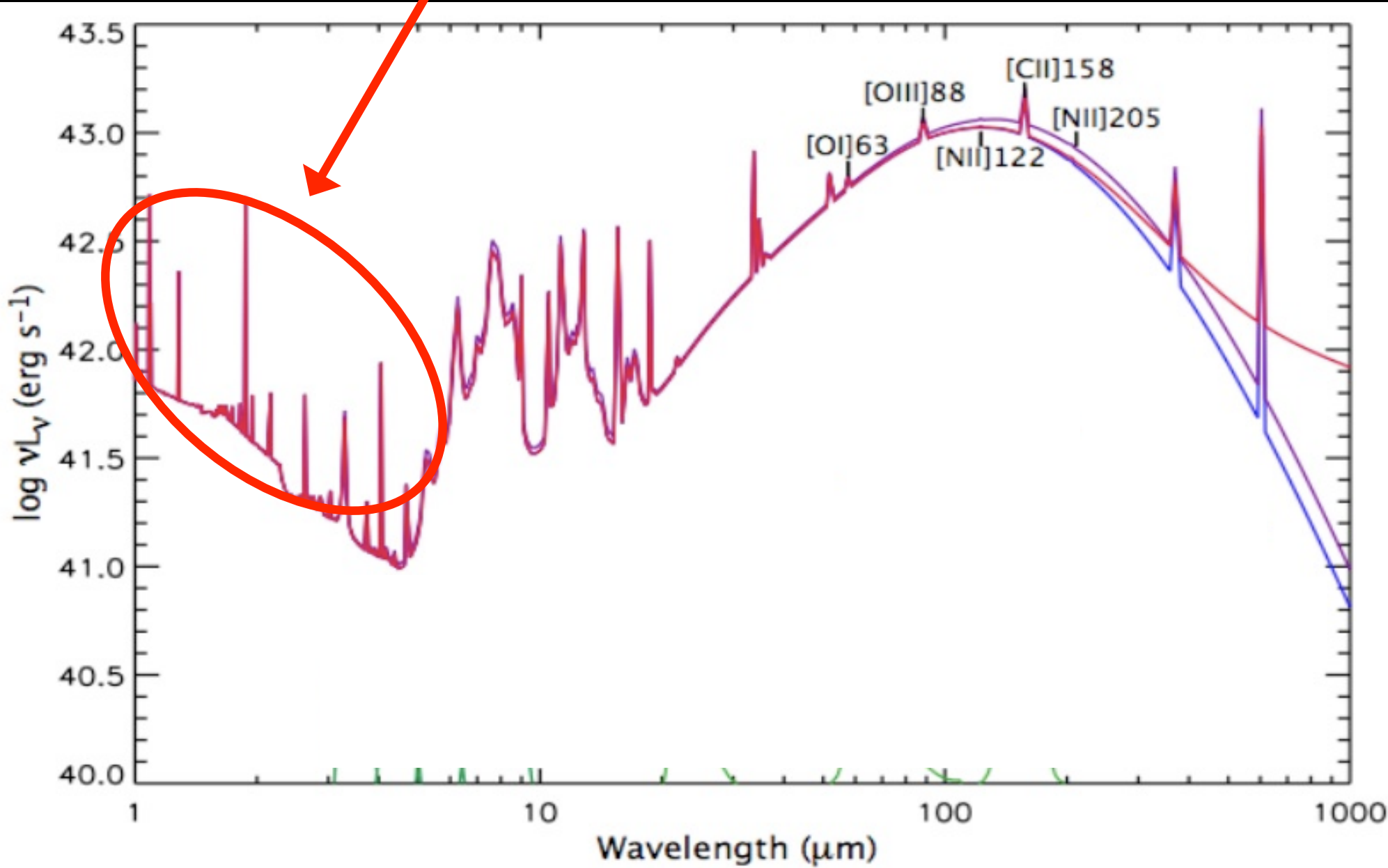
Regan et al 2004

FIG. 3.—SED and model fits to (a) the ring region and (b) the entire galaxy using the model of Li & Draine (2001, 2002b). The solid black lines and red triangles are the model-predicted fluxes, and the blue squares are the observed fluxes. The colored curves indicate the contributions of the different model components.

Note: some additional structure in continuum due to ionized gas

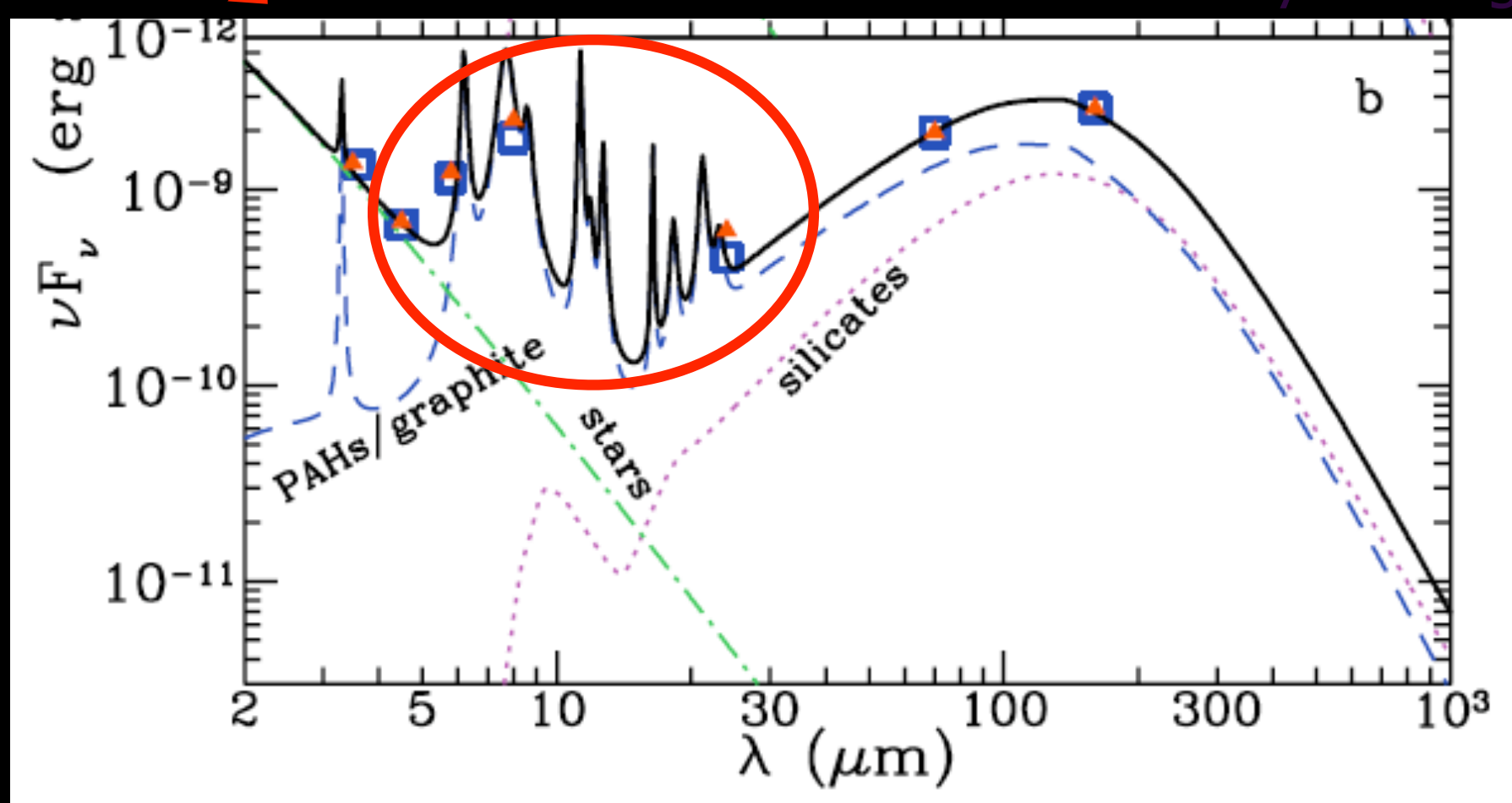


HII Region Emission Lines (Narrow)



Broad PAH features dominate emission at $5\mu < \lambda < 30\mu$

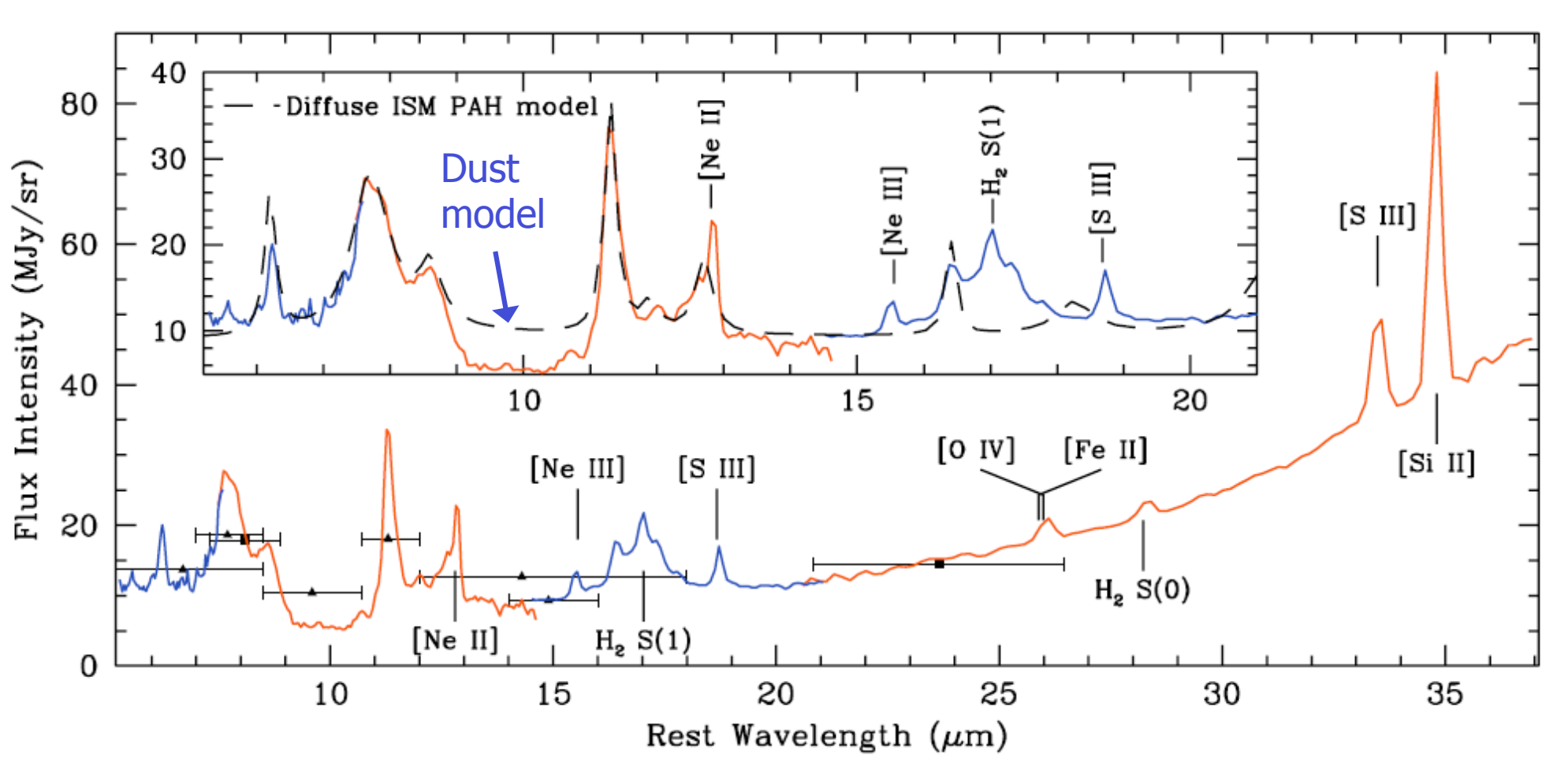
(along with some continuum from very small grains)



Regan et al 2004

FIG. 3.—SED and model fits to (a) the ring region and (b) the entire galaxy using the model of Li & Draine (2001, 2002b). The solid black lines and red triangles are the model-predicted fluxes, and the blue squares are the observed fluxes. The colored curves indicate the contributions of the different model components.

Mid-Infrared Spectrum (Spitzer)

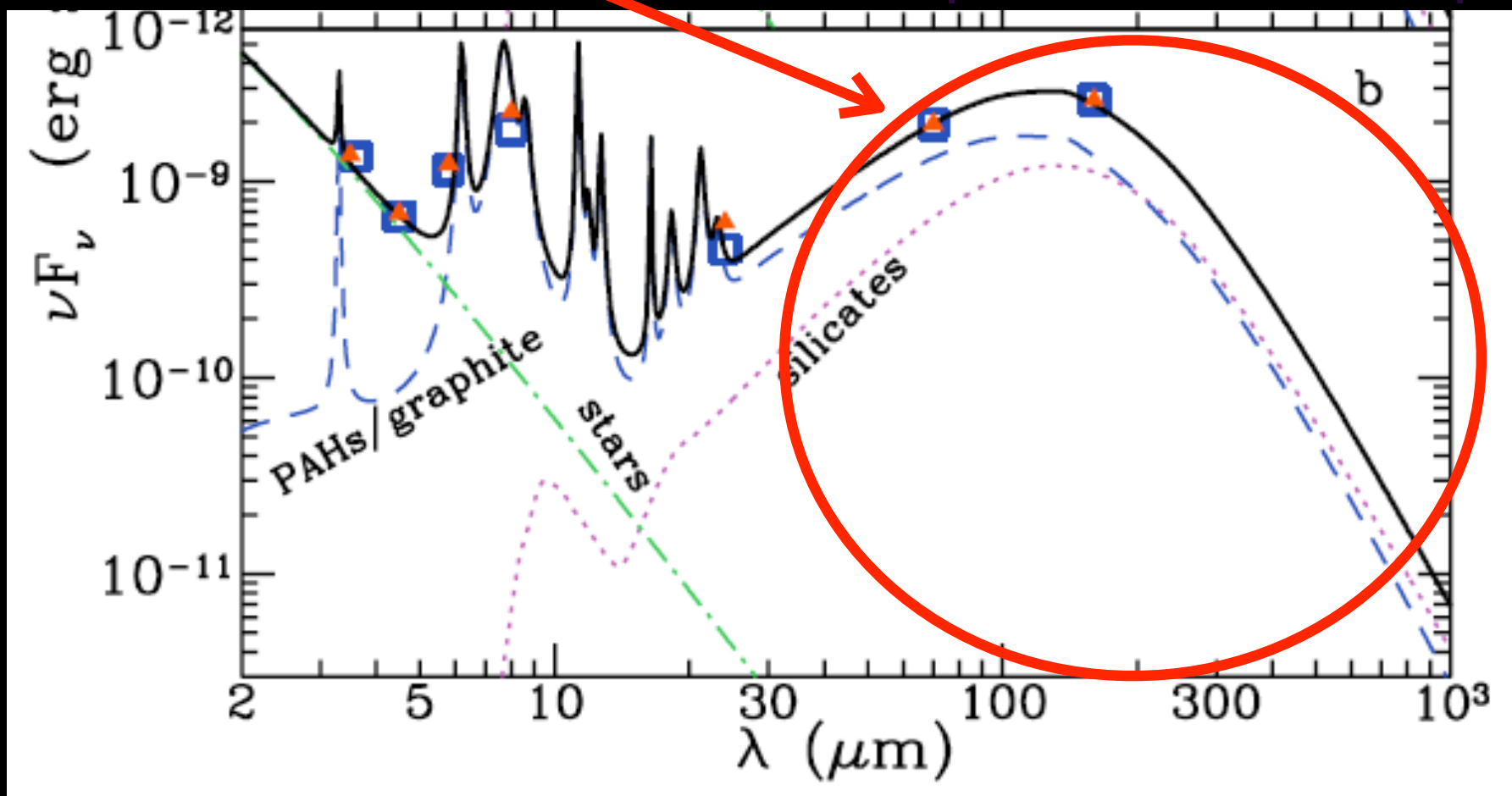


- Mostly PAH
- Some HII region lines
- Some molecular Hydrogen

FIG. 2.—Low-resolution spectrum of the inner ring and nucleus (central magenta rectangle in Fig. 1). Alternating colors indicate spectra from the four SL and LL orders. *Inset:* Expanded PAH spectrum with a diffuse ISM PAH + graphite + silicate model (Li & Draine 2001) overlaid as a dashed line, arbitrarily scaled to match the 7.7 μm peak. The broad 17 μm complex seen is blended with $\text{H}_2\text{ S}(1)$ and contains a sharp feature matching the model at 16.4 μm . Symbols represent matched photometry with filter widths shown, where squares denote IRAC 8 μm and MIPS 24 μm (Regan et al. 2004) and triangles denote ISOCAM LW2 (5.0 μm), LW6 (7.0 μm), LW7 (8.5 μm), LW8 (10.7 μm), LW3 (12.0 μm), and LW9 (14.0 μm).

Large grains dominate emission at $\lambda > 30\mu$

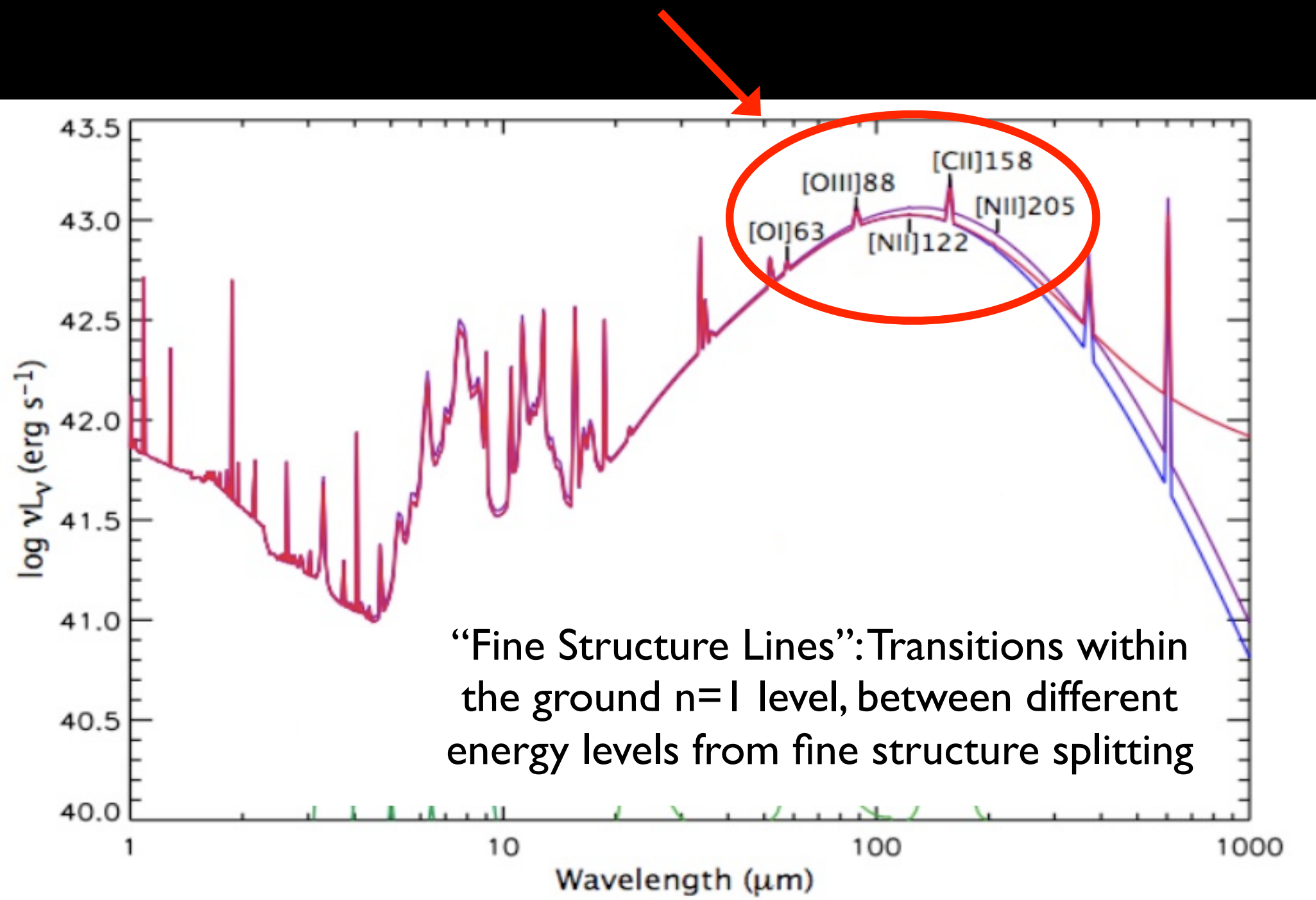
(Note: not necessarily due to a single temperature dust component)



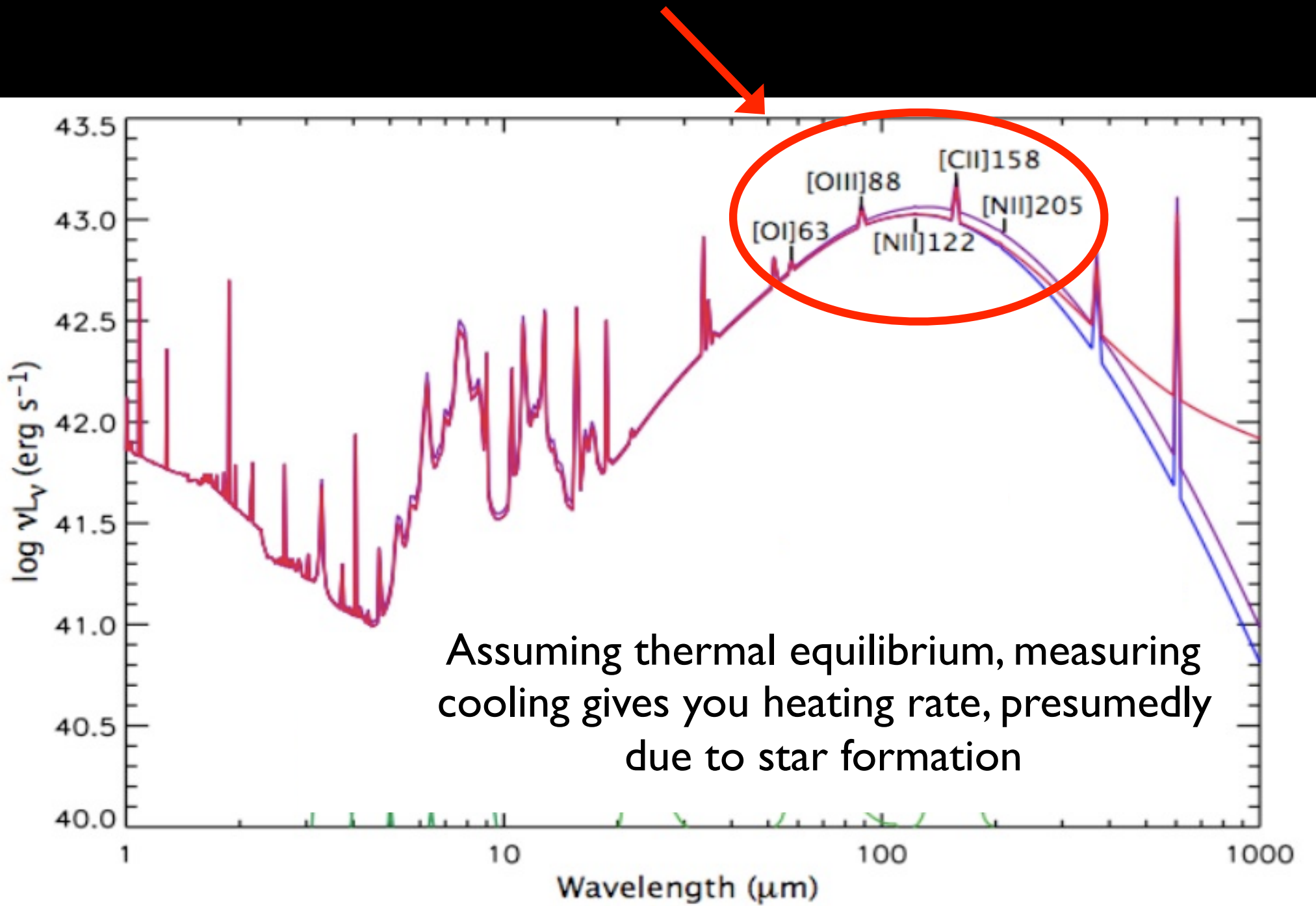
Regan et al 2004

FIG. 3.—SED and model fits to (a) the ring region and (b) the entire galaxy using the model of Li & Draine (2001, 2002b). The solid black lines and red triangles are the model-predicted fluxes, and the blue squares are the observed fluxes. The colored curves indicate the contributions of the different model components.

Fine-Structure Lines: ISM Coolants

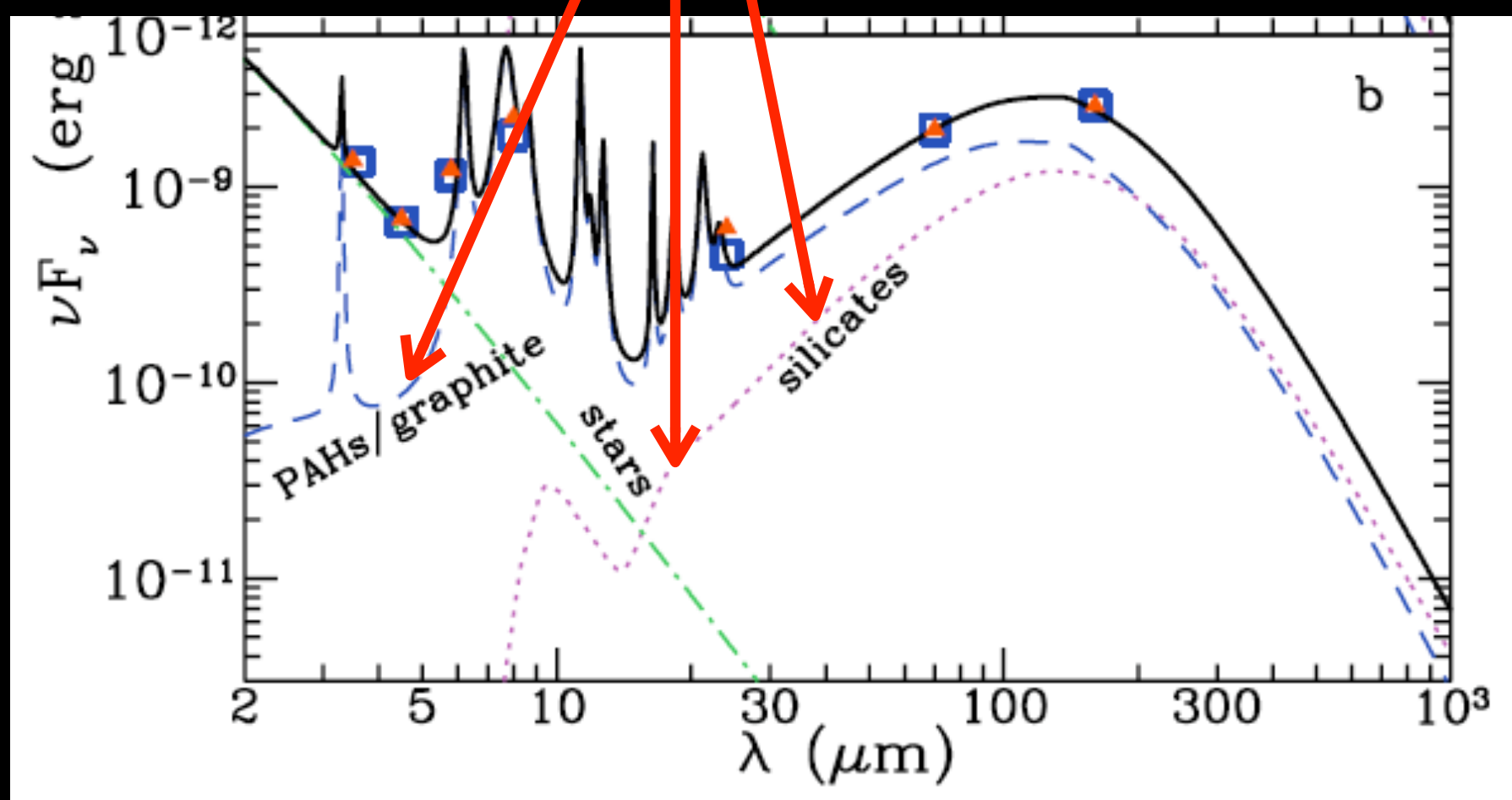


Fine-Structure Lines: ISM Coolants



Mid- and Far-IR emission typically modeled with “Drain & Li models”

See also DustEm and Themis:
<https://www.ias.u-psud.fr/DUSTEM/>
https://www.ias.u-psud.fr/themis/THEMIS_model.html

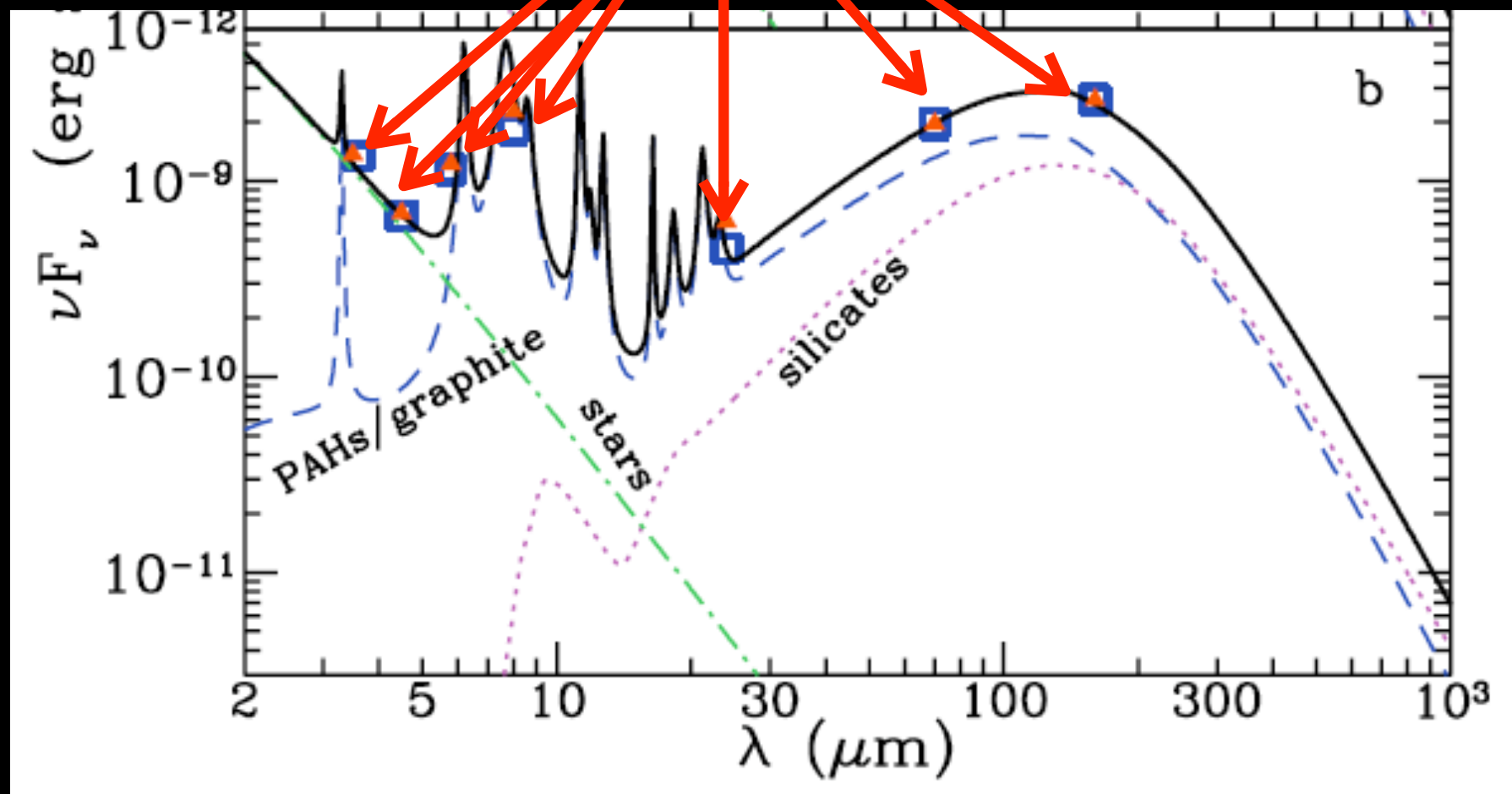


Regan et al 2004

FIG. 3.—SED and model fits to (a) the ring region and (b) the entire galaxy using the model of Li & Draine (2001, 2002b). The solid black lines and red triangles are the model-predicted fluxes, and the blue squares are the observed fluxes. The colored curves indicate the contributions of the different model components.

High resolution spectroscopy is expensive and rare, so models usually fit the broad SED

More points and more long λ coverage improves fits



Regan et al 2004

FIG. 3.—SED and model fits to (a) the ring region and (b) the entire galaxy using the model of Li & Draine (2001, 2002b). The solid black lines and red triangles are the model-predicted fluxes, and the blue squares are the observed fluxes. The colored curves indicate the contributions of the different model components.

Examples of Drain & Li parameterizations

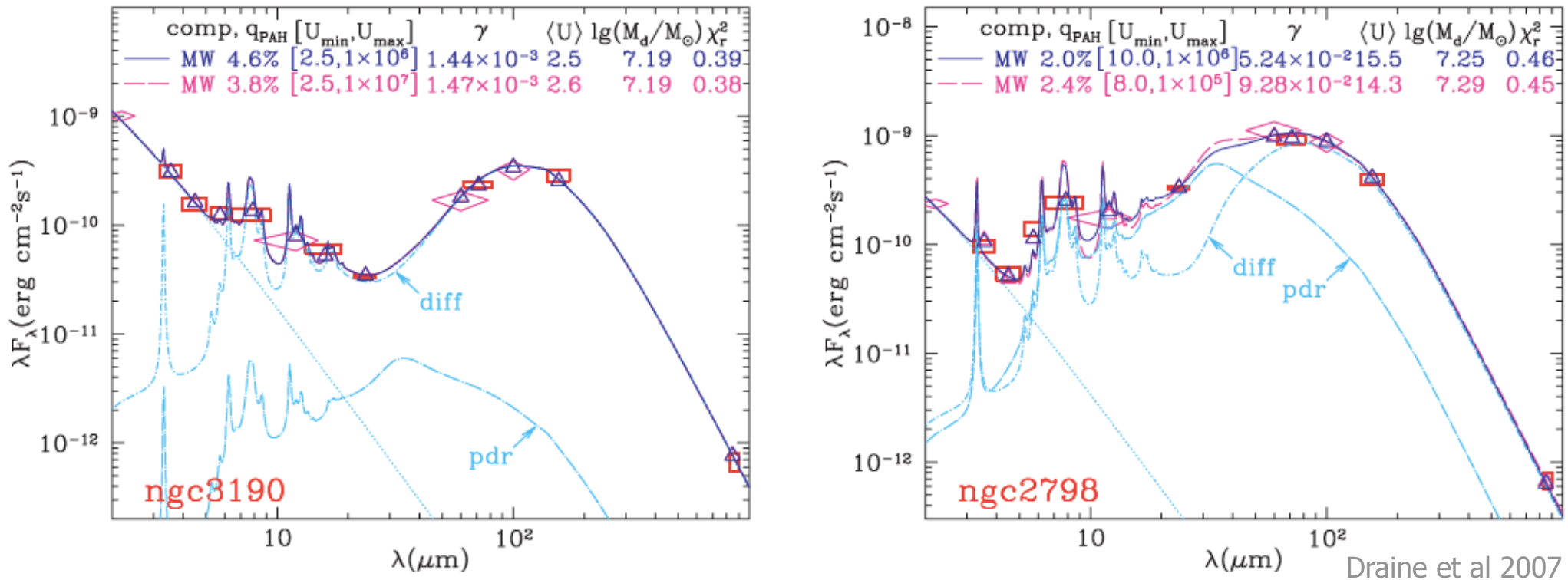


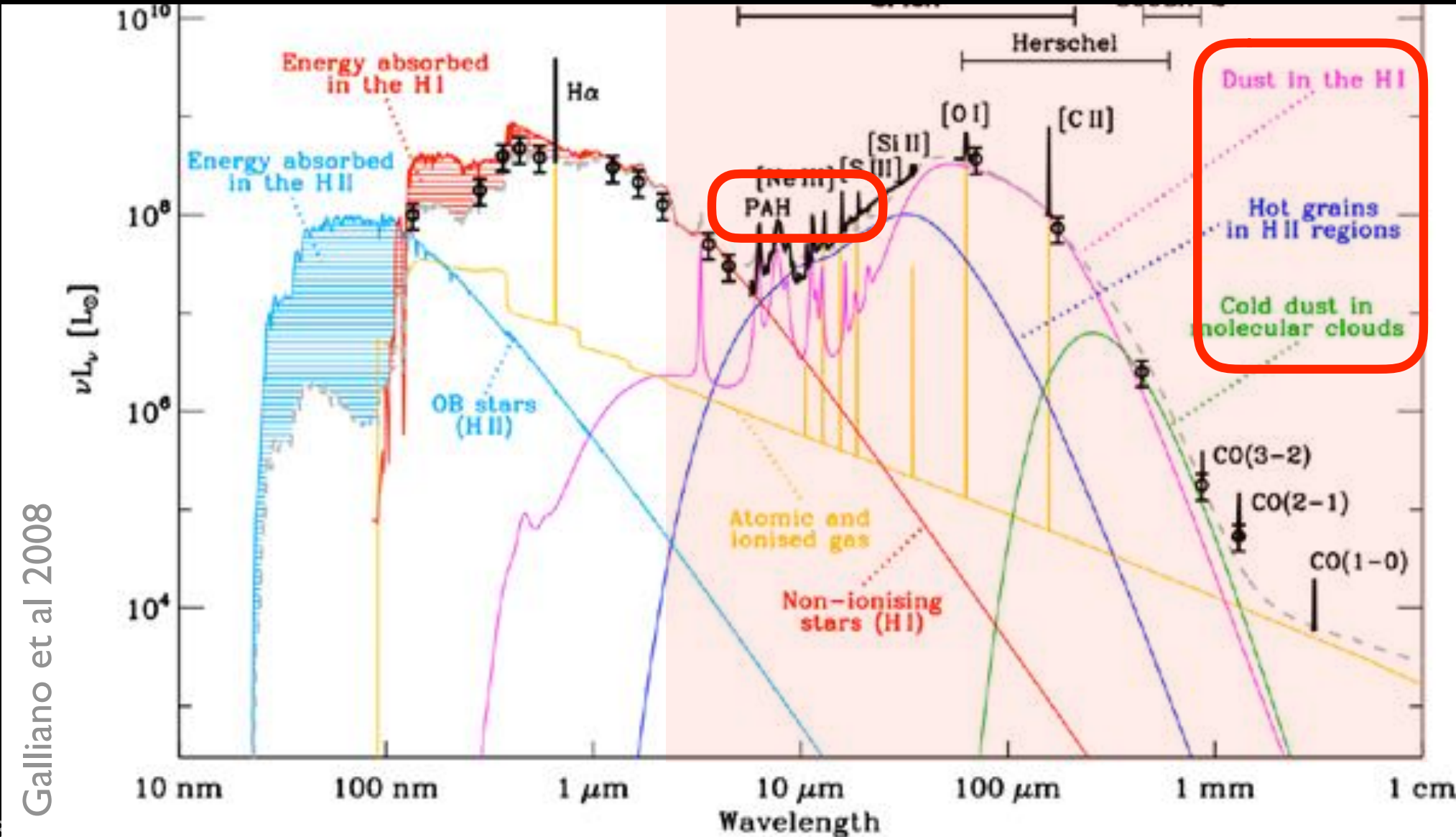
FIG. 3.—(a) SED for the SAap galaxy NGC 3190. Rectangles show observed fluxes in the IRAC, MIPS, SCUBA, and IRS 16 μm bands; diamonds show 2MASS 2.2 μm and *IRAS* 12, 60, and 100 μm fluxes. Vertical extent of rectangles and diamonds corresponds to $\pm 1 \sigma$ range, and width corresponds to nominal width of band. The solid line shows the best-fit $U_{\max} = 10^6$ model, with IRAC, MIPS, IRS 16 μm , *IRAS*, and SCUBA data used to constrain the fit; $N_b = 12$ for NGC 3190. Triangles show the model convolved with the IRAC, MIPS, IRS 16 μm , *IRAS*, and SCUBA bands. Dot-dashed lines show separate contributions of starlight and emission from dust heated by $U = U_{\min}$ (labeled “diff”) and dust heated by $U_{\min} < U < U_{\max}$ (labeled “pdr”). The long-dashed line shows the best-fit model when U_{\max} is unconstrained; for this case the model spectrum is nearly indistinguishable for the simple reason that there is relatively little dust ($\gamma \approx 0.0015$), and therefore relatively little power, in the “pdr” component. (b) Same as (a), but for the SBa galaxy NGC 2798, with $N_b = 11$ (global imaging in the IRS 16 μm band is unavailable).

- “Diffuse” dust, heated by low intensity background radiation field within the galaxy
- “PDR” dust, heated in high-intensity radiation field

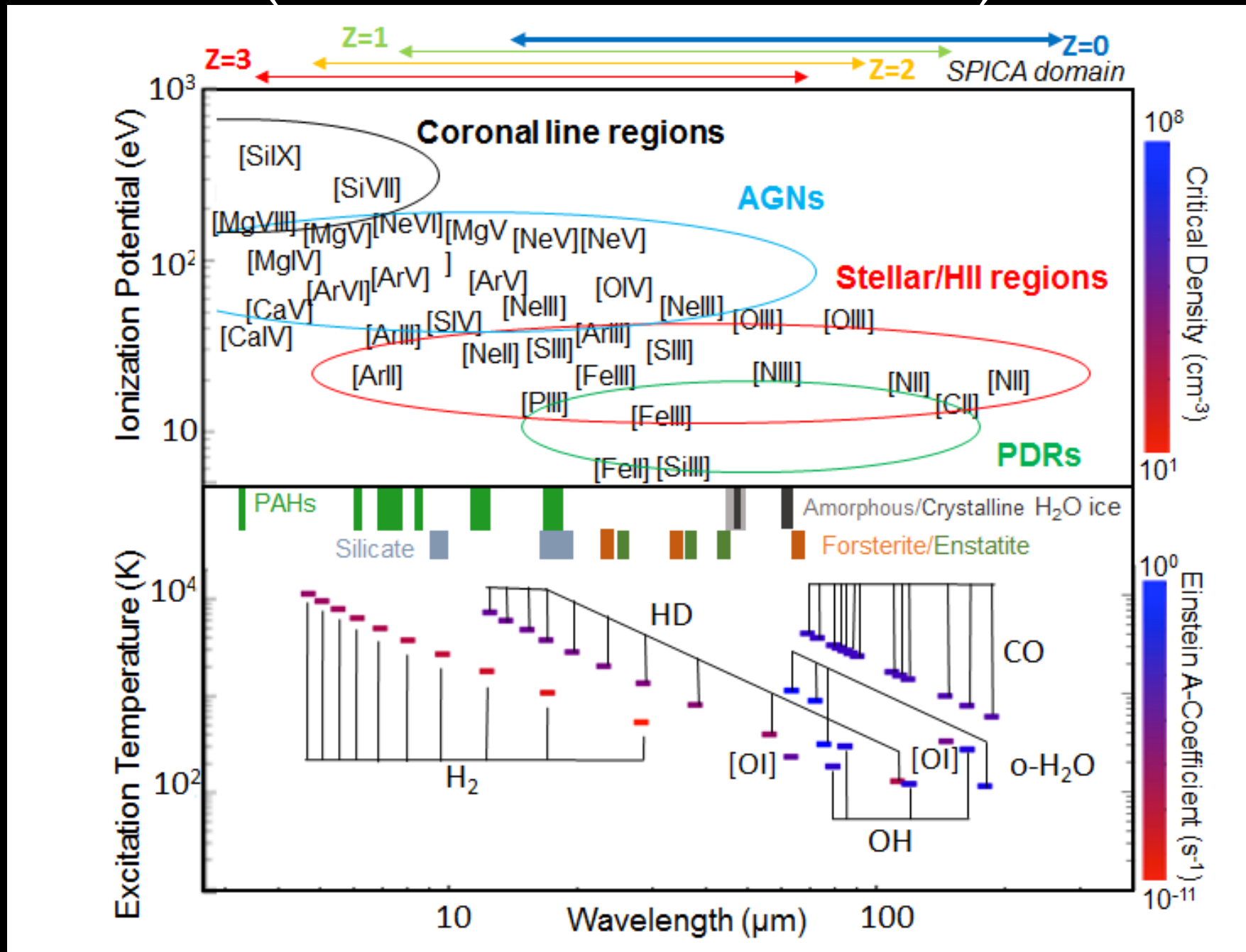
Dust is an important focus of current technology

Why look at mid- and far-IR emission?

Relative strengths of dust components are diagnostics of ISM, SFRs, AGN



Also, many useful mid- and far-IR line diagnostics
(i.e., not dust, but useful!)



MIR/FIR Telescopes (Space, mostly)

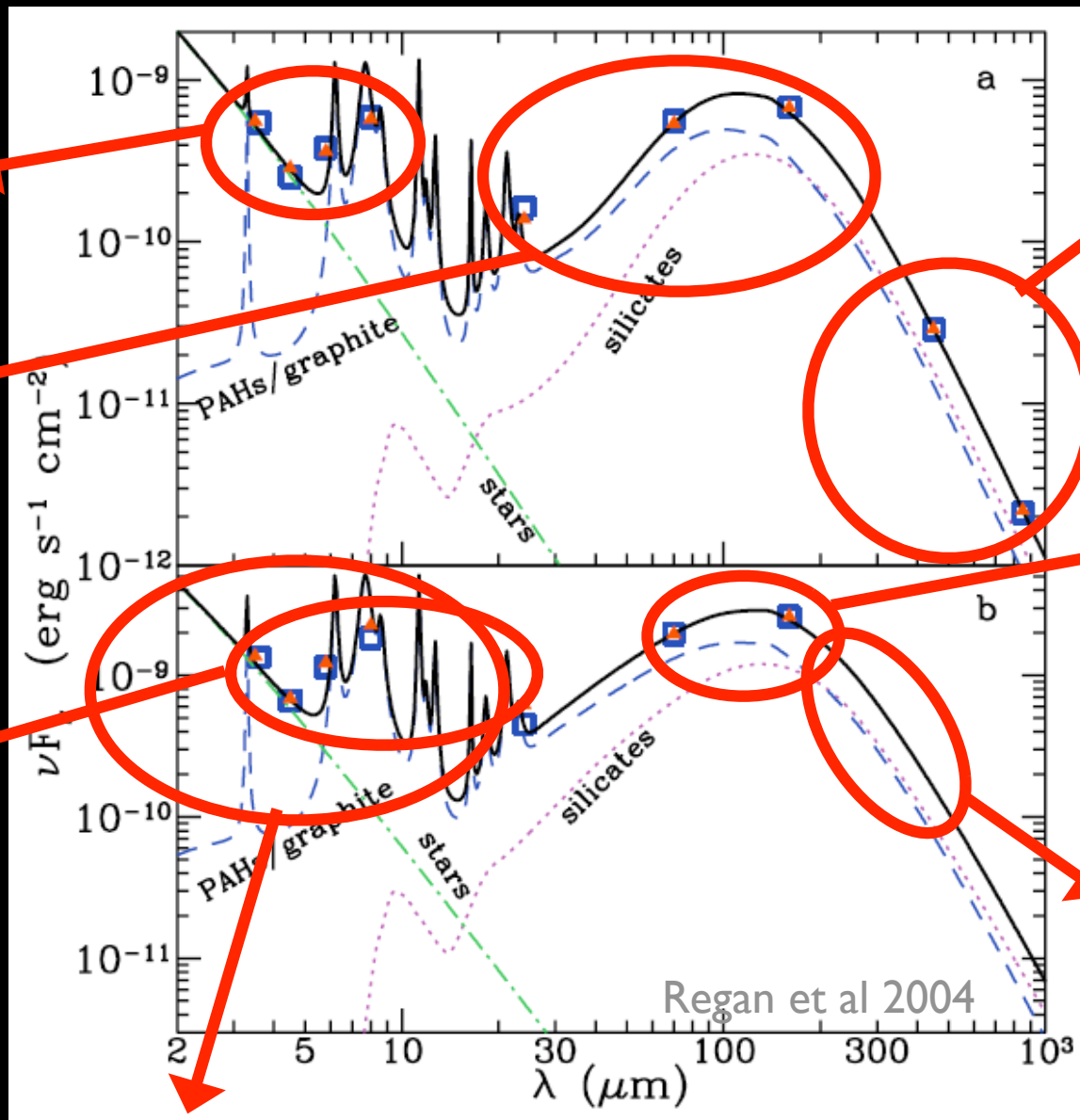
Spitzer

1. IRAC $3.6\mu\text{m}$,
 $4.5\mu\text{m}$, $5.8\mu\text{m}$,
 $8\mu\text{m}$
2. MIPS $24\mu\text{m}$,
 $70\mu\text{m}$, $160\mu\text{m}$

WISE

- 3-4 μm , 4-5 μm ,
8-16 μm ,
20-25 μm

JWST $0.8\mu\text{m} - 25\mu\text{m}$



SCUBA

$450\mu\text{m}, 850\mu\text{m}$

ALMA

$400\mu\text{m}-3\text{mm}$

Herschel

1. PACS integral field spectrograph;
 $60-85\mu\text{m}$,
 $85-130\mu\text{m}$,
 $130-210\mu\text{m}$
2. SPIRE $250\mu\text{m}$,
 $350\mu\text{m}$, $500\mu\text{m}$

$>500\mu\text{m} = \text{"sub-mm"}$

FIG. 3.—SED and model fits to (a) the ring region and (b) the entire galaxy using the model of Li & Draine (2001, 2002b). The solid black lines and red triangles are the model-predicted fluxes, and the blue squares are the observed fluxes. The colored curves indicate the contributions of the different model components.

Former State of the Art for MIR/ FIR photometry:

IRAS (5' beam)

12μm, 25μm, 60μm, 120μm

DIRBE (0.7° beam)

1-240μm

ISO

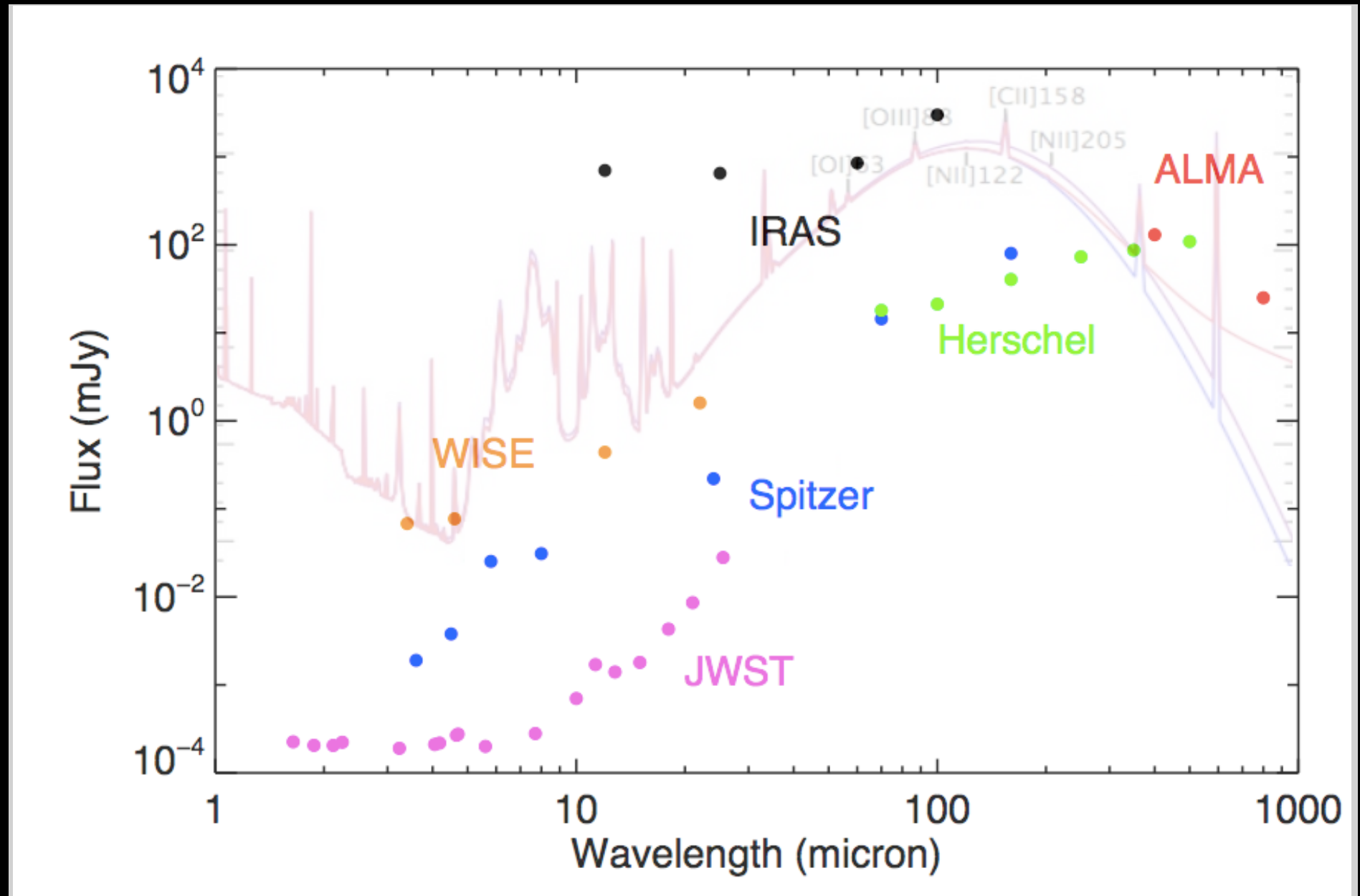
6-12μm (7" beam), 60-170μm (1.3' beam)

Also:

Planck (5-10' beam)

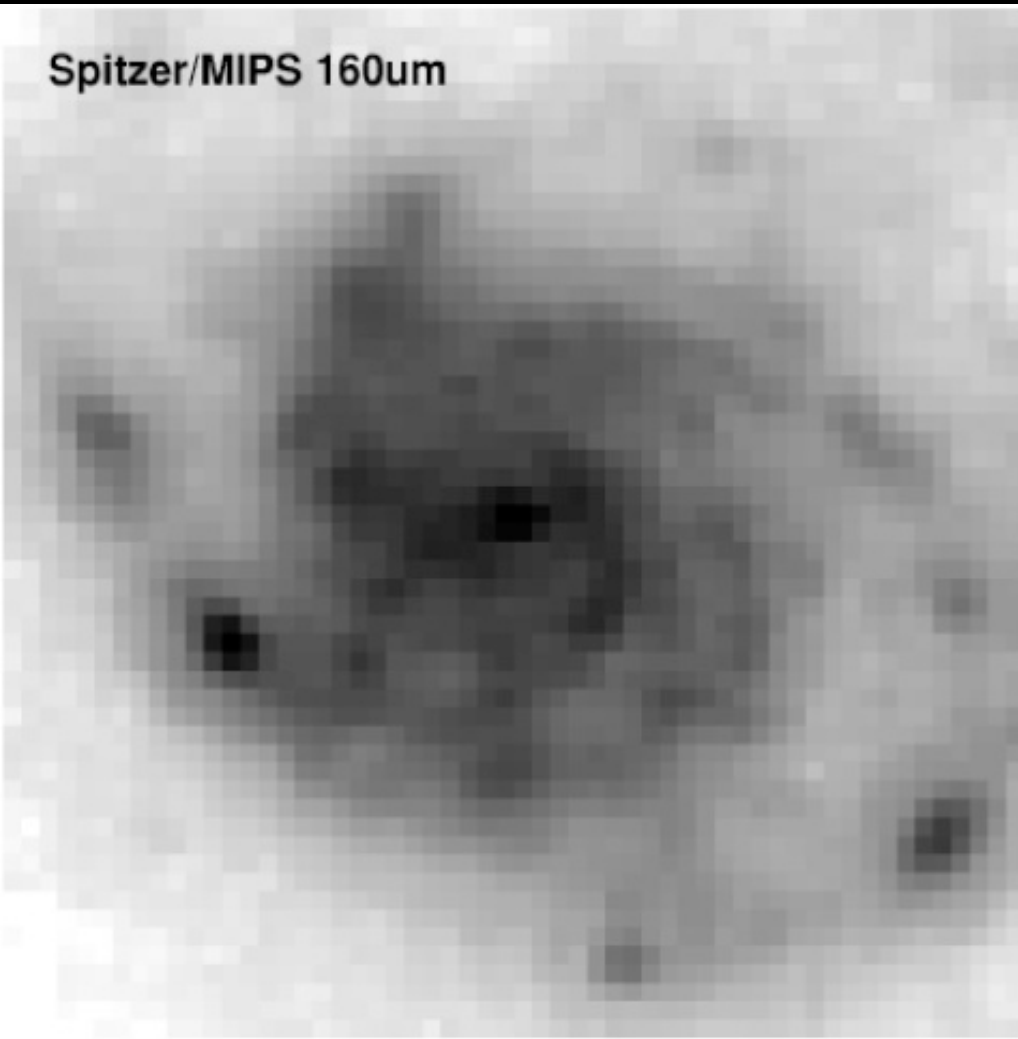
300μm-11,000μm

Limiting sensitivities are improving

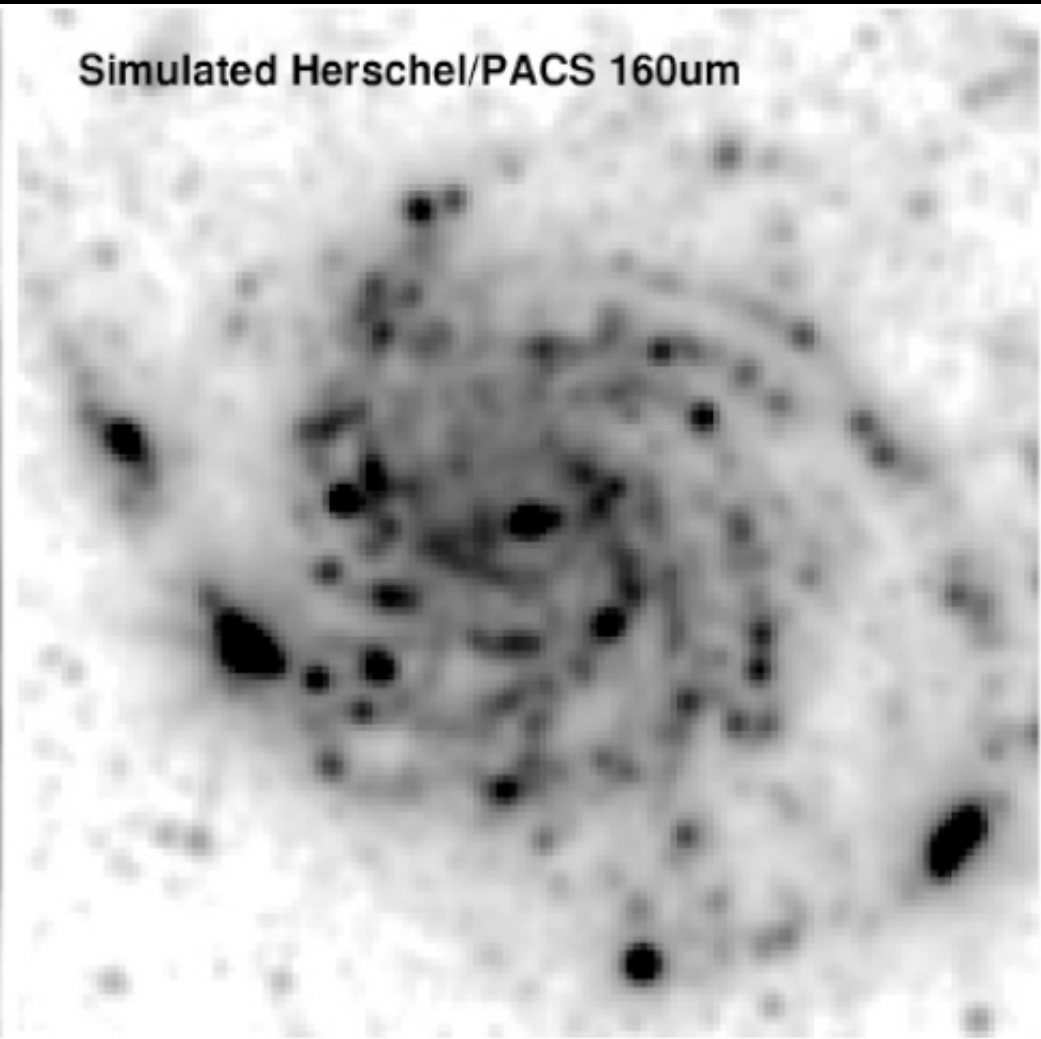


Resolution poor but also improving

Spitzer/MIPS 160um



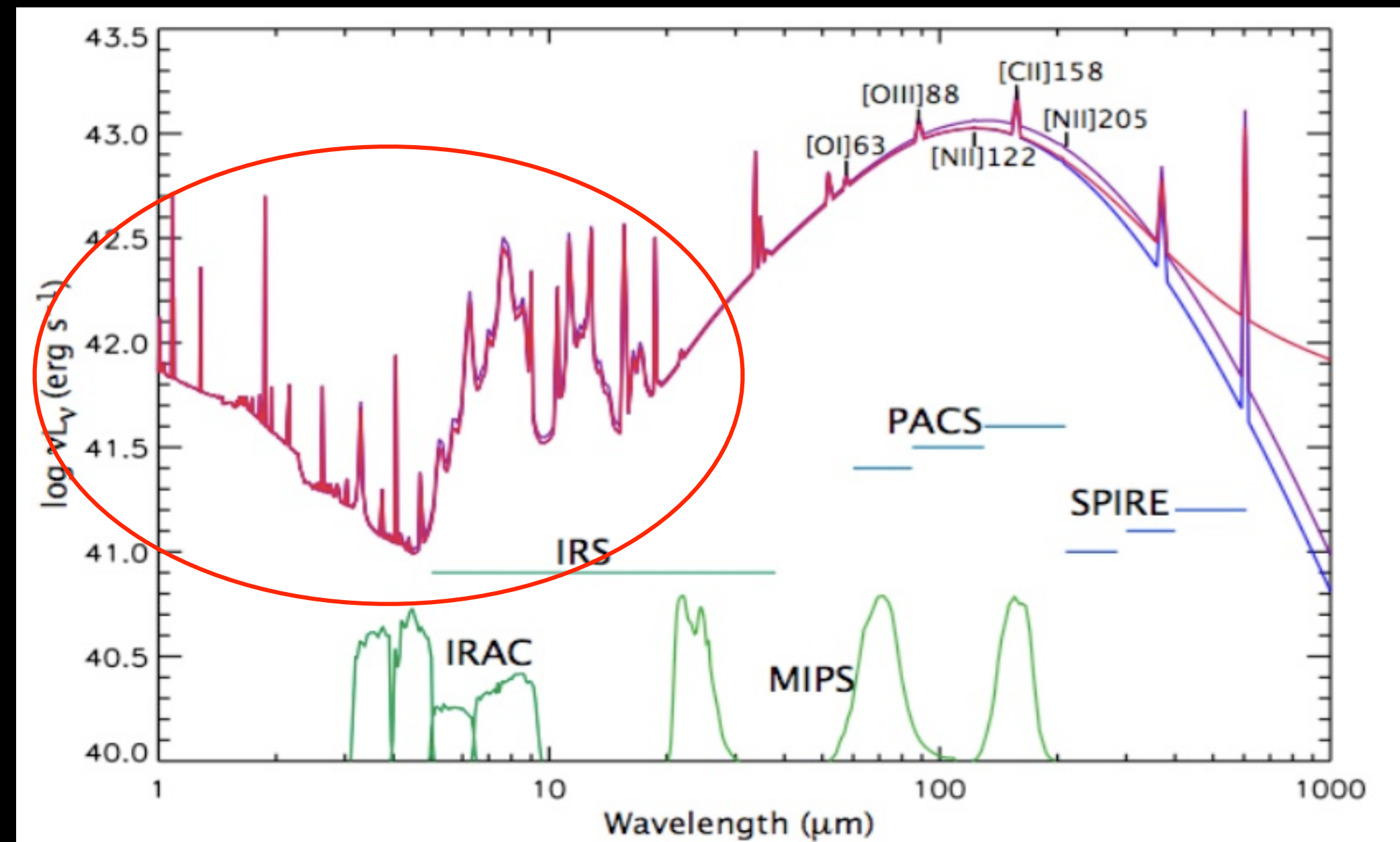
Simulated Herschel/PACS 160um



Herschel angular resolution
(PACS: 5-13'', SPIRE: 18-36'')

ALMA even better, but only very long λ

JWST (2020?): 6.5m, so better resolution



Dust Technology Questions

- How will JWST perform?
- If JWST blows up, what happens to all of NASA-funded space astronomy?

How is dust emission distributed
within galaxies?

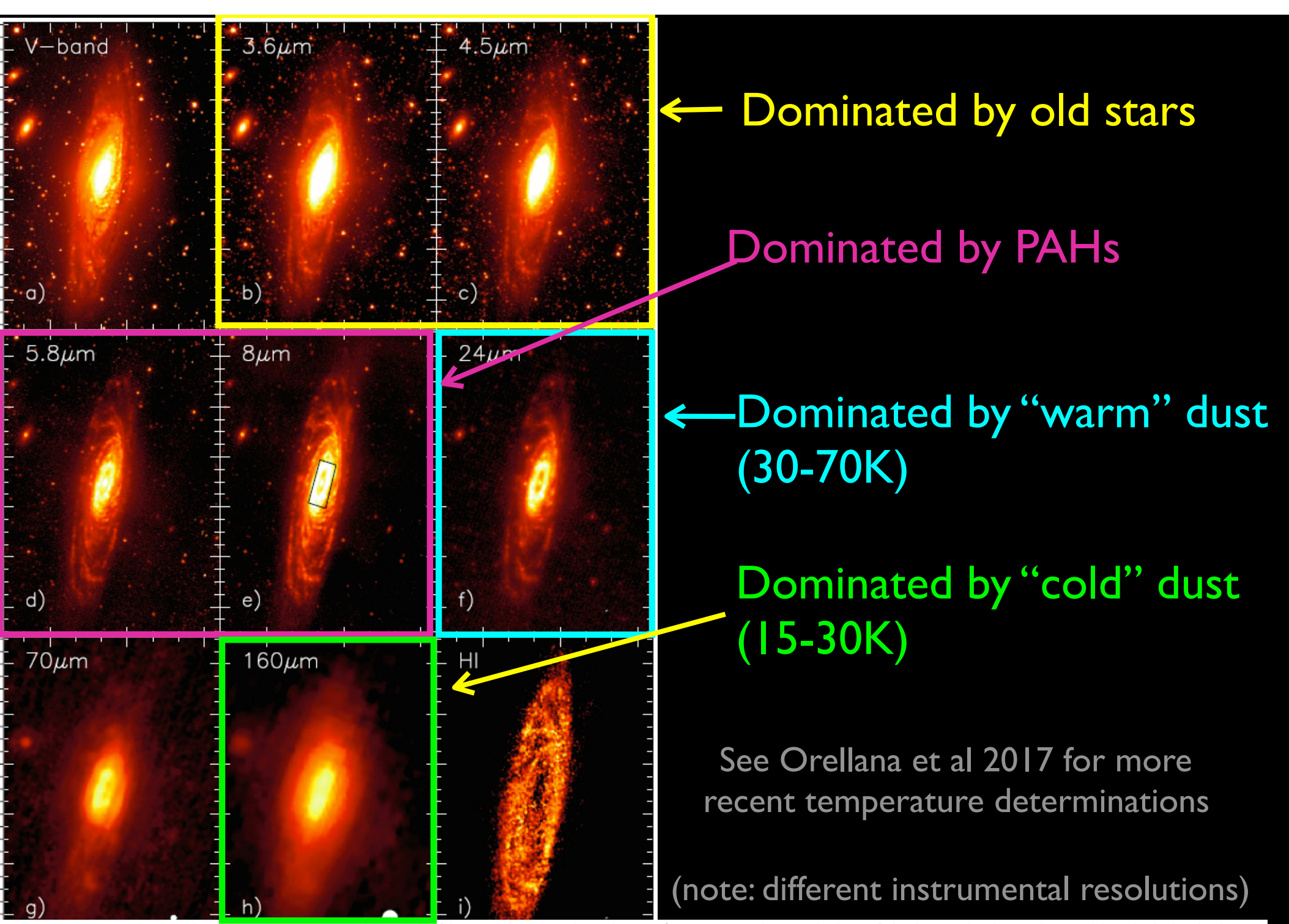
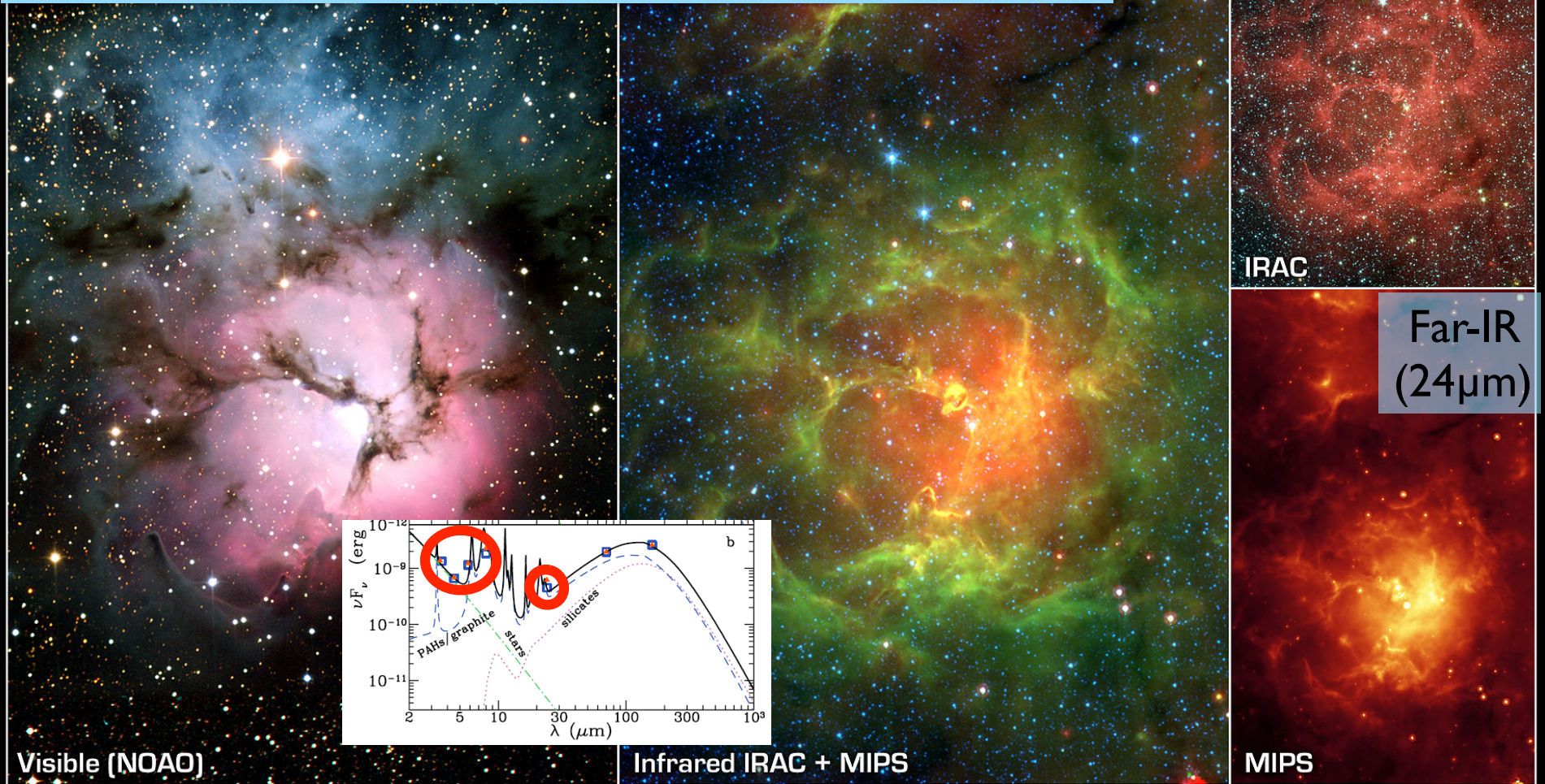


Fig. 1.—Panchromatic view of NGC 7331 in order of increasing wavelength. For $\lambda \geq 24 \mu\text{m}$, the resolution of the image is shown by a white circle in the lower right of each frame. (a) V -band ($0.54 \mu\text{m}$); (b) IRAC $3.6 \mu\text{m}$; (c) IRAC $4.5 \mu\text{m}$; (d) IRAC $5.8 \mu\text{m}$; (e) IRAC $8 \mu\text{m}$ (with a rectangle indicating ring aperture for Table 1); (f) MIPS $24 \mu\text{m}$; (g) MIPS $70 \mu\text{m}$; (h) MIPS $160 \mu\text{m}$; (i) H I (21 cm) line emission.

Regan et al 2004

Dust in HII regions

Heated by strong UV flux from O & B stars, which can also destroy PAHs

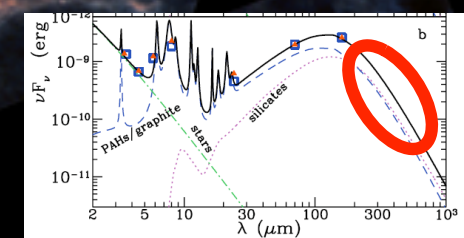
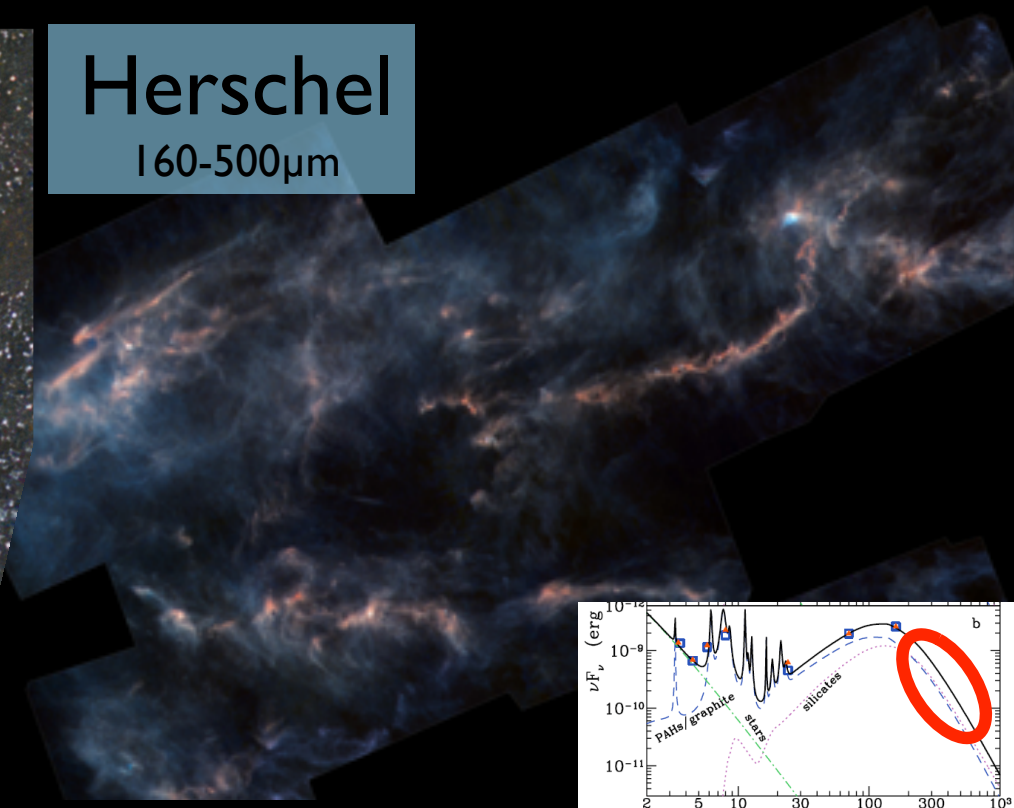


Dust in Molecular Clouds

Visible



Herschel
160-500 μ m



Mostly shielded by interstellar radiation field (ISRF),
so typically cold ($\sim 10K$) until SF starts

Taurus molecular cloud; Only forming low mass stars in the dense filament

160 μ m (blue), 250 μ m (green), 350 μ m (split between green and red) and 500 μ m (red) w/ Herschel

Cold dust in Orion

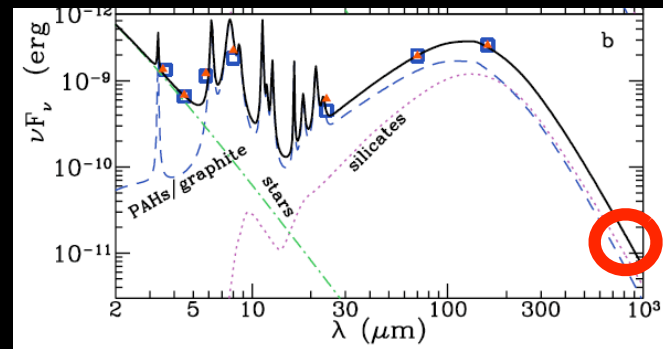
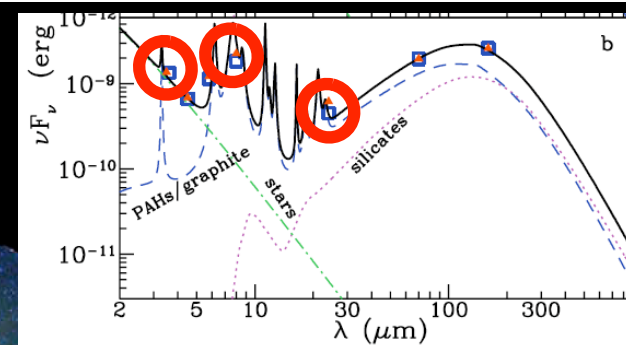


Image by LABOCA
(~870mm) on
APEX (Atacama
Pathfinder
Experiment)



Dust in neutral gas

Mid-IR
(Milky Way plane)



3.6 μm (blue; stars), 8 μm (green; PAH), 24 μm (red; warm dust) w/ Spitzer

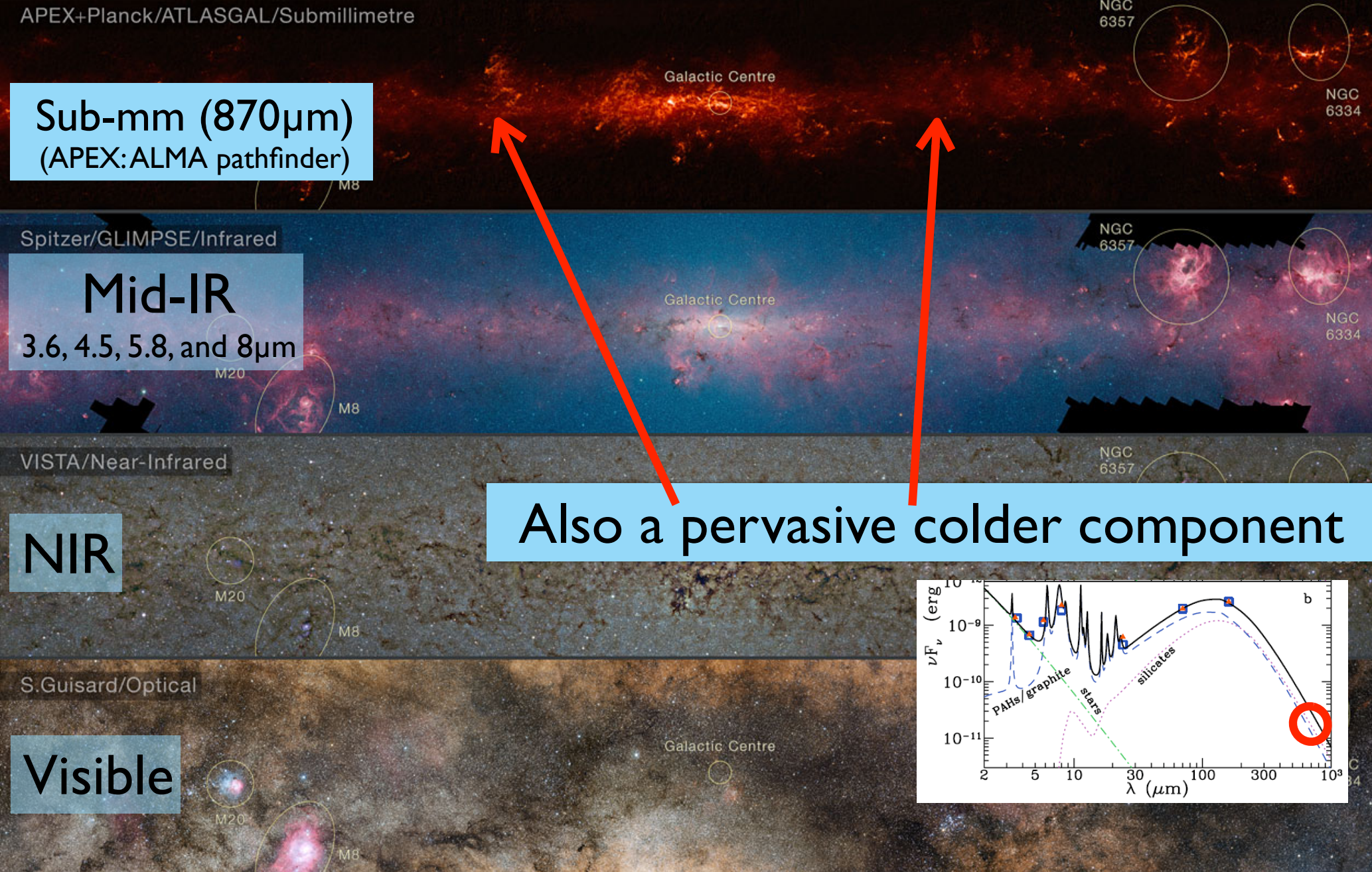
Heated by diffuse, integrated ISRF, not local SF.
Less shielded than in molecular clouds

GLIMPSE survey:

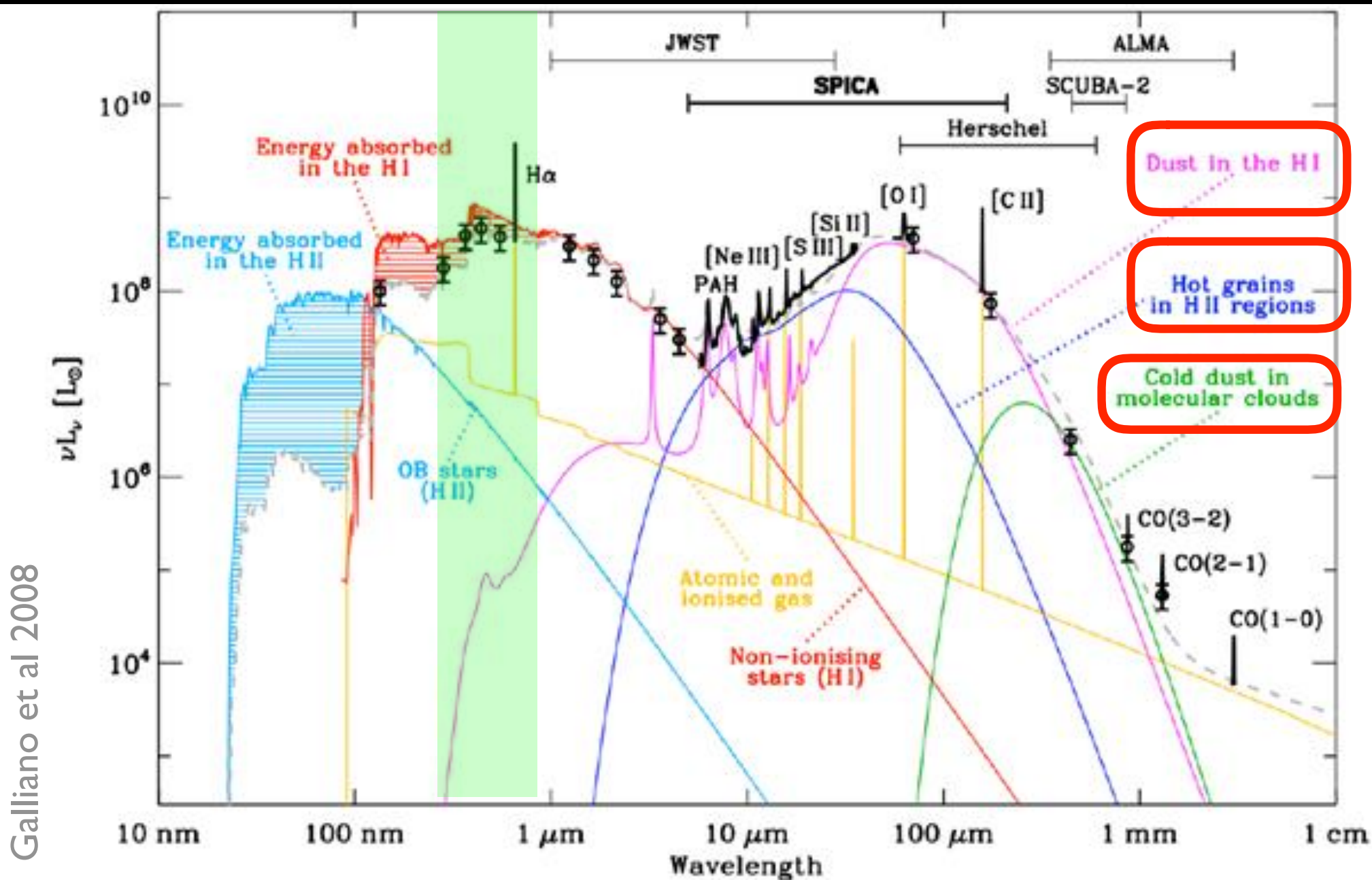
<http://www.spitzer.caltech.edu/images/3354-ssc2008-11a7-GLIMPSE-MIPSGAL-Milky-Way-7>

Dust in neutral gas

<https://www.eso.org/public/news/eso1606/>



Relative strength & temp of these components vary galaxy-to-galaxy and/or internally



$3.6\mu\text{m}$ (old stars)

peak = 1.2 MJy/sr

$4.5\mu\text{m}$ (old stars)

1.0 MJy/sr

BVRH α

H i

24 μm traces HII region dust

(a)

(e)

(i)

(b)

H α

24 μm

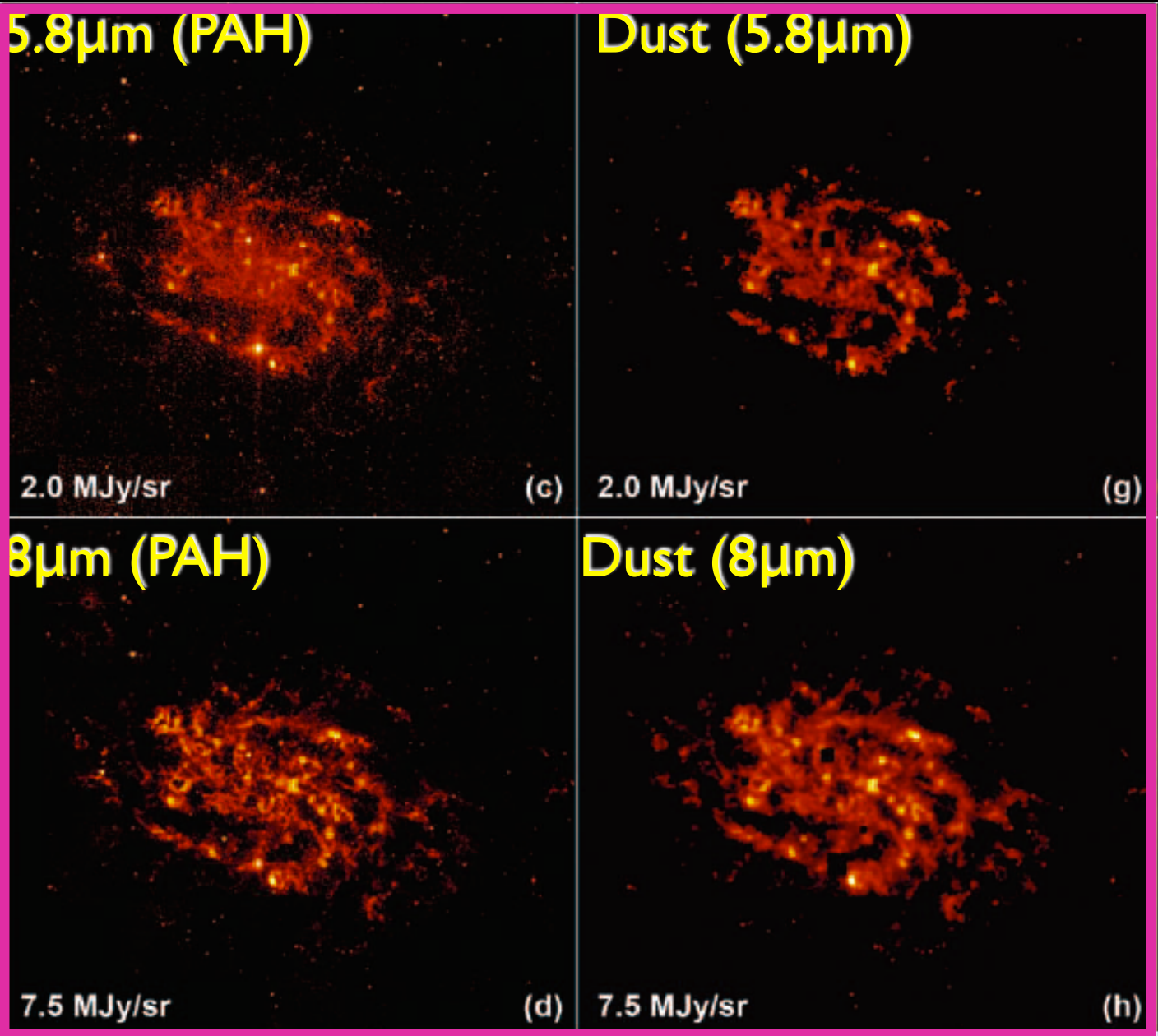
(f)

(j)

6 MJy/sr



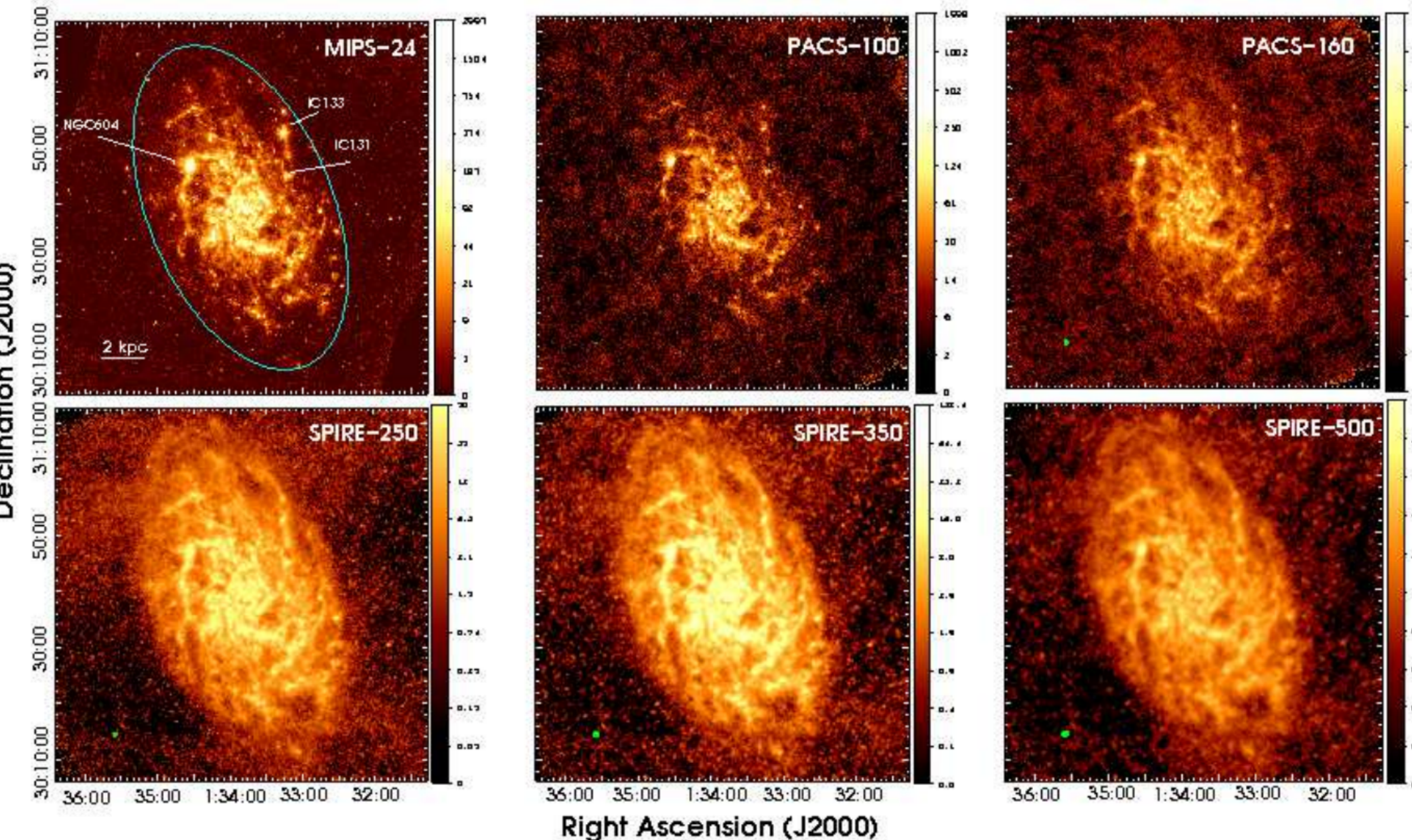
FIG. 1.—Images of NGC 300 obtained with *Spitzer* and other sources. The leftmost column shows observed maps at (a) $3.6\mu\text{m}$, (b) $4.5\mu\text{m}$, (c) $5.8\mu\text{m}$, and (d) $8\mu\text{m}$. The center column shows (e) a BVRH α composite image (credit MPG/ESO) in which *B* is coded in blue, *V* in green, and *R* and H α in red; (f) the H α map described in § 2; (g) a dust map at $5.8\mu\text{m}$; and (h) a dust map at $8\mu\text{m}$. The rightmost column shows (i) the H i map from Puche et al. (1990) and observed maps at (j) $24\mu\text{m}$, (k) $70\mu\text{m}$, and (l) $160\mu\text{m}$, with photometric apertures used in Fig. 5 superposed. Each frame contains the peak surface brightness in the background-subtracted image; all images are in logarithmic scale, except the $160\mu\text{m}$ image, which is linear. North is about 40° clockwise from vertical up, and each frame is approximately $20'$ on a side.



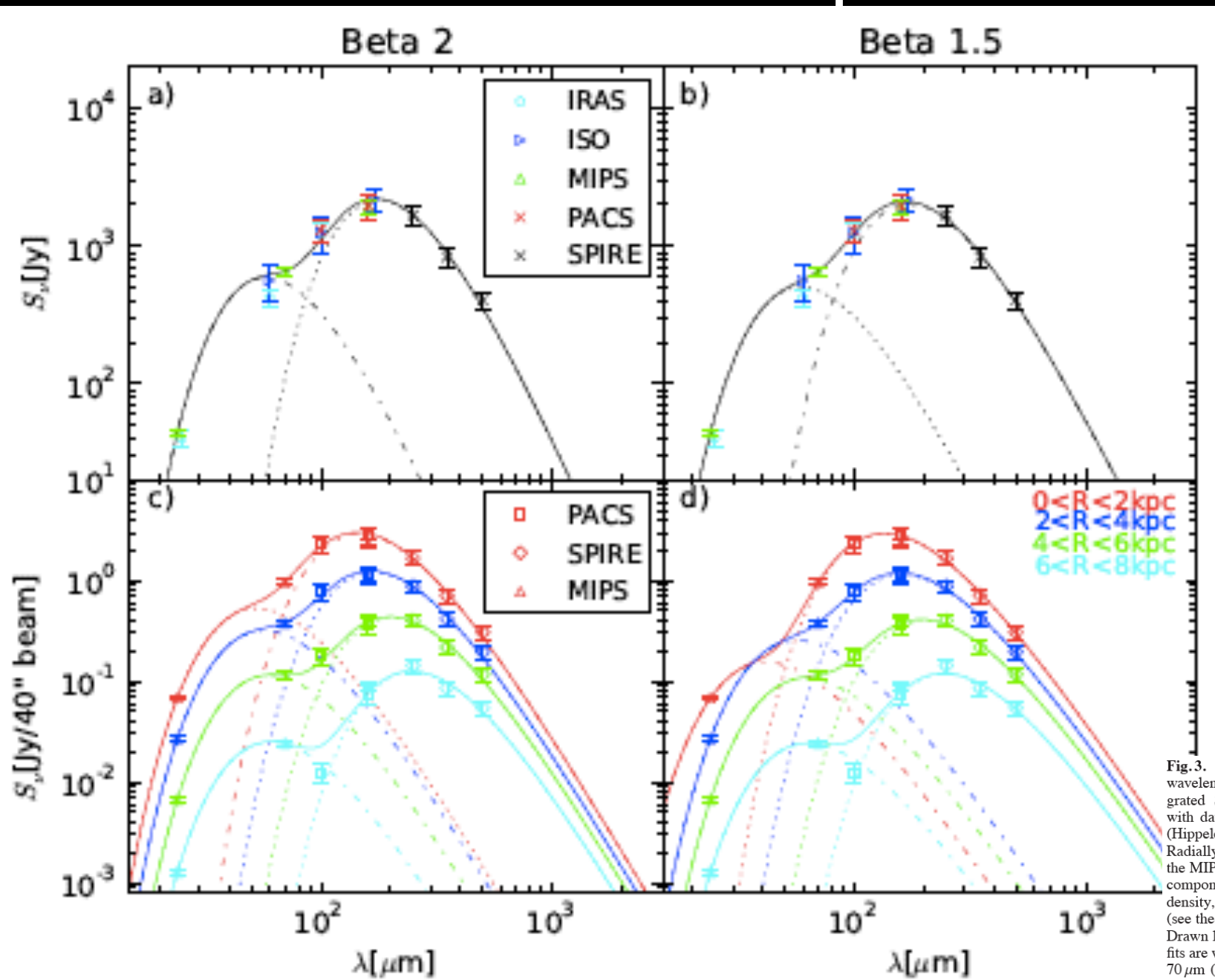
Mid-IR PAH somewhat more diffuse than H α , but still traces spiral arms

FIG. 1.—Images of NGC 300 obtained with *Spitzer* and other sources. The leftmost column shows observed maps at (a) 3.6 μ m, (b) 4.5 μ m, (c) 5.8 μ m, and (d) 8 μ m. The center column shows (e) a *BVRH α* composite image (credit MPG/ESO) in which *B* is coded in blue, *V* in green, and *R* and H α in red; (f) the H α map described in § 2; (g) a dust map at 5.8 μ m; and (h) a dust map at 8 μ m. The rightmost column shows (i) the H i map from Puche et al. (1990) and observed maps at (j) 24 μ m, (k) 70 μ m, and (l) 160 μ m, with photometric apertures used in Fig. 5 superposed. Each frame contains the peak surface brightness in the background-subtracted image; all images are in logarithmic scale, except the 160 μ m image, which is linear. North is about 40° clockwise from vertical up, and each frame is approximately 20' on a side.

>100 μ m cold dust more diffuse, though lower resolution



Radial distributions fit by combinations of cold+warm components or...



M33:
Herschel
+ Spitzer
+ Others

Kramer et al
2010

Fig. 3. Spectral energy distributions (SEDs) of M33 at wavelengths between $24 \mu\text{m}$ and $500 \mu\text{m}$. a, b: Total integrated SED of M33, combining data of PACS & SPIRE, with data of MIPS/Spitzer (Tabatabaei et al. 2007), ISOCAM (Hippelein et al. 2003), and IRAS (Rice et al. 1990). c, d: Radially averaged SEDs in zones of 2 kpc width. Here, we show the MIPS, PACS, and SPIRE data. a, c: Drawn lines show two-component grey body model fit results. The $100 \mu\text{m}$ PACS flux density, measured in the outermost zone, was not used for the fits (see the text). The dust emissivity index was set to $\beta = 2$. b, d: Drawn lines show two-component models for $\beta = 1.5$. a-d: All fits are weighted by the assumed uncertainties: 7% for MIPS $24, 70 \mu\text{m}$ (Spitzer Observers Manual v8.0), 20% for PACS, 15% for SPIRE. The SEDs have not been de-projected.

...or by fitting SED models (Drain & Li 07, MAGPHYS; da Cunha et al 2010, GRASIL, CIGALE, etc; see Hunt et al 2018)

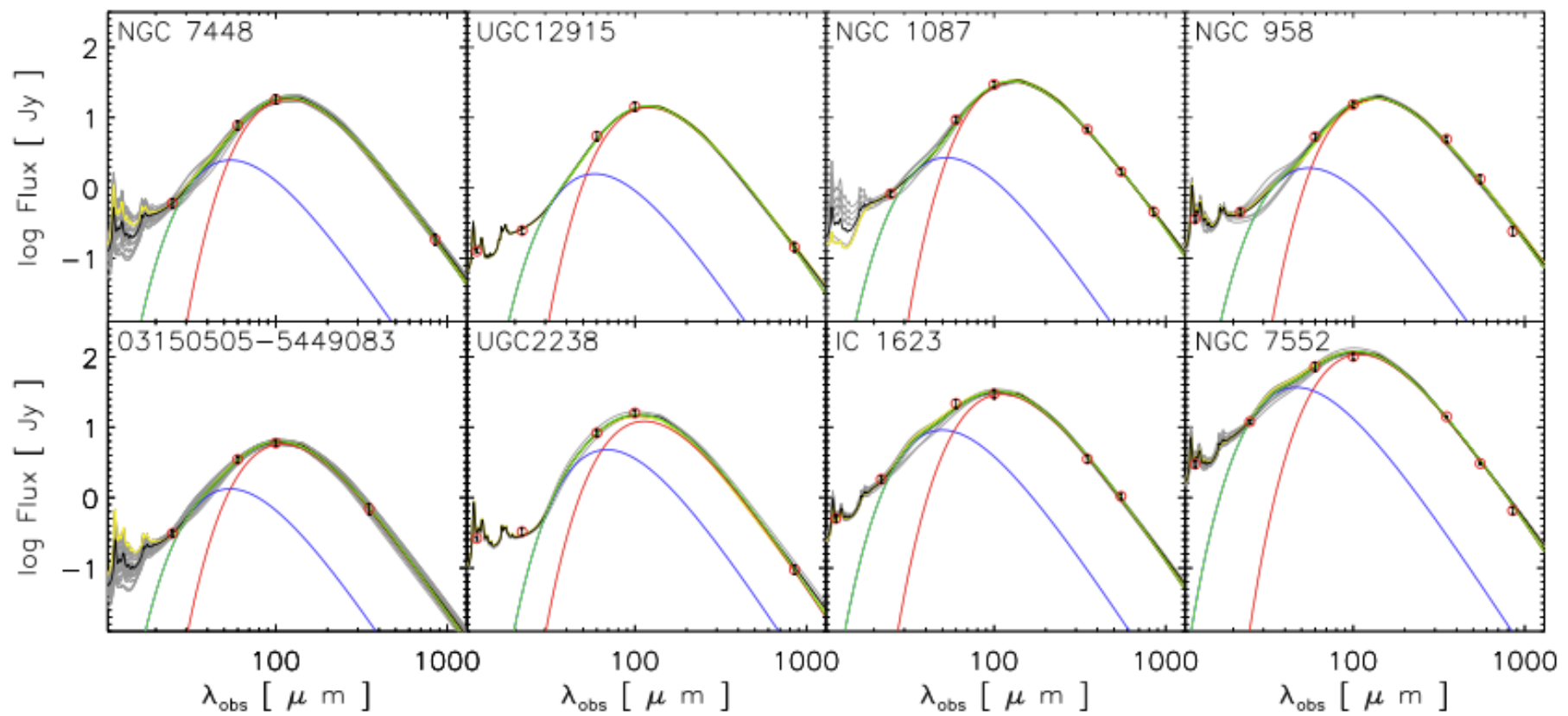


Fig. 4. Examples of DL07 spectral energy distribution (SED) fits to galaxies in our sample, as named in each panel. Photometric data points are shown with red circles and corresponding black error bars. Panels are organized (left to right) by the number of photometric data points (4 to 7 points). The top (bottom) row shows 'normal' star forming (starburst; SB) galaxies; (see Sect. 4.3). The single best-fit DL07 template SED is shown in yellow. All SEDs which satisfy the reduced χ^2 criterion (see Sect. 3) are shown in gray; the weighted geometric mean of these is used as our final template fit (FTF; shown in black). The two temperature component model fits (eqn. 7) are shown in red (cold dust component), blue (warm dust component), and green (sum of cold and warm dust components).

General results

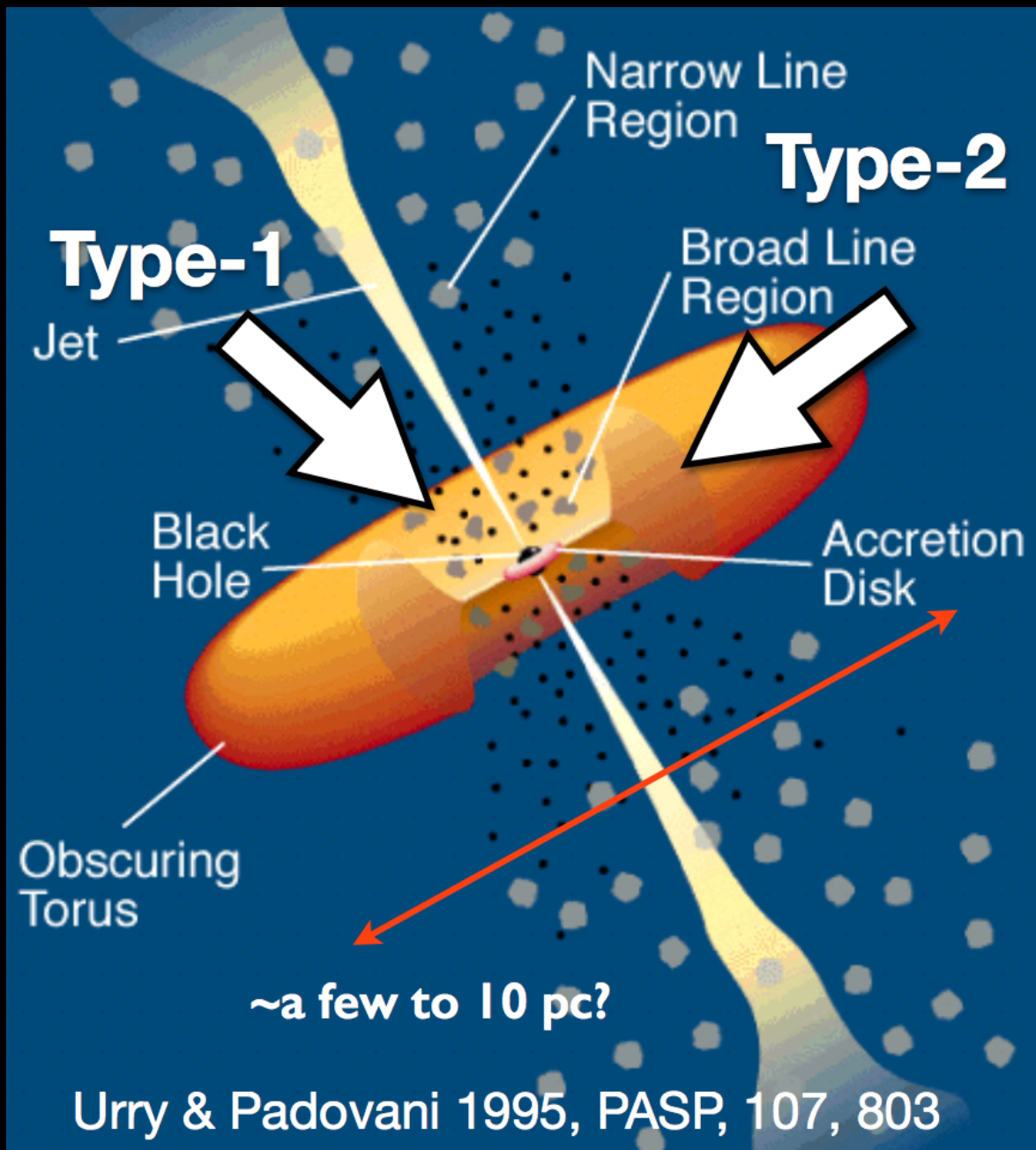
- Average dust temperature drops at larger radii in nearby disks
- Cold dust drastically outweighs warmer dust
- $24\mu\text{m}$ and $70\mu\text{m}$ are heated locally, but PAH and longer wavelengths are heated more by ISRF.

Dust emission questions

- How do we map limited mid- or far-IR observations onto total IR luminosity?
- What is the exact relationship between dust emission measurements and star formation?
- Do we really understand dust heating sources?
- Are the models that fit the SED appropriate and self-consistent?
- What are the actual sources of PAH emission, and what do the line strengths tell us?

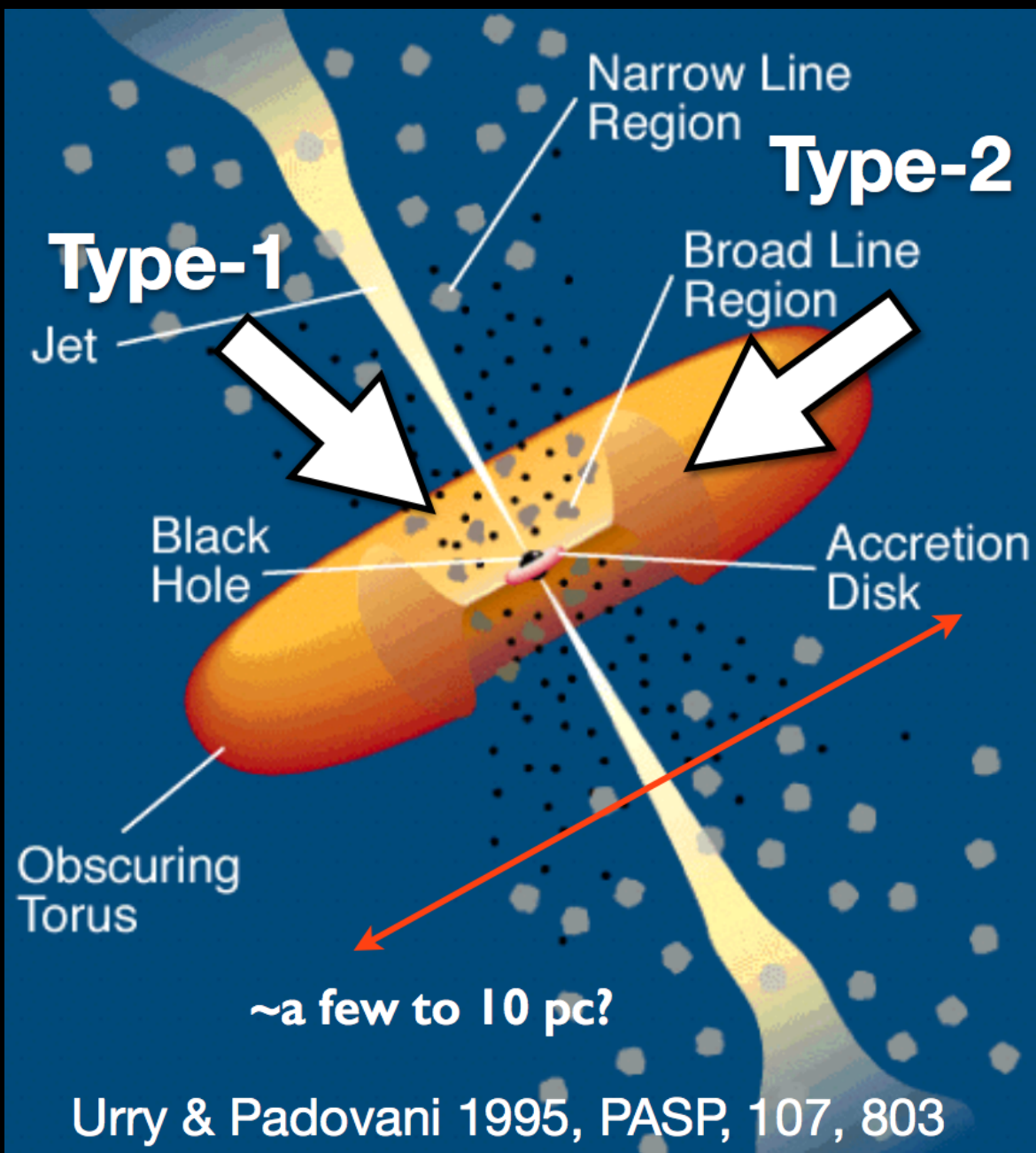
Dust emission can be due to Active
Galactic Nuclei (AGN)

Dust in “Active Galactic Nuclei” (AGN)



AGN are powered
by accretion disk
funneling gas onto
a supermassive
black hole (SMBH)

Dust in “Active Galactic Nuclei” (AGN)

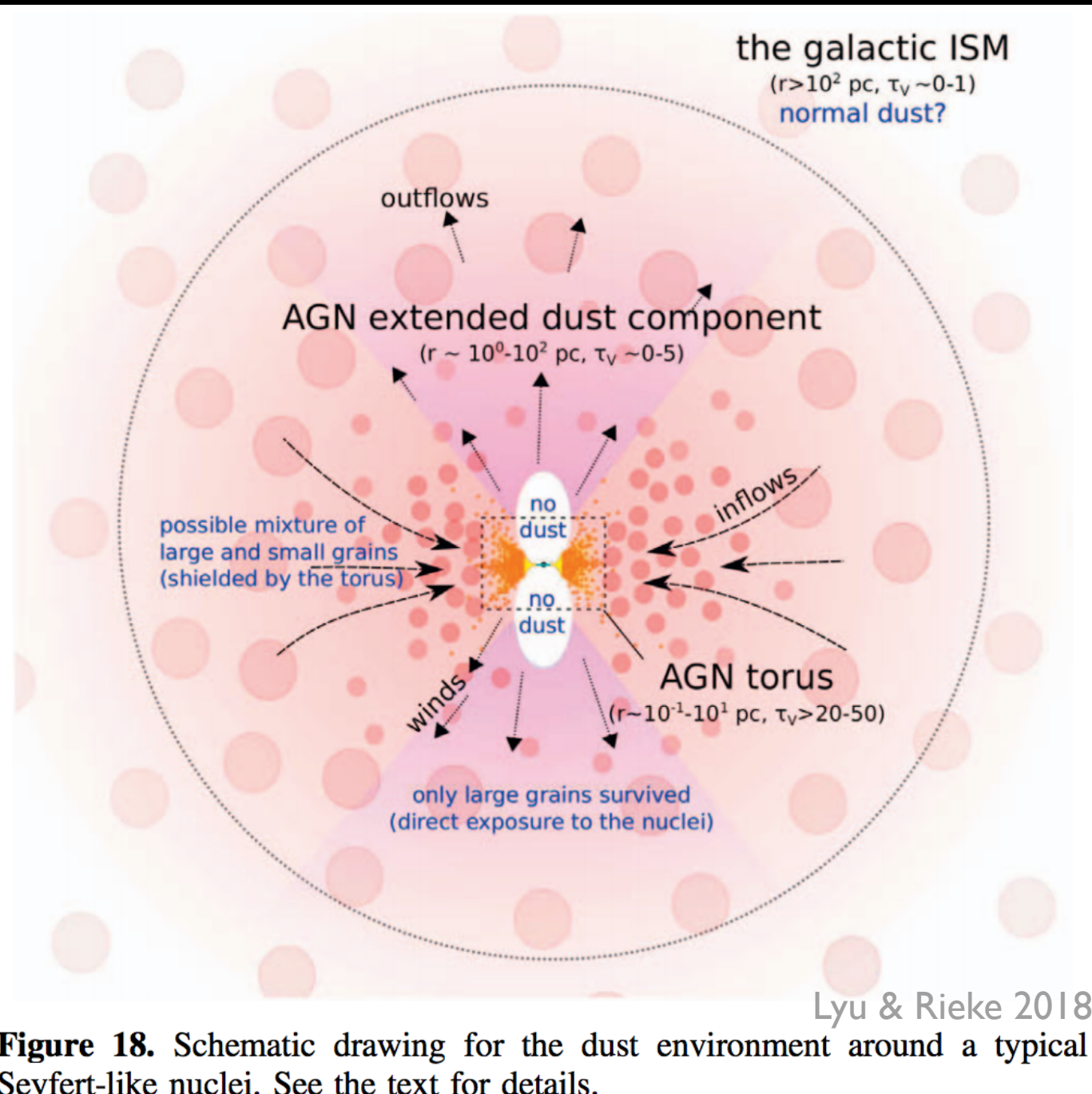


“unification model” invokes a “dusty torus” to hide very center from some viewing angles

This dust will be heated by the AGN, and emit in the IR

See Antonucci 1993 ARAA

Dust in AGN



AGN dust is
likely to be
complex

Also varies
galaxy to
galaxy

Dust in AGN

AGN can have significant,
variable impact on SED
(relative strength? deficient
in warm or hot dust?)

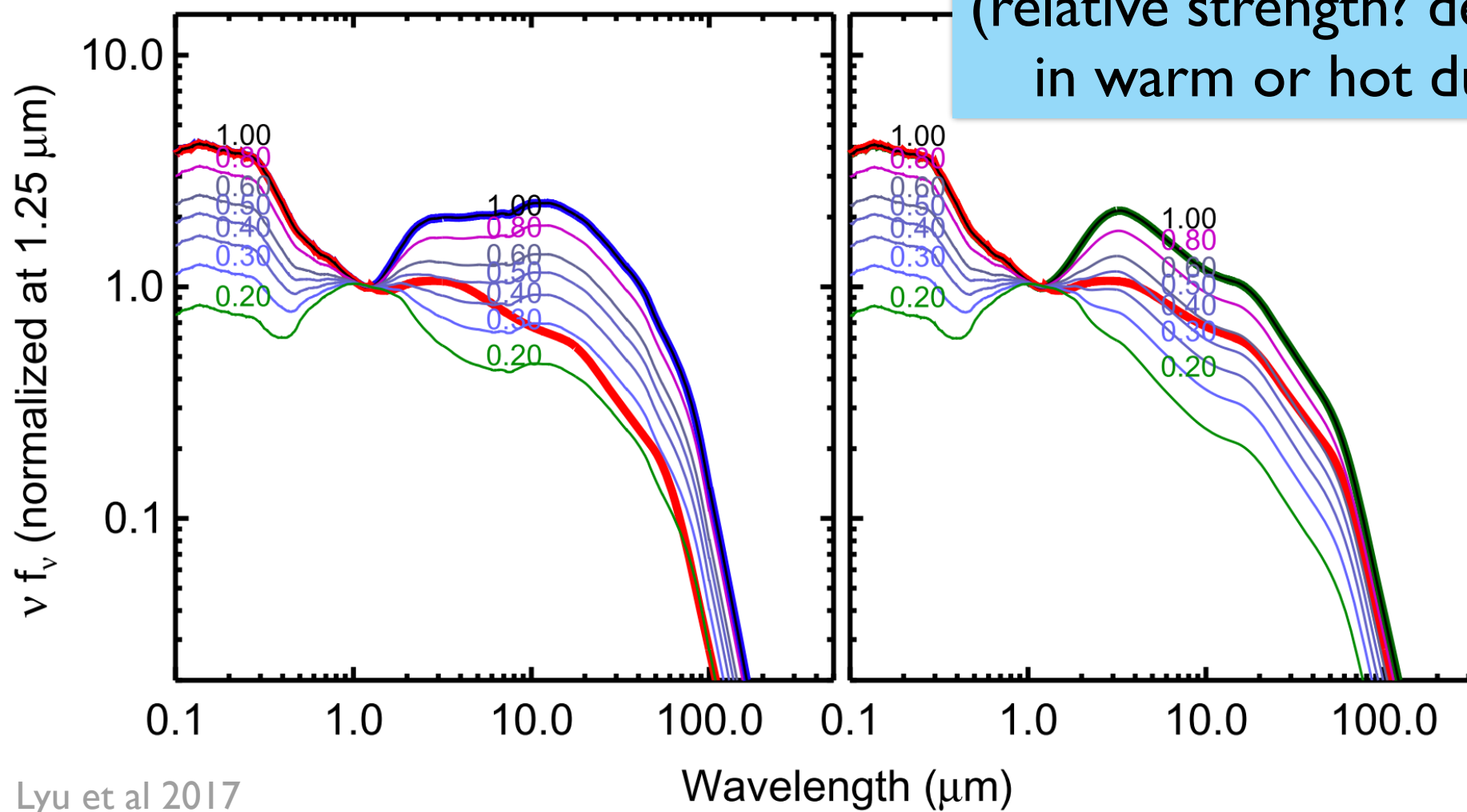


Figure 4. Mock SEDs of quasars. The left panel presents the composite SEDs of the Elvis AGN template and an old stellar population template, with the numbers indicating the fraction of the AGN contribution at 1.25 μm . The normal AGN template is shown as the red line. The right panel shows the composite SEDs of the WDD AGN template and an old stellar population template. The WDD AGN template is denoted as the green line. In both panels, the HDD template is shown as the blue thick line.

Separating contributions of AGN-heated vs SF-heated dust is challenge in unresolved observations!

Dust in AGN questions

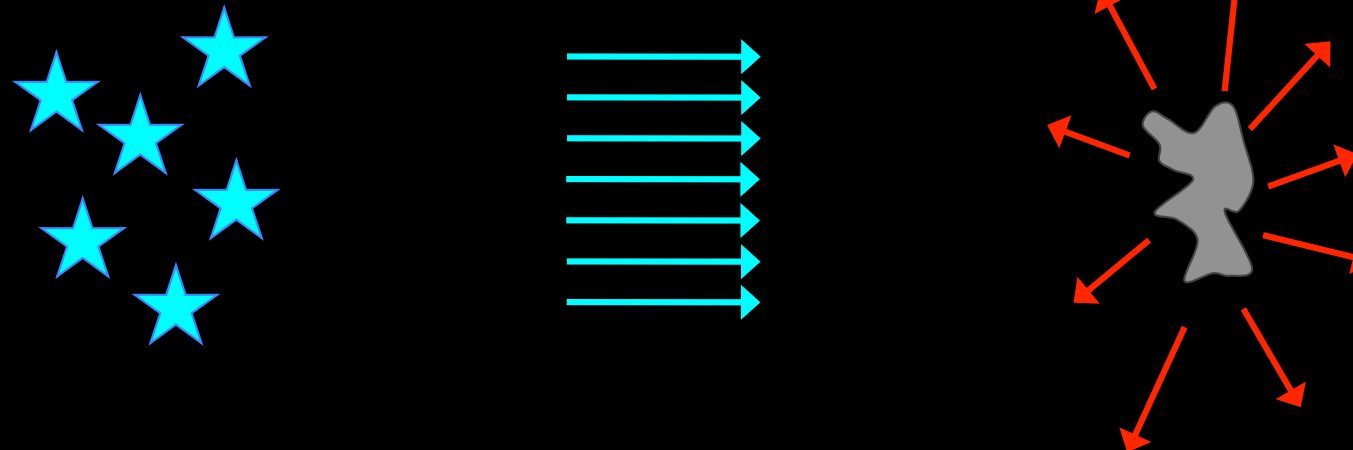
- Is there actually a dust “torus”?
- What drives variation in AGN dust (i.e., why are some kinds of dust emission absent, sometimes)?
- How clumpy and structured is the dust?
- What is the physical size scale of the dust heated by the AGN?
- How can we infer what fraction of the total IR luminosity is powered by AGN rather than SF?
- How should we use PAH diagnostics?

Fuller discussion of physics of dust emission

Extinction implies energy has been absorbed by dust.

Dust obeys Kirchoff's Law:

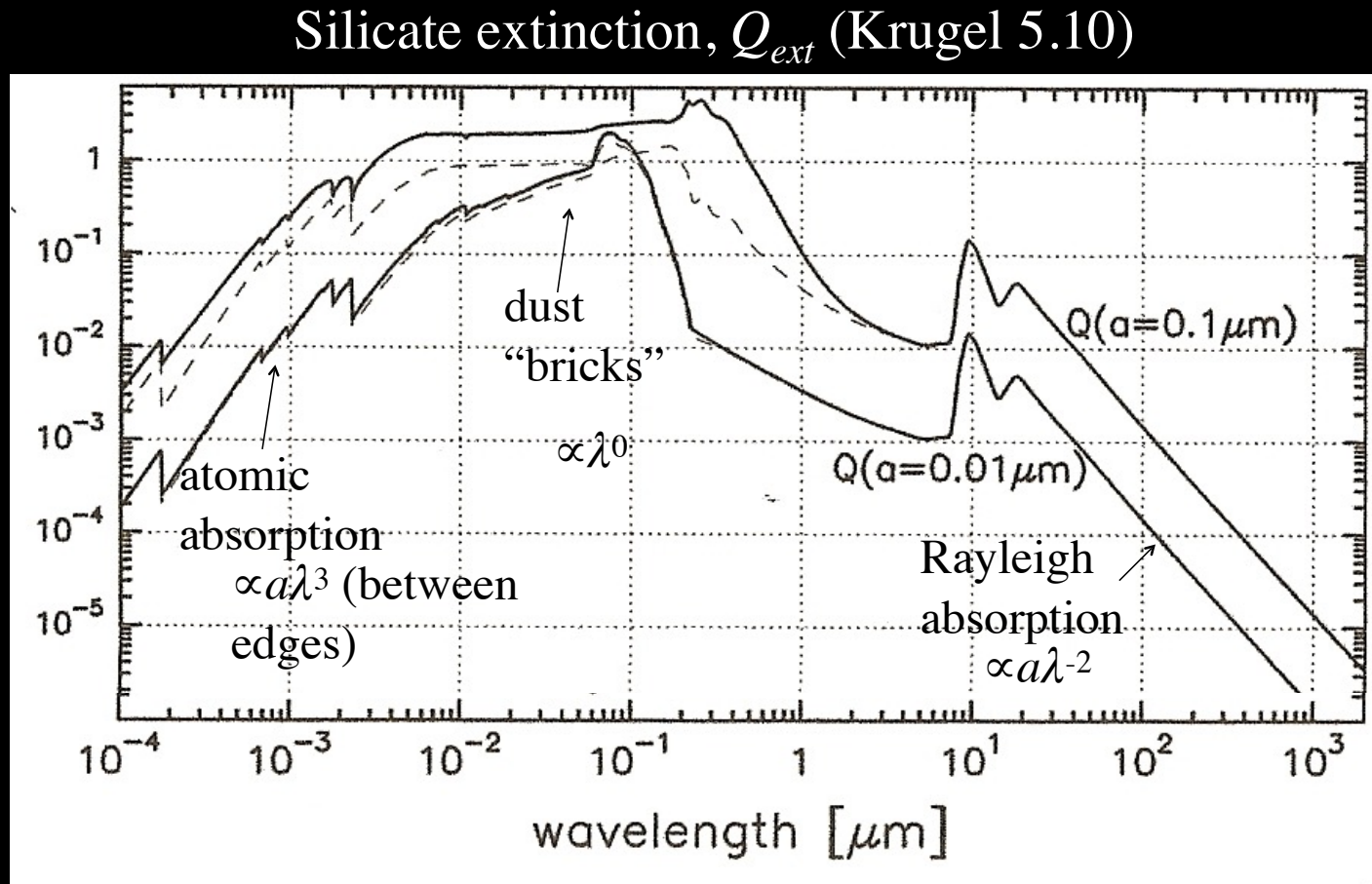
$$\varepsilon_v = \kappa_v^{abs} B_v(T_d)$$



$$\int Q_v^{abs} J_v dv = \int Q_v^{abs} B_v(T_d) dv$$

$\kappa_v \propto Q_v$ where Q is the “extinction coefficient”, set by dust properties

The extinction coefficient Q_{ext} will vary for different types of dust grains

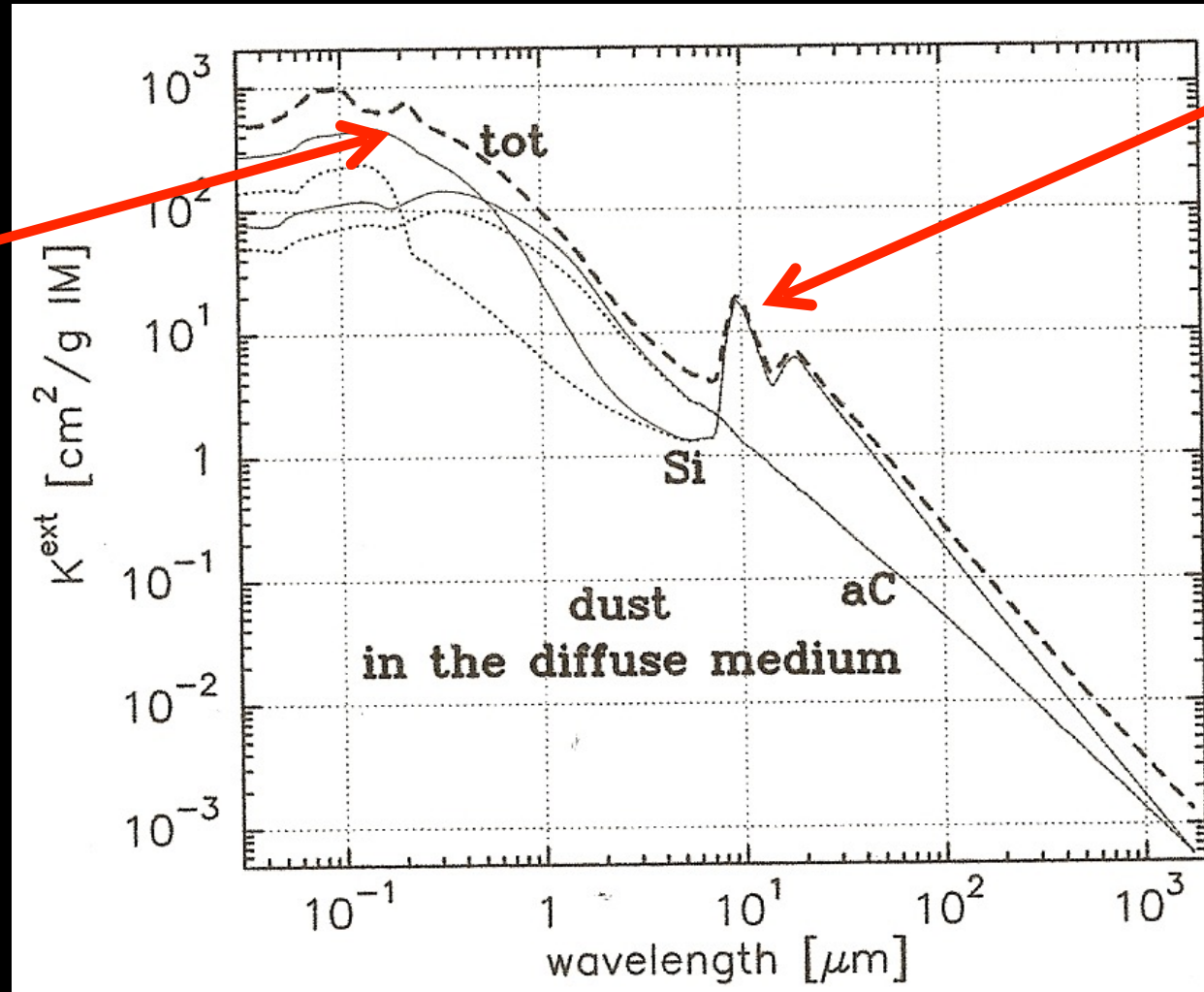


Discrete Dipole Approximation – can treat arbitrary dust shapes & varied composition – most sophisticated dust scattering codes

The total extinction depends on the mixture of dust grains

“2200 Å
feature”

Silicate
Features



Total extinction (Krugel Fig. 10.7)

Emission from heated dust: Blackbody-ish

Emission from dust grain w/ optical depth τ_λ :

$$I_\lambda = B_\lambda(T_d) \left(1 - e^{-\tau_\lambda}\right)$$

At high optical depth:

$$I_\lambda = B_\lambda(T_d)$$

At low optical depth where
 $(1 - \exp(-\tau)) \sim \tau$:

$$I_\lambda = \boxed{\tau_\lambda} B_\lambda(T_d) = \boxed{\kappa_\lambda^{\text{abs}} \sum_d} \frac{\varepsilon_\lambda}{\kappa_\lambda^{\text{abs}}} = \varepsilon_\lambda \sum_d$$

Remembering:

$$\varepsilon_\nu = \kappa_\nu^{\text{abs}} B_\nu(T_d)$$

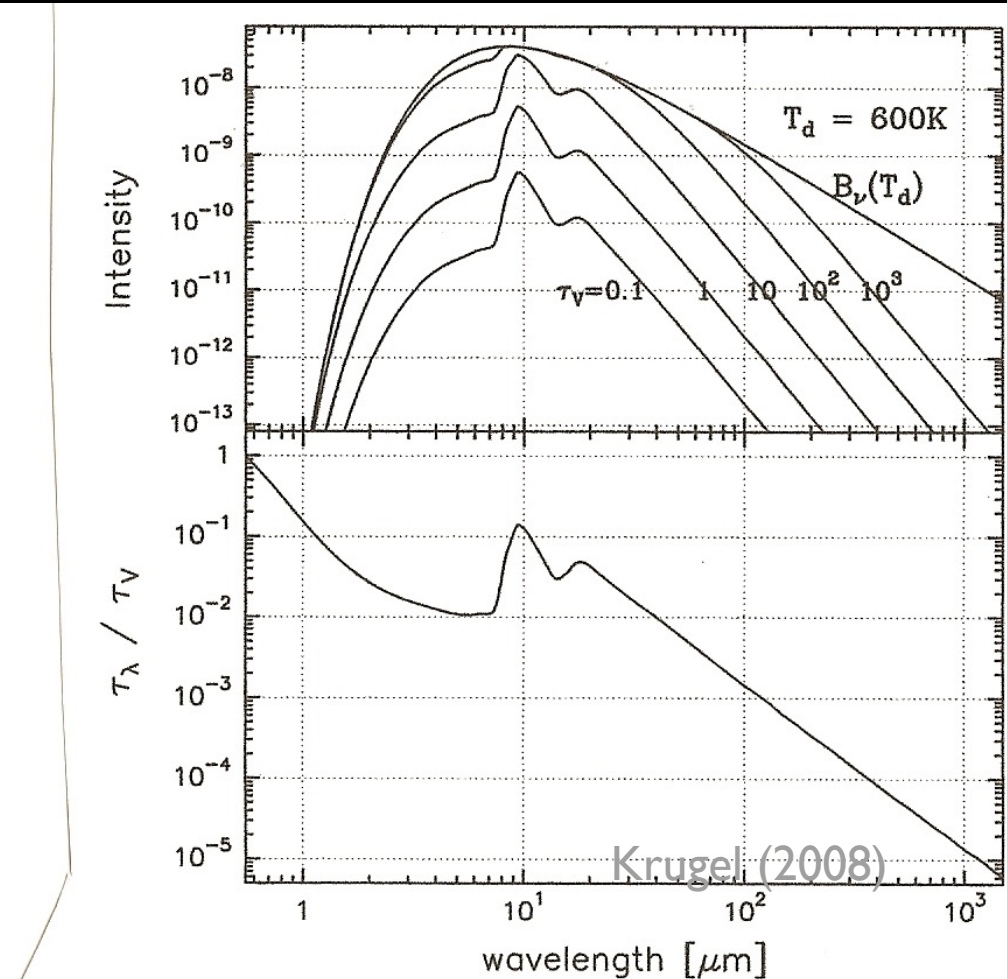


FIGURE 6.4 *Bottom:* The normalized optical depth of silicate grains with 600\AA radius. The wavelength scale starts at $0.55\mu\text{m}$ where $\tau_\lambda/\tau_V = 1$. *Top:* The intensity (in units $\text{erg s}^{-1} \text{cm}^{-2} \text{Hz}^{-1} \text{ster}^{-1}$) towards a cloud with temperature $T = 600\text{K}$ filled with such grains for visual optical thickness from 0.1 and 1000.